THE BEHAVIOUR OF

COMPOSITE CELLULAR BEAMS

THE INFLUENCE OF CELL GEOMETRY ON THE BEHAVIOUR OF COMPOSITE CELLULAR BEAMS

by

VICTOR PERCY LANE, B. ENG.

A Thesis

Submitted to the Faculty of Graduate Studies

in Partial Fulfilment of the Requirements

for the Degree

Master of Engineering

McMaster University

November, 1964

MASTER OF ENGINEERING(1965) McMASTER UNIVERSITY
(Civil Engineering) Hamilton, Ontario

TITLE: The Influence of Cell Geometry on the Behaviour of Composite Cellular Beams

AUTHOR: Victor Percy Lane, B. Eng. (Liverpool University)

SUPERVISOR: Dr. H. Robinson

NUMBER OF PAGES: ix, 118

SCOPE AND CONTENTS: Two types of tests are reported in this thesis: (1) tests of push - out specimens and (2) tests of composite cellular T - beams. The components of the composite members tested were short lengths of steel I - beams and concrete ribbed slabs. The ribbed slabs were formed by the inclusion of cellular sheet steel decking. Various rib sizes were used by varying the cell height and cell width of the decking. The components of a specimen were tied together by stud shear connectors.

The tests were made to investigate the influence of cell geometry on the behaviour of composite cellular members and to provide a rational approach to their design.

ACKNOWLEDGEMENTS

The author wishes to express sincere gratitude to his research director, Dr. H. Robinson, for suggesting the problem and for giving invaluable assistance and encouragement throughout the course of this work.

Thanks are also due to Canadian Sheet Steel Building Institute whose financial assistance made it possible to carry out the work, to Robertson - Irwin Ltd., Hamilton, Ontario, who provided the sheet steel, to Algoma Steel Corporation Ltd., who provided the steel beams, and to Gregory Industries Inc., Lorain, Ohio, who supplied the connectors and did all the welding.

CONTENTS

CONTENTS (Continued)

LIST OF FIGURES

LIST OF FIGURES (Continued)

LIST OF FIGURES (Continued)

LIST OF TABLES

CHAPTER 1

INTRODUCTION

1.1 Introduction

A reinforced concrete cellular slab formed by a galvanized steel deck, which is supported on a number of steel I - beams, is a well established form of floor construction. In this type of structure, a noncomposite structure, each I - beam carries the entire load transmitted to it by the concrete slab. If adequate shear connection is provided between the beam and the slab, they will act as a composite T - beam to carry the load.

The major factor in standard composite construction, without cells, is the manner of connecting the two units. It has been suggested that bond between the concrete slab and the beam is a sufficient shear connection. VIEST, SIESS, APPLETON & NEWMARK* in 1952, showed that bond, as long as it was present, was a very effective shear connection, but that repeated loading would break this connection; they concluded that bond was an unreliable shear connection. A variety of mechanical connectors have been used, such as channels, angles, plates, studs, hooked bars and spirals. The stud connector, a relatively recent development, has been used extensively because of its ease of installation. Studs, which may be considered as a flexible type of connector, allow a relative movement between the slab and the beam i.e. they permit "slip". Slip is

---

*References are given in chronological order in the BIBLIOGRAPHY.

a necessary requirement before the resistance of the studs can be developed. The studs are welded to the steel beam and embedded in the concrete to resist the horizontal shear (or limit the slip) and to prevent the slab lifting from the beam.

A preliminary investigation by ROBINSON in 1963, of a full scale composite T - beam with cellular slab incorporating stud connectors, demonstrated the feasibility of this method of construction. He observed that the use of studs to connect the steel beam to the concrete caused the concrete slab above the cells to resist compressive stresses in the manner of the more conventional composite T - beam; and that the strain distribution across the section was linear within the elastic range.

The advantages of the composite cellular T - beam over the non-composite form are:-

(a) the decking acts as a form and work platform prior to pouring the concrete

(b) the ducts can be used for electrical services and for circulating air

(c) the materials are positioned rationally in respect of their tensile and compressive strength.

(d) the slab serves a dual role, transmitting the load to the beam and acting as the compressive flange of the T - beam

(e) the beam may be reduced in size and weight and

(f) the greater stiffness reduces live load deflections.

The testing described herein is of push - out specimens and beams using studs as the connectors between the steel beam and the concrete cellular slab.

1.2 Object and Extent of Investigation

The primary objectives of the tests were to investigate the influences of change of cell geometry on the behaviour of composite steel and concrete T - beams with cellular slabs, and to provide a rational approach to the design of composite cellular members.

Since the investigations were broad in scope, small scale models were employed, so that specimens covering a wide range of cells could be tested economically. The types of specimens used were push - out specimens and T - beams.

The push - out specimens consisted of an I - beam with two concrete cellular slabs, one attached to each flange. Each slab included three concrete ribs and two cells separating the ribs; the central rib was connected to the I - beam by a pair of studs which were welded to the flange of the I - beam. The push - out test has been used universally to investigate the shear strength and load - slip characteristics of shear connectors. Despite its shortcomings, it provides a useful indication of the relative performance of different types of connectors. A wide range of cell proportions are used in the decking of standard non-composite floors. The push - out tests were employed to study the effect of cell geometry on the performance of stud connectors.

T - beams were tested with a two - point loading system. Again, the height and width of the cells were the variables investigated. The data from these tests have been analysed by the Newmark theory for incomplete interaction in composite beams. This theory is presented in the Appendix. Comparisons are made between the theory and the test data to show the validity and applicability of the Newmark approach to composite

beams with cellular slabs.

On the basis of the push - out and the beam tests, attempts have been made to describe the working characteristics of the connections and to describe how the characteristics are affected by change in cell geometry. The Newmark incomplete interaction theory is used with these results to illustrate a method of developing design curves.

The computations were simplified by the use of an I.B.M. 7040 digital computer.

The recommendations herein are based on tests of six small scale beams and forty-five push - out tests.

1.3 Definitions

The following terms are used throughout the text and for convenient reference are listed below:

- A COMPOSITE CELLULAR T - BEAM is a beam consisting of an I - beam and a concrete cellular slab interconnected in such a manner that they act together as one unit.
- A SHEAR CONNECTOR is a device for connecting the I - beam to the slab. In conventional composite beams with flat slabs, the connector resists horizontal shear and prevents the slab lifting from the I - beam. Studs are often used as connectors. In order to avoid confusion, "the connectors" is reserved herein to mean the studs and is not used to describe the complete connecting arrangement.
- A SHEAR CONNECTION in a composite cellular beam is the intricate arrangement of the stud connectors, the concrete ribs and the decking, through which the I - beam is connected to the solid slab. It resists horizontal shear and prevents the slab lifting from the I - beam. All

connections are imperfect in that they permit horizontal movement between the I - beam and the slab, i.e. slip.

- THE TOTAL SHEAR CONNECTION consists of a number of individual shear connections and in accordance with the Newmark theory means connections with spacing and modulus uniform throughout the length of the beam.
- SLIP is the relative horizontal movement between the I - beam and the slab at any position along the beam.
- THE MODULUS OF A SHEAR CONNECTION, k, is that load on the connection which causes unit slip.
- THE LOAD ON A SHEAR CONNECTION, Q, is the horizontal force transmitted by the connection from the slab to the I - beam.
- THE BREAKDOWN LOAD FOR A SHEAR CONNECTION, Q_{cb}, is the load on the connection at which the load - slip curve levels off. The break down load and the modulus of a connection can be used to obtain a simple idealized load - slip curve.
- COMPLETE INTERACTION exists between the I - beam and the slab if the connection is perfectly rigid i.e. if there is no slip.
- INCOMPLETE INTERACTION exists between the I - beam and the slab if slip occurs, as is the case with real connections.
- NO INTERACTION is that case in which the slab and the beam act independently and move freely at the contact surface.
- THE INTERACTION COEFFICIENT, 1/C, is a dimensionless expression indicating the degree of interaction. It is equal to zero for no interaction and to infinity for complete interaction. It is a function of the modulus of the connection, the spacing of the connections, the properties of the slab and the I - beam and the

span of the composite beam (see Appendix)

- THE THEORETICAL YIELD MOMENTFOR COMPLETE INTERACTION, M_{yf} is that moment which the beam with complete interaction would theoretically support when the strain in the steel in the lower fibre is at the yield strain.

CHAPTER II

PUSH - OUT TESTS

2.1 Description of Specimens and Materials

The push - out specimens were approximately one half scale. The form of the specimens is indicated in Figures 2.1 and 2.2. Each specimen consisted of a short length of steel I - beam, and two concrete cellular slabs, one slab attached to each flange of the steel beam. In each concrete slab two cells were formed using galvanized steel decking. This decking formed an integral part of the push - out specimen. The cells were separated and bounded by concrete ribs, and each central rib was connected to the I - beam by a pair of studs. These studs were welded to the steel beam and passed through holes in the decking; their lengths were chosen so that the heads of the studs projected out of the ribs into the main slab.

The tests of push - out specimens were made for the primary purpose of investigating the influence of cell geometry on the behaviour of pairs of studs used as connectors in a composite cellular beam. The principal variables were the cell width and the cell height. The values selected for the cell width were 1 1/2 in., 2 1/4 in., and 3 in., and for the cell height 3/4 in., 1 1/2 in., 2 1/4 in., and 3 in. In all cases, the distance between cell centres or rib centres was 4 1/2 in.

The beams used were 5 in. by 3 in. Standard I - beams at 10 lb. per ft. All slabs were 1 1/2 in. thick and 12 in. wide. The shear connectors used were 3/8 in. in diameter and varied in length such that their

heads had 3/8 in. cover in the slabs. The lengths of studs for cell sizes are given in TABLE 2.1. The decking was formed from U. S. No. 24 gauge galvanized sheeting, weighing 1 lb. per sq. ft.

The concrete used was a nominal 3500 psi commercial ready - mix concrete, containing a maximum aggregate size of 3/8 in. The slabs contained no reinforcement.

TABLE 2.1

SUMMARY OF DETAILS AND RESULTS FOR PUSH - OUT SPECIMENS

Cell Dimensions		Slabs[a]	Method*	Maximum	Slip at	Type+	Breakdown Load**	Length of 3/8	Rib Dimensions	
Height (inches)	Width (inches)	Laterally	of Loading	Load (Kips)	Max. Load (inches x 10^{-4})	of Failure	For one Slab (Kips)	in. dia. studs (inches)	Height (inches)	Width (inches)
3	1 1/2	R	C	18.00	498	TFS(1)	6.0	4 1/8	3	3
3	1 1/2	F	Rep.	19.90	1216	TFS(1)	5.0	4 1/8	3	3
3	1 1/2	F	C	20.68	1885	TFS(2)(1)	4.8	4 1/8	3	3
3	2 1/4	R	C	12.14	590	SFR(2) TFS(1)	4.5	4 1/8	3	2 1/4
3	2 1/4	F	Rep.	13.20	259	SFR(1)	4.5	4 1/8	3	2 1/4
3	2 1/4	F	C	13.00	132	TFS(1)	4.6	4 1/8	3	2 1/4
3	3	R	C	8.80	528	SFR(1)(2)	4.0	4 1/8	3	1 1/2
3	3	F	Rep.	8.00	323	SFR(2)(1)	3.3	4 1/8	3	1 1/2
3	3	F	C	7.60	96	SFR(2)(1)	3.5	4 1/8	3	1 1/2
2 1/4	1 1/2	R	C	23.25	654	TFS(1)(2)	6.0	3 3/8	2 1/4	3
2 1/4	1 1/2	F	C	21.14	430	TFS (1) SFR (1)	5.5	3 3/8	2 1/4	3
2 1/4	1 1/2	F	Rep.	20.50	600	TFS(1)(2) SFR (1)	5.0	3 3/8	2 1/4	3

TABLE 2.1 (Continued)

Cell Dimensions Height (inches)	Cell Dimensions Width (inches)	Slabs[a] Laterally	Method* of Loading	Maximum Load (Kips)	Slip at Max. Load (inches x 10^4)	Type+ of Failure	Breakdown Load** For one Slab (Kips)	Length of 3/8 in. dia. studs (inches)	Rib Dimensions Height (inches)	Rib Dimensions Width (inches)
2 1/4	2 1/4	R	C	12.50	223	TFS(2)	5.0	3 3/8	2 1/4	2 1/4
2 1/4	2 1/4	F	Rep.	12.80	158	TFS(1)	5.0	3 3/8	2 1/4	2 1/4
2 1/4	2 1/4	F	Rep.	13.80	214	TFS(2)(1)	4.8	3 3/8	2 1/4	2 1/4
2 1/4	3	R	C	11.00	480	TFS(2)(1)	4.0	3 3/8	2 1/4	1 1/2
2 1/4	3	F	C	11.18	337	SFR(2)	3.8	3 3/8	2 1/4	1 1/2
2 1/4	3	F	Rep.	11.00	413	TFS(2)SFR(1)	3.6	3 3/8	2 1/4	1 1/2
1 1/2	1 1/2	R	C	24.30	400	TFS (1,2) SFR (1,2)	7.5	2 5/8	1 1/2	3
1 1/2	1 1/2	F	C	24.20	317	TFS (1,2) SFR (1,2)	7.0	2 5/8	1 1/2	3
1 1/2	1 1/2	F	C	22.65	325	TFS (1,2) SFR (2)	6.8	2 5/8	1 1/2	3
1 1/2	2 1/4	R	C	18.80	303	TFS(1)SFR(1)	6.0	2 5/8	1 1/2	2 1/4
1 1/2	2 1/4	F	C	19.10	274	TFS(1)SFR(1)(2)	6.0	2 5/8	1 1/2	2 1/4
1 1/2	2 1/4	F	C	16.40	402	SFR(2)TFS (1)	5.0	2 5/8	1 1/2	2 1/4
1 1/2	3	R	C	12.84	270	TFS (1)	3.3	2 5/8	1 1/2	1 1/2
1 1/2	3	F	C	14.40	400	TFS (1)	3.8	2 5/8	1 1/2	1 1/2
1 1/2	3	F	C	13.75	315	SFR (1)	4.0	2 5/8	1 1/2	1 1/2

TABLE 2.1 (Continued)

Cell Dimensions		Slabs[a] Laterally	Method* of Loading	Maximum Load (Kips)	Slip at Max. Load (inches x 10^4)	Type+ of Failure	Breakdown load** For one Slab (Kips)	Length of 3/8 in dia. studs (inches)	Rib Dimensions	
Height (inches)	Width (inches)								Height (inches)	Width (inches)
3/4	1 1/2	R	C	34.50	630	TFS (2)	9.0	1 7/8	3/4	3
3/4	1 1/2	F	C	32.10	646	TFS (1) (2)	9.0	1 7/8	3/4	3
3/4	1 1/2	F	C	32.80	960	TFS (2) (1)	8.3	1 7/8	3/4	3
3/4	2 1/4	R	C	29.00	673	TFS (1) (2)	7.0	1 7/8	3/4	2 1/4
3/4	2 1/4	F	C	29.70	665	TFS (1) (2)	8.0	1 7/8	3/4	2 1/4
3/4	2 1/4	F	C	28.00	1104	TFS (1) (2)	7.0	1 7/8	3/4	2 1/4
3/4	3	R	C	23.60	191	TFS(1)SFR(2)	6.0	1 7/8	3/4	1 1/2
3/4	3	F	C	21.20	414	SFR(1)Stud.	6.0	1 7/8	3/4	1 1/2
3/4	3	F	C	21.50	464	TFS(2)SFR(1)	5.5	1 7/8	3/4	1 1/2
No	Cells	R	C	33.65	870	TFS(1,2)	12.	1 1/8	No Ribs	
No	Cells++	F	C	20.0	412	Vertical Crack	12.5	1 1/8	No Ribs	
No	Cells	F	C	29.8	1211	Studs (2)	15.0	1 1/8	No Ribs	

(a) R = slabs laterally restrained;
F = slabs laterally free;

* C = continuously loaded;
Rep = repetitive loading;

\+ TFS = tension failure slab;
SFR = failure of central rib;
(1)(2) = first cast slab followed by second cast slab;
(1,2) = both slabs almost simultaneously;
(2) = failure apparent in slab 2 only;

** Determined from load - slip curves and taken as one half of load on specimen;

++ Concrete damaged before testing.

2.2 Manufacture of Specimens

The first step in the manufacture of push - out specimens was the welding of pairs of studs to each flange of the I - beams. Then the shaped decking, with holes for passing over the studs, was placed on the flanges of the beams. The formwork was then attached. In order to minimize bond between the concrete and the steel flanges, oil was poured on every flange around the base of the studs; care was taken to keep the studs free from contact with this oil. A one-half inch diameter hole was cut in the decking of the central rib of each slab, alongside the studs, for slip measurement.

In a building, the concrete is cast in a horizontal position on top of the beam. Therefore to simulate these conditions, the slabs were cast horizontally. This necessitated a time delay between the casting of the two slabs of one specimen. The slab on one side of the beam was cast first, and this was allowed to set for twenty-four hours. This slab is referred to as slab 1. On the following day, the specimen was turned over, and the other slab, slab 2, was poured.

In each slab, the concrete was worked around the studs and into the ribs of the decking with a steel trowel and a one-inch diameter poker vibrator. The slabs were levelled off and after a few hours were finally trowelled to give a smooth finish. The specimens were cured under wet burlap for the first seven days, after which the formwork was removed and the specimens dry-cured until tested.

The first pour of concrete was used for the first slabs of twenty-four push - out specimens with cellular slabs and three push - out specimens without ribs or cells, and for the three composite beams reported in Chapter 3. The second pour completed the manufacture of these push -

out specimens. Two specimens were made of each cell arrangement listed in Table 2.1, and they were separated to give two complete series, each series having all of the twelve listed cell arrangements. These series are referred to as Series 1 and Series 2.

At a later date, twelve more cellular slab push - out specimens were cast. These again covered the whole range of cell sizes and are referred to as Series 3.

Before starting any pour of concrete, water was added to the mix such that the concrete had a one inch slump. Control cylinders were made at intervals during each pour and these cylinders were cured together with their corresponding slabs. The cylinders were tested either at 28 days, the beginning of the push - out test period or at a time when the push - out tests were completed. Since the slabs were cast from different concrete batches, the strengths varied as indicated in Table 2.2 and Table 2.3. The variations in concrete strength had no effect on the validity of the results of the T - beam tests, but in the case of the push - out specimens, resulted in slab 2 being stronger than slab 1. This may account for the observation that twenty push - out specimens cracked in slab 1 initially, whereas only thirteen cracked in slab 2 initially. Before the concrete cracked, the variation of concrete did not appear to affect the behaviour of the push - out specimens and the test results were consistent and satisfactory for comparing connection performances.

TABLE 2.2

COMPRESSIVE STRENGTH AND MODULUS OF

ELASTICITY OF CONCRETE CYLINDERS

Identification	Age (days)	Compressive Strength (psi)	Modulus of Elasticity (psi)
Push-out Specimens	28	4940	3.78×10^6
Series 1 and 2	28	4950	3.88×10^6
Slab 1	28	4740	3.18×10^6
	28	4330	3.78×10^6
	111	4950	3.91×10^6
Composite B I	28	5180	3.70×10^6
Beams B II	28	5200	3.84×10^6
B III	28	5100	3.58×10^6
B I	111	5970	4.15×10^6
B II	111	5890	4.34×10^6
B III	111	5480	4.27×10^6
Push-out Specimens	28	6950	4.10×10^6
Series 1 and 2	28	7300	4.38×10^6
Slab 2	28	7300	4.25×10^6
	28	7000	4.04×10^6
	111	7500	4.85×10^6
Push-out Specimens	29	5580	4.03×10^6
Series 3	29	5380	3.22×10^6
Slab 1	29	5410	4.00×10^6
	29	5820	4.07×10^6
	29	4950	3.85×10^6
	30	5610	3.95×10^6
Push-out Specimens	29	6800	4.80×10^6
Series 3	29	6400	4.73×10^6
Slab 2			

TABLE 2.3

SPLITTING TENSILE STRENGTH OF CONCRETE CYLINDERS

Identification	Age (days)	Cylinder Details		Maximum Load (Kips)	Proportion of Coarse Aggregate Fractured (%)	Splitting Tensile Strength (psi)
		Length (inches)	Diameter (inches)			
Push-out Specimens	28	12.0	6.00	57.4	60	510
Series 1 and 2	28	12.0	6.00	58.8	55	520
Slab 1	110	12.0	6.02	72.5	60	640
Beams B I	28	12.0	6.00	53.4	45	475
B II	28	12.0	6.00	52.0	50	460
B III	28	12.0	6.00	54.0	60	480
B I	110	12.1	6.01	58.2	60	510
B II +	110	12.0	6.04	60.6	40	535
B III	110	12.0	6.02	69.2	80	610
Push-out Specimens	28	12.0	6.00	71.0	70	630
Series 1 and 2	28	12.0	6.00	70.4	65	625
Slab 2	109	12.0	6.01	83.0	90	735
Push-out Specimens	30	12.0	6.03	66.4	40	585
Series 3	30	12.0	6.00	64.8	80	575
Slab 1	30	12.0	6.02	67.8	70	595
Push-out Specimens Series 3, Slab 2	29	12.0	6.02	78.0	80	690

Failure of cylinders resulted in a vertical diagonal crack for all specimens except the specimen marked +

The test procedure followed is that recommended in "Tentative Method of Test for Splitting Tensile Strength of Molded Concrete Cylinders", ASTM designation C496 - 62T.

2.3 Instrument and Loading Apparatus

The specimens were tested on a mechanical screw type Universal testing machine of 120,000 lb. capacity, with the load applied to the steel beam through a ball platen to achieve an equal distribution of load. The bases of the concrete slabs were embedded in Soiltest CT55 concrete cylinder capping compound on machined steel moulds to limit displacements due to bedding in of the concrete slab.

Unlike the conventional push - out specimen with solid slabs, interfacial slip measurements do not detect the total movement of the slab relative to the I - beam. It was hoped that measurement of the cross-head movement of the testing machine would indicate this total movement. However, tilting of the bases of the specimen complicated interpretation of this measurement. Interfacial slip between the I - beam and the cellular slab was measured at the base of the central rib. The displacement of the solid part of the slab relative to the bottom of the rib was also measured. It is thought that this displacement is due in large part to the rotation of the rib. The interfacial slips of each slab were measured at the level of the studs, at the extremities of the flanges of the I - beam, by means of a Sanborn Differential Transformer. The core of the transformer rested on a small metal bracket which was cemented to the concrete at least one day prior to testing. A view of this general arrangement is shown in Figure 2.2 (a). In later tests the differential transformers were replaced by dial gauges as illustrated in Figure 2.2 (b). The rotation of the ribs was measured by four dial gauges as shown in Figures 2.1 and 2.2(b). Two gauges were used on each central rib; one gauge was positioned on the slab and the other gauge on the central rib. Cantilever extension arms were attached to the dial

stems, and these arms rested on brackets cemented to the concrete at the level of the studs.

Measurements were also made to determine the settlement, if any, of the specimen after capping the bases of the concrete slabs. The maximum settlement measured on any specimen was 0.001 inches and in most cases was even less.

2.4 Test Procedure

The load was applied to the push - out specimen from zero load to failure in increments of 1000 lb. At each load increment, the differential transformers which were coupled to a Moseley Autograf X - Y Recorder, and the dial gauges, were read to the nearest 0.0001 in.

This procedure was modified with four specimens of Series 2 and three specimens of Series 3. For these specimens the load was removed at each increment and the residual slip measured. This procedure was followed until failure was imminent, at which time the load was applied in 500 lb. increments until the specimen failed.

Preliminary tests indicated, that during the testing of a push-out specimen with cellular slabs, there was a tendency for the slabs to separate from the beam in the lower half of the specimen. Previous investigators, VIEST, SIESS, APPLETON and NEWMARK in 1952, had commented on this occurrence in push - out tests without cells and on the necessity of holding the slabs and the beam firmly together. It was decided to test Series 1 of the specimens using a lateral restraining device as illustrated in Figure 2.2(a). Series 2 and Series 3 were tested without this device, so that slabs of these specimens were free to move laterally.

2.5 Test Results and Observations

Results of the push - out tests are summarized in Table 2.1. In this table and in the following discussion, it is assumed that the load applied to the I - beam was transmitted to the concrete slabs through the studs alone, and that the load was shared equally between the slabs. Inaccuracies, arising due to uneven distribution of the load between the slabs, were partly compensated for by averaging the slip readings for each side.

The assumption of load transmission by the studs alone, ignores the presence of kinetic friction and of bond. The eccentricity of the force transmitted to the concrete slabs by the studs, causes the slabs to rotate and to exert a pressure on the I - beam above the level of the connection. Therefore part of the load on the beam is transferred to the slabs by friction. Any specific contribution to resistance by friction has been ignored in evaluating the performance of the specimen. In all specimens, an attempt was made to destroy the development of bond between the slab and the beam, by greasing the surface of the flanges in the immediate vicinity of the stud welds prior to concreting. This was satisfactory on the push - out specimens of Series 1 and Series 2, but, despite the oil, the results of many specimens of Series 3 were obviously affected by bond. This can be seen in Figure 2.3 showing the load - slip curves for two specimens from Series 2 and two specimens from Series 3 with rib sizes 3 in. wide by 1 1/2 in. high, and 1 1/2 in. wide by 1 1/2 in. high. These curves and similar curves indicate that the normal curve, where bond is not noticeable, takes the form of an initial linear portion, followed by a flat part in which small load increase causes large increase in slip movement. In specimens affected by bond, the linear part of the curve is

almost vertical, when little or no slip is recorded and the bond is broken near the limit of the normal linear portion.

The load required to produce unit slip of the connection or the gradient of the load - slip curve, is known as the modulus of the connection. For comparison purposes, the modulus used is that obtained from the linear part of the load - slip curves. In many specimens of Series 3, the initial modulus indicated was large because of bond. Therefore, in drawing conclusions such magnitudes of the modulus are considered to be invalid. Nevertheless, for specimens affected by bond in the early stages of loading, the values of the load at which the load - slip curve flattens out, and the values of the maximum load supported, are considered satisfactory for inclusion in further discussion, since such load values show little indication of variation due to bond.

The modes of failure are listed in Table 2.1. The most common type of failure was that in which the slab cracked suddenly in tension as the maximum load was reached. Generally, this crack was horizontal and started at the outer face of the slab at the level of the lower edge of the concrete rib, as indicated in Figure 2.4, before spreading inwards until the slab was completely broken. Such a tensile slab failure is shown in Figure 2.5. This type of failure occurred most frequently in push - out specimens having rib width greater than slab thickness. No similar type of collapse was observed in the T - beams. In the T - beams, the cracking of the concrete occurs across the ribs at the junction of the slab and the ribs, causing the solid part of the slab to separate from the ribs. Failure of the central rib of the push - out specimen, due to cracking along the top of the rib as shown in Figure 2.4, was observed in eight instances. Push - out specimens with slender ribs, such as those with

dimensions 3 in. high and 1 1/2 in. wide, were most prone to rib failure. The specimen illustrated in Figure 2.2(a) failed in this way, and a close - up view of the rib after testing is shown in Figure 2.6(a). Another type of failure which might occur in a composite beam is that of a break of a stud connector, within the weld or within the stud. In a beam, this behaviour of a stud, or a pair of studs, would result in redistribution of the load to those studs functioning satisfactorily, so that the effects would be less apparent than in a push - out test, where the effect on the slip would be instantaneous and would cause lateral movement of parts of the specimen. Figure 2.6(b) shows a push - out specimen after stud failure. Three tests had to be terminated because of stud failure. Two of these were push - out specimens without cells and the third had ribs 3/4 in. high by 1 1/2 in wide. The results in the latter case were not seriously affected. Since the stud failures occurred in three specimens with shallow ribs or without ribs, it is probable that the behaviour of specimens, with shallow ribs, at or near to the maximum load is a function of the stud strength. This indicates a limit for curves based on the results of the push - out tests.

The data obtained from the push - out tests were reasonably consistent for any particular connection. Therefore, it is considered sufficient to present the load - slip curves for a typical series of specimens, Series 2, as shown in Figures 2.7, 2.8, and 2.9. The total slip for one slab was taken as the sum of the interfacial slip and the relative movement due to rib rotation. The abscissa of the load - slip curve is the average of the total slips for the two slabs of the same specimen.

2.6 Modulus and Breakdown Load

The modulus, k, of a particular specimen having a specific rib size, is related to the slope of the linear part of the load - slip curve. To ensure that the effect of bond was minimized, a secant modulus was calculated at a point close to the limit of the linear part of the load slip curve.

Two values of load were considered on each load - slip curve for comparison of the effect of geometry on behaviour of the push - out specimens with cellular slabs. One was the maximum load and the other the magnitude of the load at which the load - slip curve levels off. This is a critical load for the connection and will be called the breakdown load, to prevent confusion with "critical load" as defined by VIEST in 1955. If the linear portion of the load - slip curve was well defined, the breakdown load, Q_{cb}, was taken as the limit of the linear part; in other cases, such as the plot for the push - out specimens with ribs 3/4 in. high by 3 in. wide, tangents were drawn to the initial and to the flat sections of the curve, and breakdown load considered as the intersection of the two tangents. Figures 2.7, 2.8, and 2.9 are marked to indicate these values.

2.7 Effect of Testing Technique

The twelve specimens of Series 1 were tested so that the concrete slabs were restrained, to prevent lateral movement. The effect that this had on the load - slip curves was consistent for all specimens, and for this reason the results from only six tests are listed in Table 2.4

It can be seen in Table 2.1 that the restraining device did not affect the maximum load. However, the magnitude of the slips for a

TABLE 2.4

EFFECT OF RESTRAINING CONCRETE SLABS

Rib Height (inch)	Rib Width (inch)	Slabs Laterally	Q_{cb} Pair of Studs (Kips)	Slip at Load Q_{cb} (inches x 10^4)	Load (P_{MAX}) (Kips)	Corresponding Slip (inches x 10^4)
2 1/4	1 1/2	Restrained	4.0	130	11.0	480
2 1/4	1 1/2	Free	3.8	63	11.0	227
2 1/4	2 1/4	Restrained	5.0	43	12.1	224
2 1/4	2 1/4	Free	5.0	34	12.1	135
2 1/4	3	Restrained	6.0	78	20.0	473
2 1/4	3	Free	5.5	43	20.0	342
3	1 1/2	Restrained	4.0	145	7.0	130
3	1 1/2	Free	3.3	69	7.0	96
3	2 1/4	Restrained	4.5	95	10.0	115
3	2 1/4	Free	4.5	75	10.0	79
3	3	Restrained	6.0	90	17.0	540
3	3	Free	5.0	70	17.0	409

"restrained" push - out were larger than those for the similar "laterally-free" specimens at all corresponding stages of loading, and likewise the modulus for a "restrained" specimen was smaller than that for its "free" counterpart. In some cases, the magnitude of the breakdown load for a restrained specimen differs from that for the similar "laterally - free" specimen. This difference is probably due to difficulties in interpreting the load - slip curve. Therefore, the breakdown loads obtained from tests on "restrained" push - out specimens are considered satisfactory for inclusion in further discussion.

The "restrained" load - slip curves showed less agreement with the behaviour of the beams than the "laterally free" curves.

VIEST, 1955 and 1956, used a repetitive loading method on push - out specimens with solid flat slabs to illustrate that at low loads, practically all the slip was recoverable on removal of the load; and that at higher loads large residual slips resulted. Viest defined a critical load as that load at which the residual slip was 0.0030 in., or as the value of the load at transition from small to large residual slips, if this occurred when the residual slip was less than 0.0030 in.

The "critical load", as defined by Viest is obtained from a load - residual slip curve; whereas the breakdown load (the load at which a load - slip curve levels - off) is obtained from a load - slip curve.

The specimens tested with repetitive loading are indicated in Table 2.1, and the results shown in Figure 2.10. The "critical loads" and the breakdown loads are compared in Table 2.5. In each case, the "critical load" is smaller than the breakdown load.

The connection in composite cellular members is weaker and

TABLE 2.5

CRITICAL AND BREAKDOWN LOADS

Rib Dimensions Height (inches)	Rib Dimensions Width (inches)	Critical Load, Q_c (Kips)	Breakdown Load Q_{cb} (Kips)	
		Series 3	Series 1	Series 2
2 1/4	3	4.0	6.0	5.5
2 1/4	2 1/4	2.7	5.0	5.0
2 1/4	1 1/2	1.8	4.0	3.8
		Series 2	Series 1	Series 3
3	3	4.5	6.0	4.8
3	2 1/4	4.3	4.6	4.5
3	1 1/2	2.6	4.0	3.5

more flexible than the connectors used by Viest. Therefore, larger residual slips may be tolerated in composite cellular structures. If the method of finding "critical loads" as described by Viest, is applied to the results of tests on push - out specimens with cellular slabs, and allowance is made for larger permissible residual slips, the magnitudes of the "critical loads" increase and give closer agreement with the breakdown loads.

2.8 The Effect of Variation of Rib Size on Slip Components

Change of the rib size of a push - out specimen causes change of the magnitude of the interfacial slip, the slip due to rotation and the total slip, which occur when a specific load is applied to the specimen. The overall result is a change in the load - slip curve.

Table 2.6 shows at different stages of loading the variation of the components of slip with change of the rib dimensions. For cases in which the rotational component appears to be the dominant figure, it is necessary to ascertain that the presence of bond has not caused a reduction in the interfacial slip. For example, if bond is present in a push - out specimen with slender ribs the bond is difficult to break during testing, even with repetitive loading. In such a case, application of load, causes only the ribs to rotate and may result in the concrete ribs cracking before the bond is broken. The results listed above are not perfectly consistent but the trends described below are apparent.

From Table 2.6, it is evident that when the rib height is small, the interfacial slip is the larger component; and as the rib height increases, the component of the total slip due to rib rotation increases.

The relationship between the interfacial slip and the slip due

TABLE 2.6

RELATIONSHIP BETWEEN INTERFACIAL SLIP AND SLIP DUE TO RIB ROTATION AS MEASURED IN THE PUSH - OUT SPECIMENS OF SERIES 2

Rib Dimensions		Value of Interfacial Slip ÷ Relative Moment Due to Rib Rotation		
Height (inches)	Width (inches)	Initially	At Breakdown Load	At Maximum Load
3	3	2/1	3/1	3/1
2 1/4	3	1/100	1/8	1/1
1 1/2	3	100/1	9/1	9/1
3/4	3	100/1	100/1	95/1
3	2 1/4	1/3	2/3	2/1
2 1/4	2 1/4	1/2	1/1	1/1
1 1/2	2 1/4	15/1	6/1	4/1
3/4	2 1/4	15/1	15/1	5/1
3	1 1/2	2/1	2/1	2/5
2 1/4	1 1/2	1/3	4/5	1/1
1 1/2	1 1/2	100/1	20/1	15/1
3/4	1 1/2	100/1	100/1	6/1

to rotation, changes with the stage of loading. In the initial stages, the component due to rib rotation is always relatively small but as the load increases, its share of the total slip increases. As the maximum load is reached, the magnitude of the slip due to rib rotation is affected by the cracking of the specimen, whether failure is due to tension in the slab or is due to collapse of the rib. This results in the rotational component of the slip contributing a larger part to the total slip at collapse of the specimen than at other stages of loading.

2.9 Effect of Variation of Rib Size on Load - Slip Characteristics

It has been shown in Figures 2.7, 2.8 and 2.9 that the load - slip characteristics vary with change in cell size. This section deals with the comparison of essential characteristics of the load - slip curves. The characteristics considered are the maximum load, the modulus, k, and the breakdown load, Q_{cb}, and their variation is studied with changes in width of rib and with height of rib.

The results of the tests on Series 1, 2 and 3 indicate similar trends for the maximum loads and for the breakdown loads. For clarity, only a few of these results are presented in Figures 2.11 to 2.14. In diagrams showing the variation of modulus the results of Series 2 are plotted.

Figures 2.11 and 2.12 show the influence of the width of the concrete rib on the maximum load, on the modulus, and on the breakdown load. In the three diagrams, for constant width, the variables show an increase due to a reduction of rib height; and for constant depth, the variables increase with widening of the concrete rib. For a given depth the maximum load and the breakdown load are directly proportional to the

square of the width of the concrete rib, but the modulus variation is less regular. The moduli show less variation between the 1 1/2 in. wide rib specimens and the 2 1/4 in. wide rib specimens, than between the 2 1/4 in. wide and the 3 in. wide. It is probable, although not necessarily conclusive, that with wide ribs the concrete rib is the dominant contributor to the stiffness of the connection; but as the ribs narrow, the effect of the concrete rib reduces, and the stud behaviour exercises a great influence on the stiffness of the connection.

The second parameter considered was the reciprocal of the concrete rib height. Its influence on the three characteristics was examined before comparisons were made as indicated in Figures 2.13, 2.14 and 2.15.

Figure 2.13 indicates that change of depth has more effect on the maximum load for specimens with narrow ribs. The plot indicates that:

the maximum load α 1/ (height of rib)^n

where $n = 0.39$ for ribs 3 in. wide,

$n = 0.62$ for ribs 2 1/4 in. wide,

and $n = 0.69$ for ribs 1 1/2 in. wide.

Figure 2.15 shows a similar relationship between the breakdown load and the height of the rib, for heights of rib between 1 1/2 in. and 3 in., that is:

the breakdown load, Q_{cb} α 1/(height of rib)^n

where $n = 0.50$ for ribs 1 1/2 in. wide and 3 in. wide

and $n = 0.43$ for ribs 2 1/4 in. wide.

As indicated in Figure 2.12, the moduli of specimens with ribs 1 1/2 in. wide show little variation with change in height between 1 1/2

in. and 3 in. In Figure 2.14, only values for specimens with ribs 3 in. wide, and ribs 2 1/4 in. wide are plotted. As before the relationship is:

the modulus, $k \propto 1/(\text{height of rib})^n$

where $n = 0.50$ for ribs 3 in. wide

and $n = 0.53$ for ribs 2 1/4 in. wide

To obtain a graphical representation of the combined effect of the two parameters, height and width of ribs, Figures 2.16, 2.17 and 2.18 were drawn. In all cases, the 3/4 in. deep ribs fall above the trend indicated by the deeper specimens. This is particularly noticeable with the results from specimens with 1 1/2 in. wide and 2 1/4 in. wide ribs of 3/4 in. high.

The trends indicated by the push - out tests may be written in the following form:

$$\text{maximum load (kips)} = A_1 + B_1 \frac{w^2}{\sqrt{h}}$$

where $A_1 = 3.23$

and $B_1 = 1.26$

$$\text{modulus, k (kips per inch)} = A_2 + B_2 \frac{w^2}{\sqrt{h}}$$

where $A_2 = 188$

and $B_2 = 156$

and

$$\text{breakdown load, } Q_{cb}\text{(kips)} = A_3 + B_3 \frac{w^2}{\sqrt{h}}$$

where $A_3 = 2.80$

$B_3 = 0.572$

In the above expressions w and h are the width in inches and height in inches of the concrete rib, respectively.

The above relations are presented to demonstrate the influence of the parameters, width and height of the concrete rib, on the behavior of push - out specimens. It is not meant to imply that the maximum load and the breakdown are necessarily variables of importance. Push - out tests are quite acceptable for comparison of various types of connectors, as demonstrated by SIESS, VIEST, and NEWMARK in 1952, but specific information concerning the connectors as observed in the push - out tests should only be used in composite beam analysis after their validity in beam behaviour has been confirmed. Certainly the significance of the maximum load in push - out tests is questionable, since it often corresponds to a tensile failure of the concrete slab (a type of failure not observed in composite beam tests). On the other hand, the breakdown load occurs at an acceptable stage in the testing and is more confidently accepted for comparison with beam results. The parameter, k, has an exact equivalent in the beams but the modulus given by a push - out test is generally much smaller than the modulus indicated by beam tests.

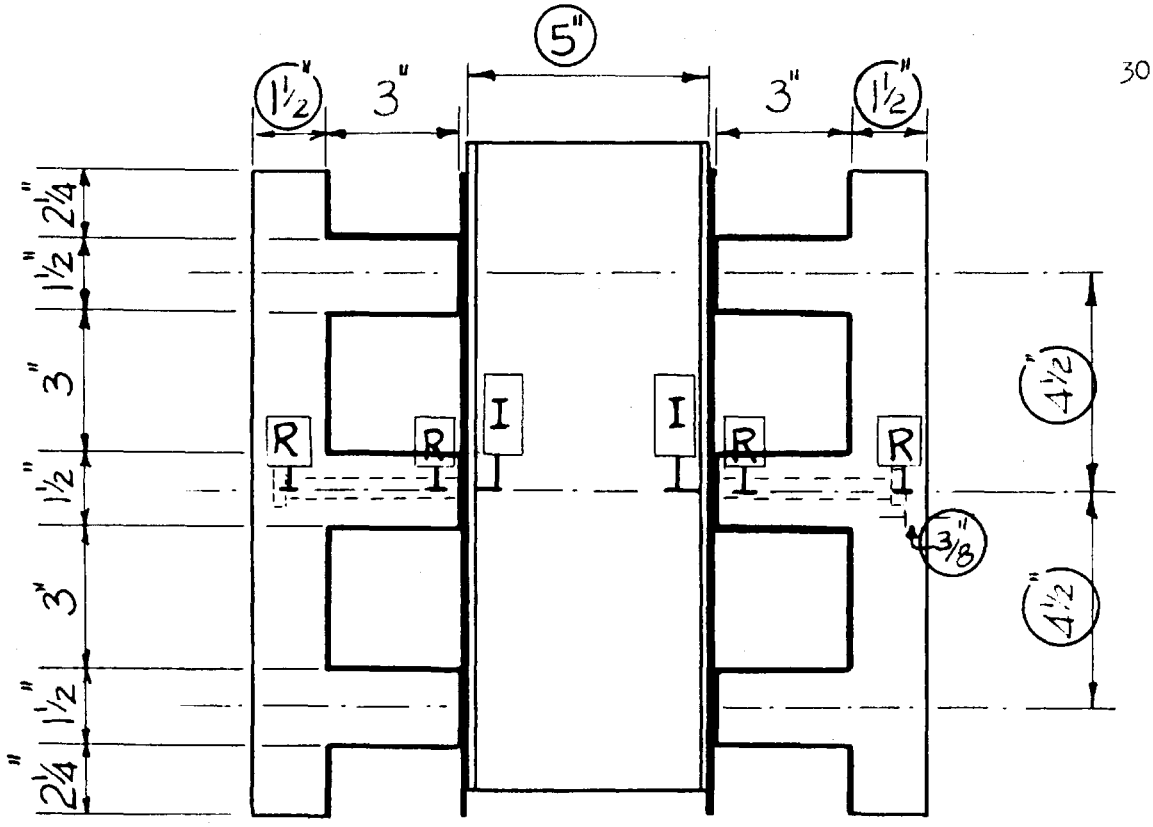

Dimensions marked ◯ are constant for all push-out specimens.

Gauges for determining relative movement due to rib rotation shown R

Instruments for determining Interfacial Slip shown I

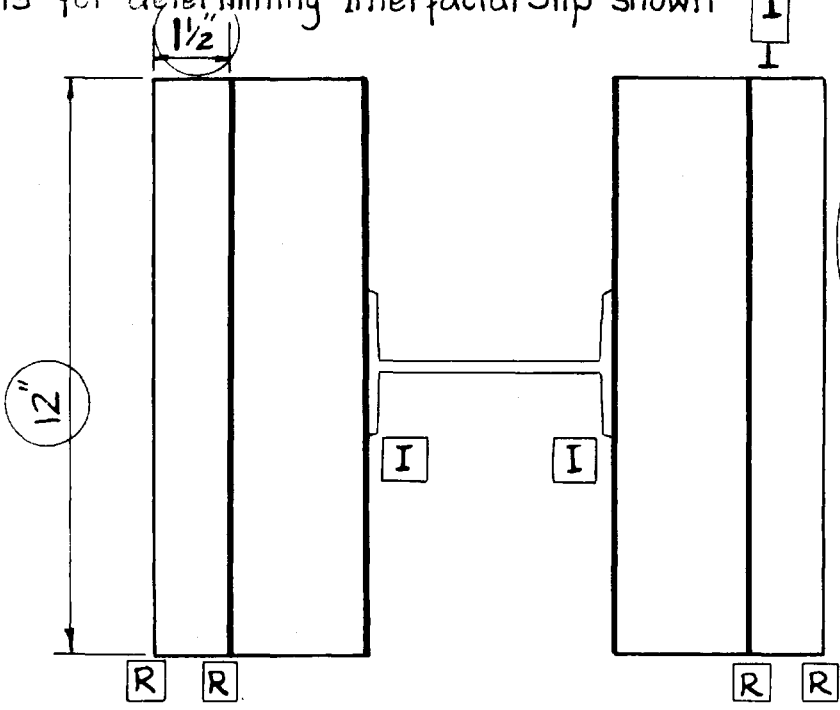

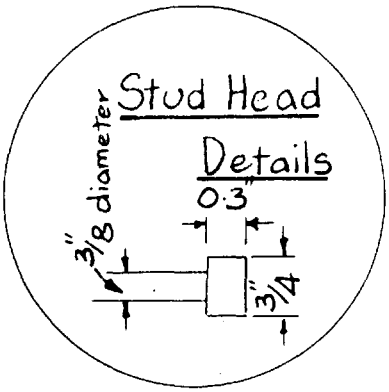

Figure 2.1 Details of Push - Out Specimens and Positions of Gauges

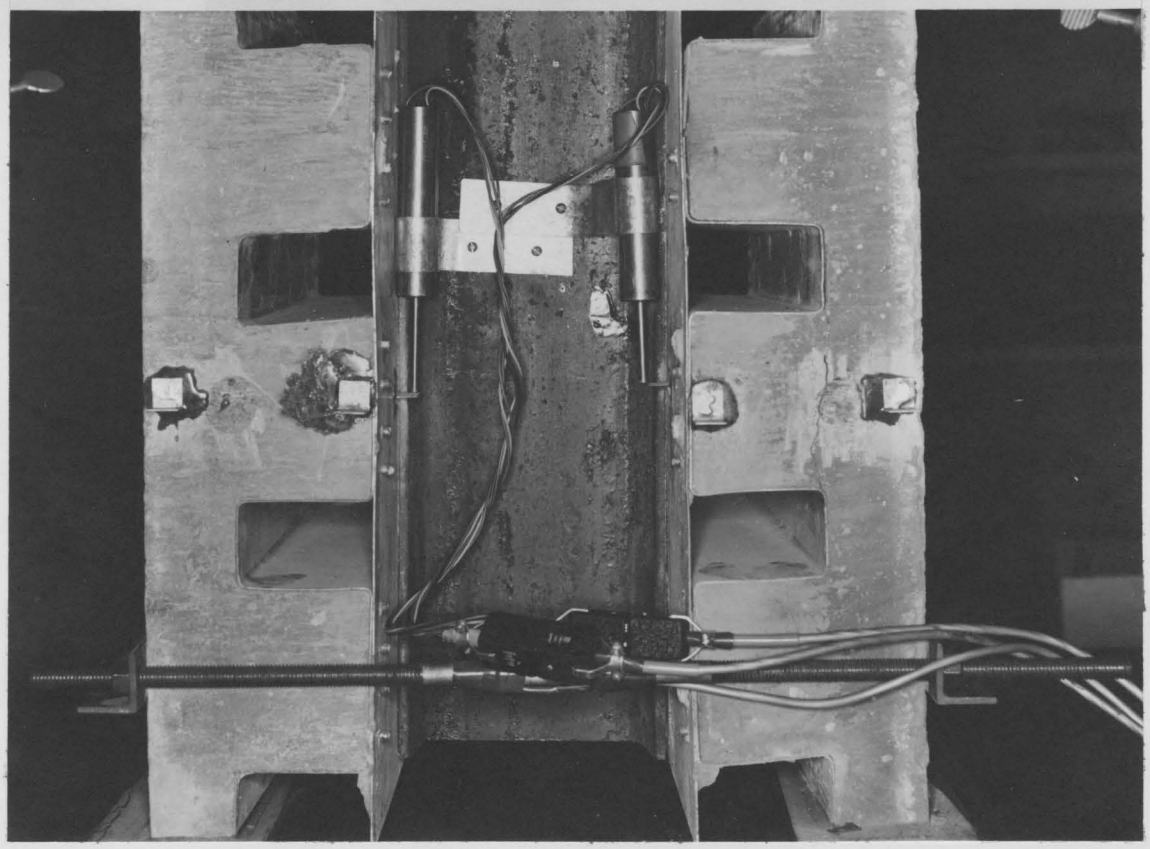

(a) Differential Transformers and Lateral Restraining Device

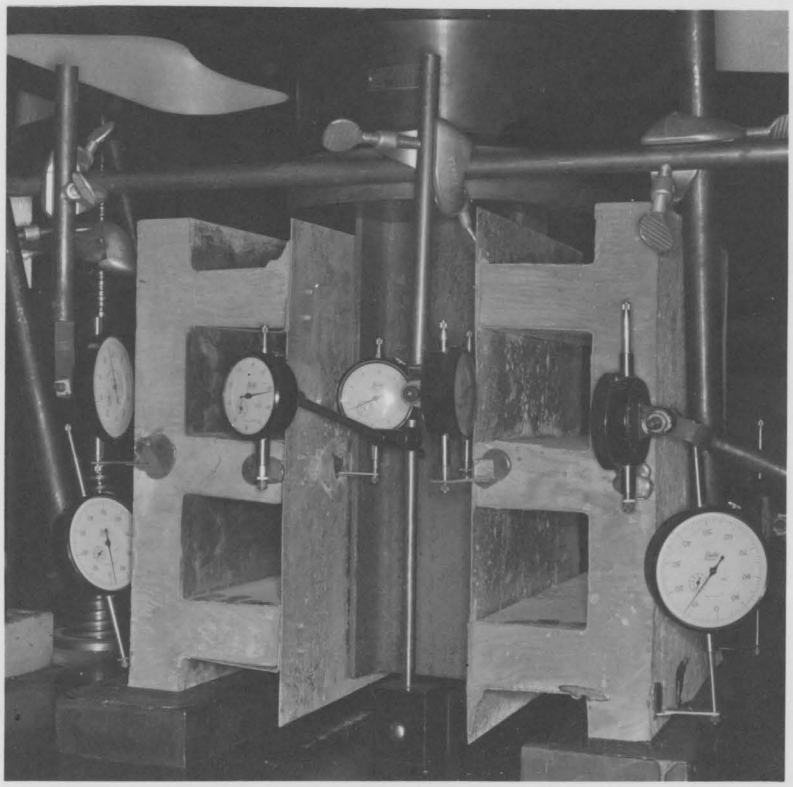

(b) Dial Gauges

Figure 2.2 Instrument Arrangement for Testing Push - Out Specimens

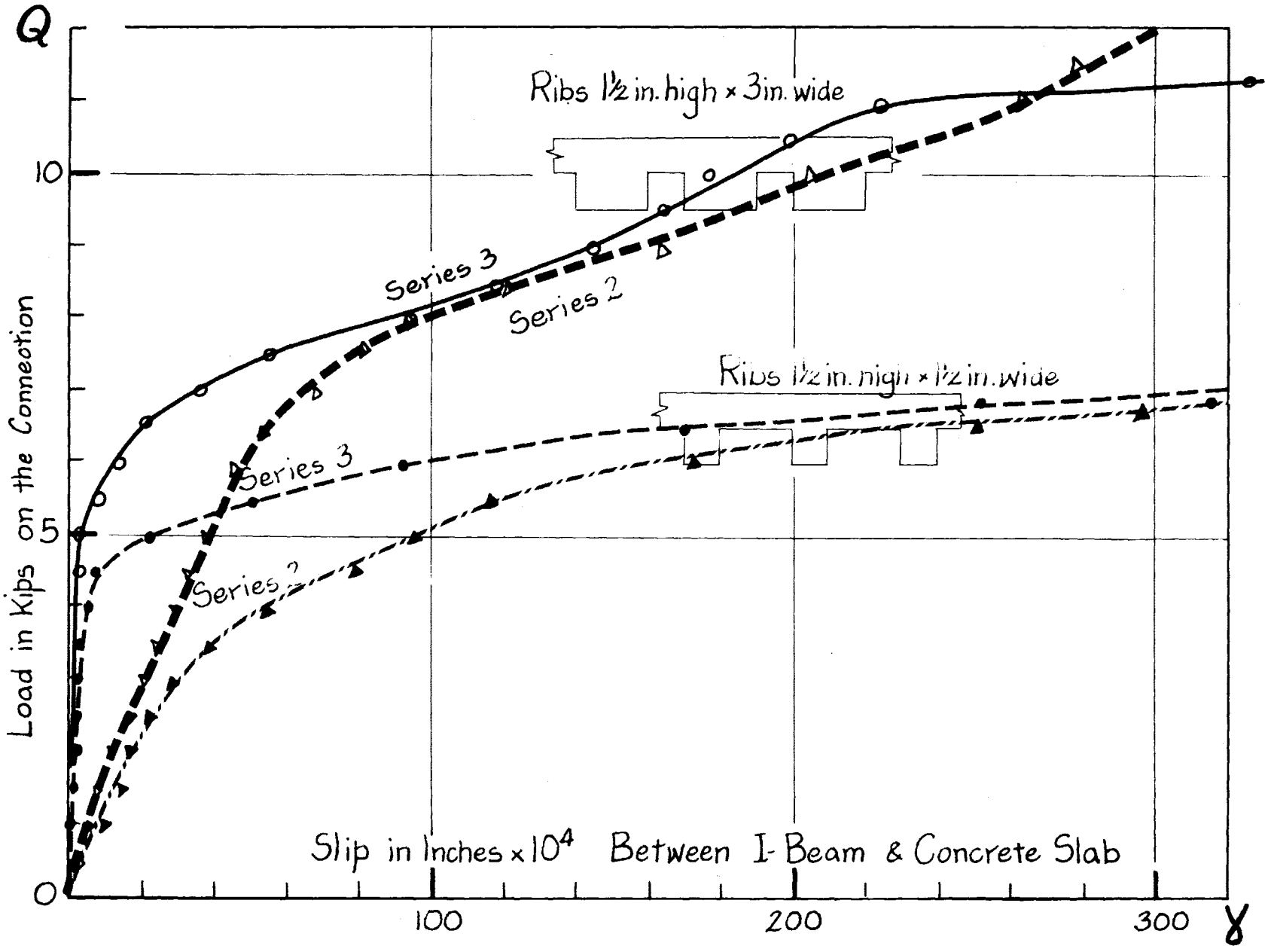

Figure 2.3 Effect of Bond on Slip Measurement

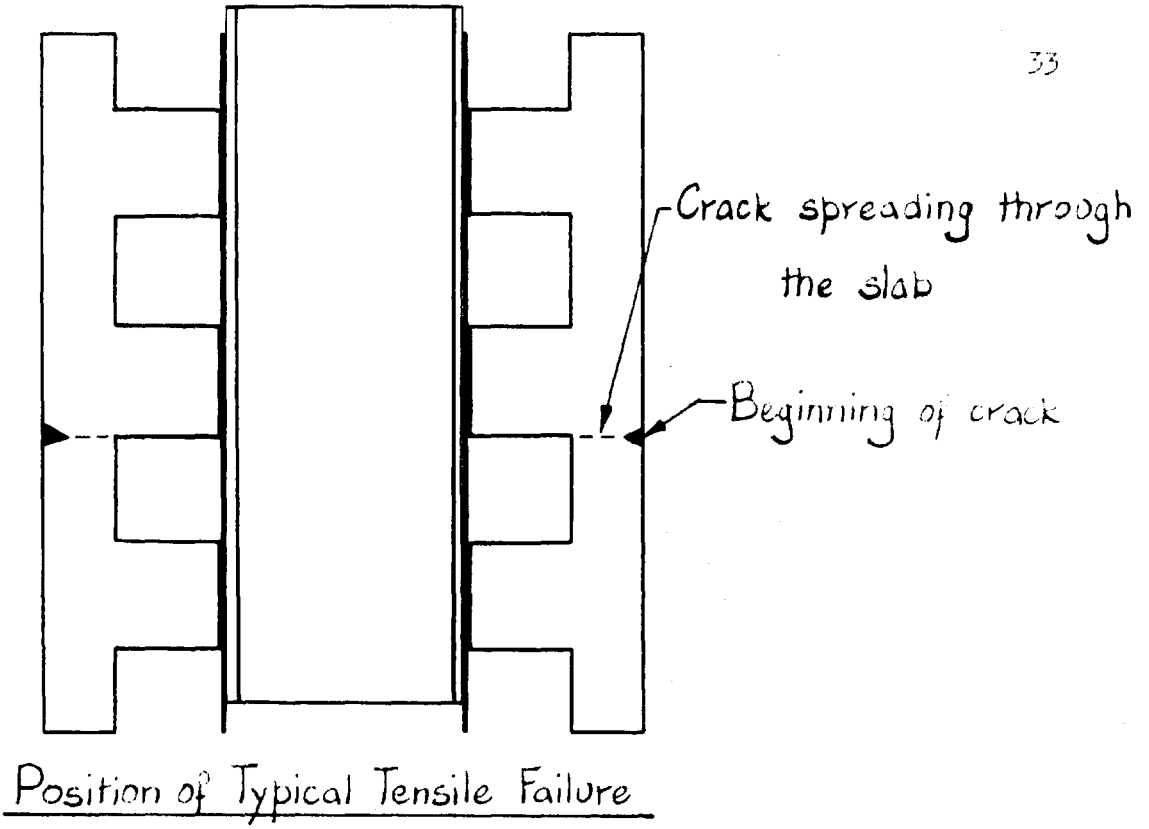

Figure 2.4 Position of Cracks at Failure of Push - Out Specimens

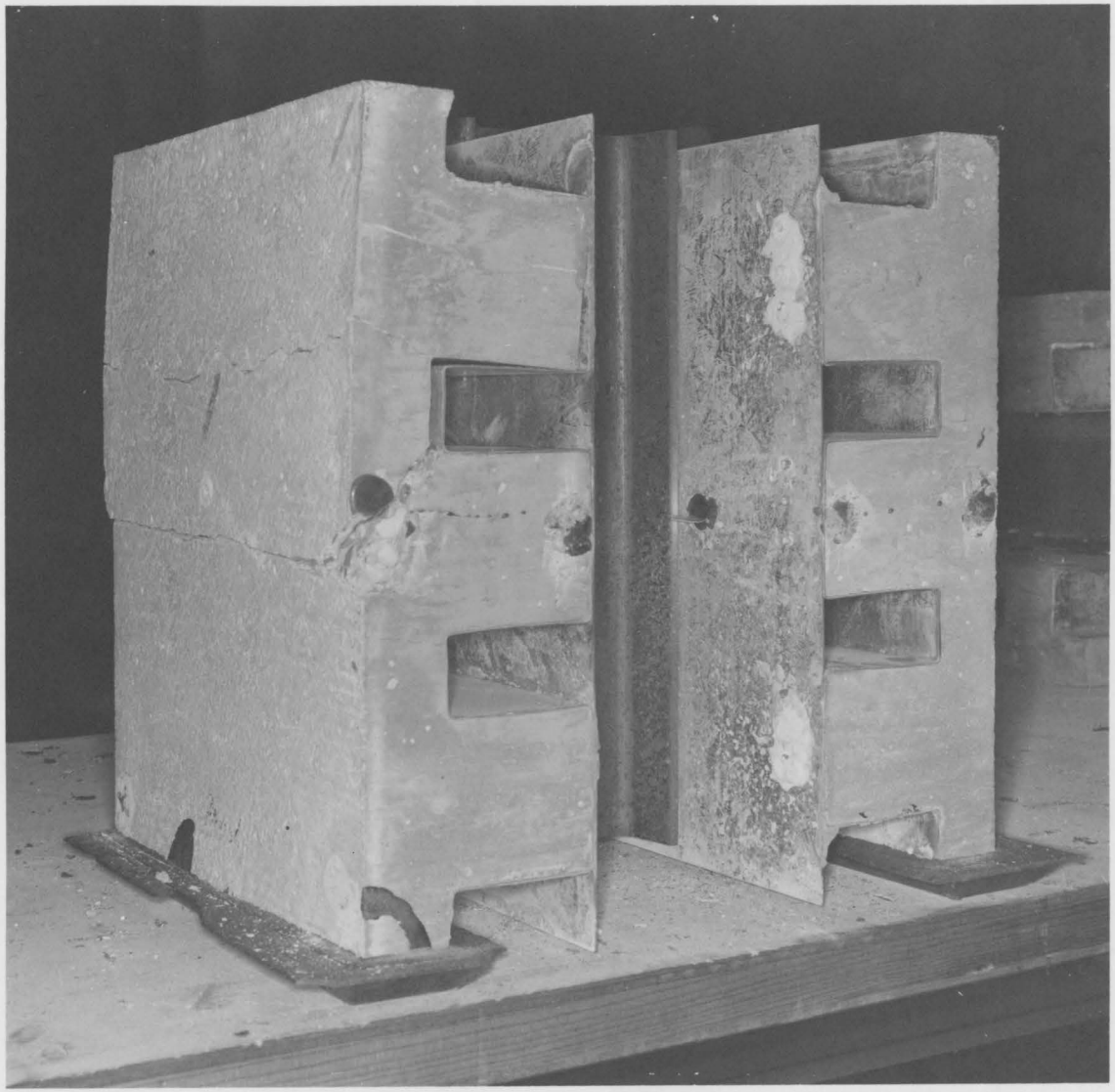

Figure 2.5 Push - Out Specimen, Failure due to Tensile Cracking of Concrete Slab

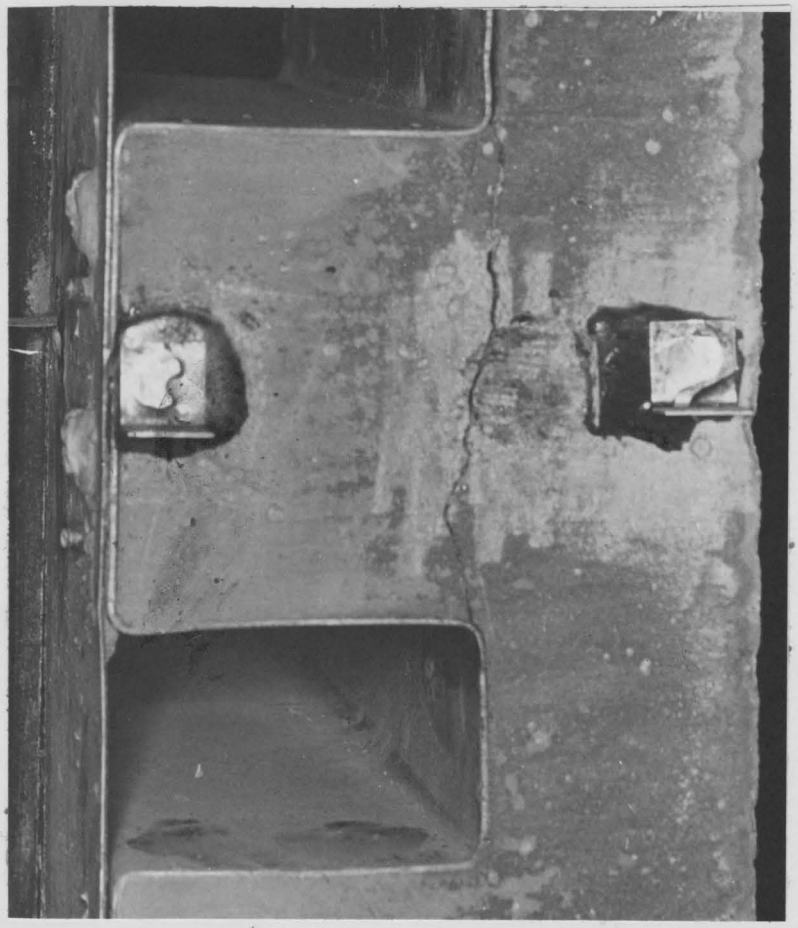

(a) Cracking of Concrete Rib

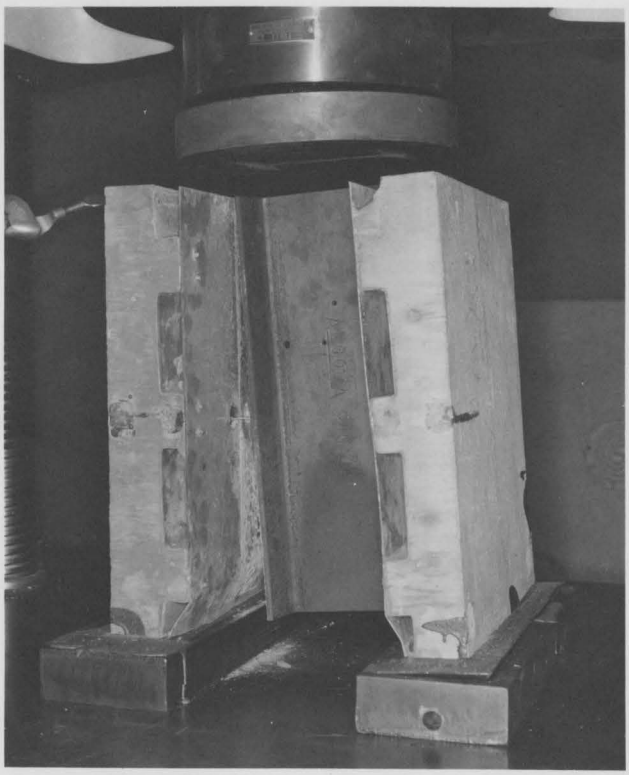

(b) Stud Failure

Figure 2.6 Push - Out Specimen Failure

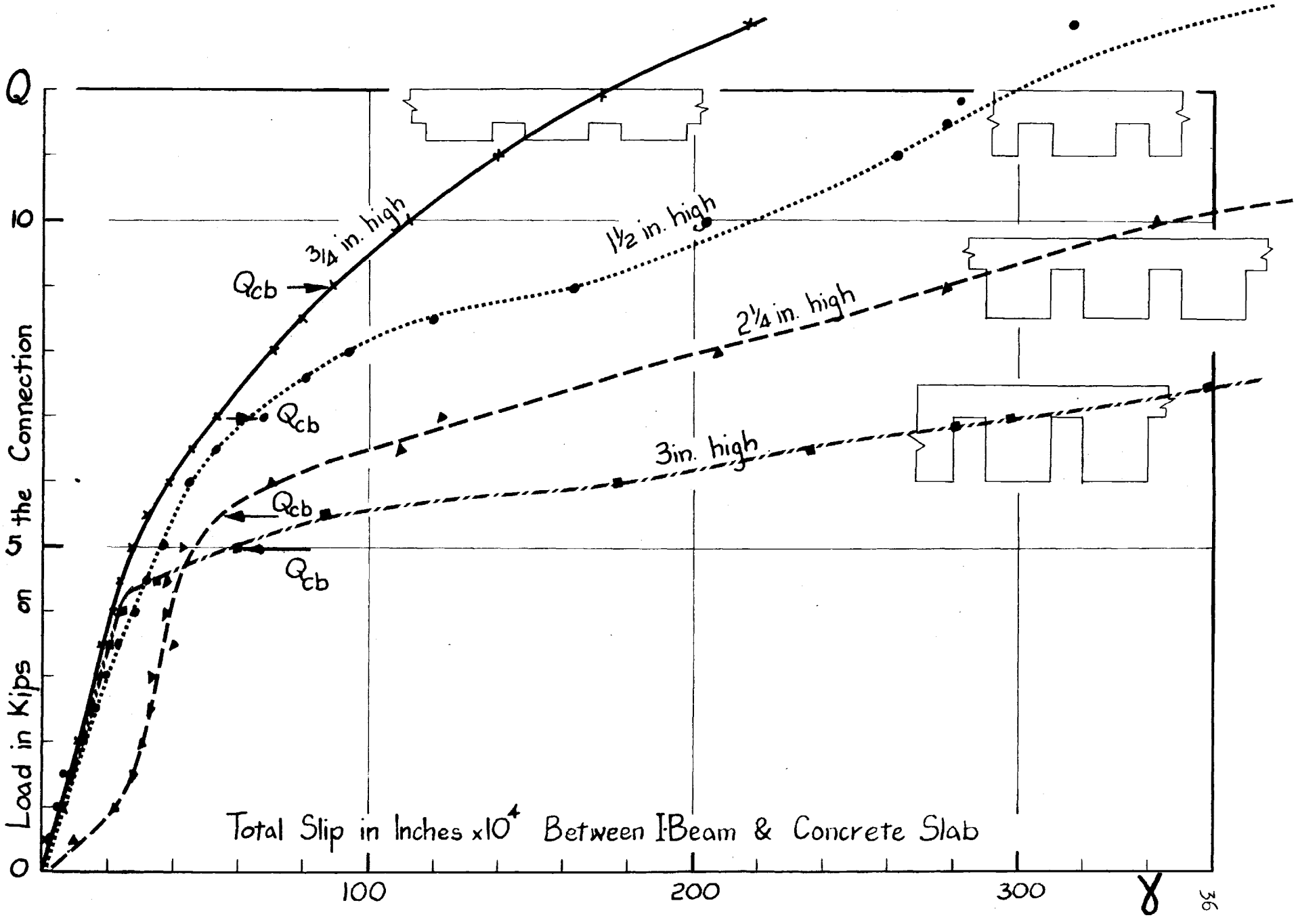

Figure 2.7 Load - Slip Curves for Specimens with Ribs 3 in. Wide

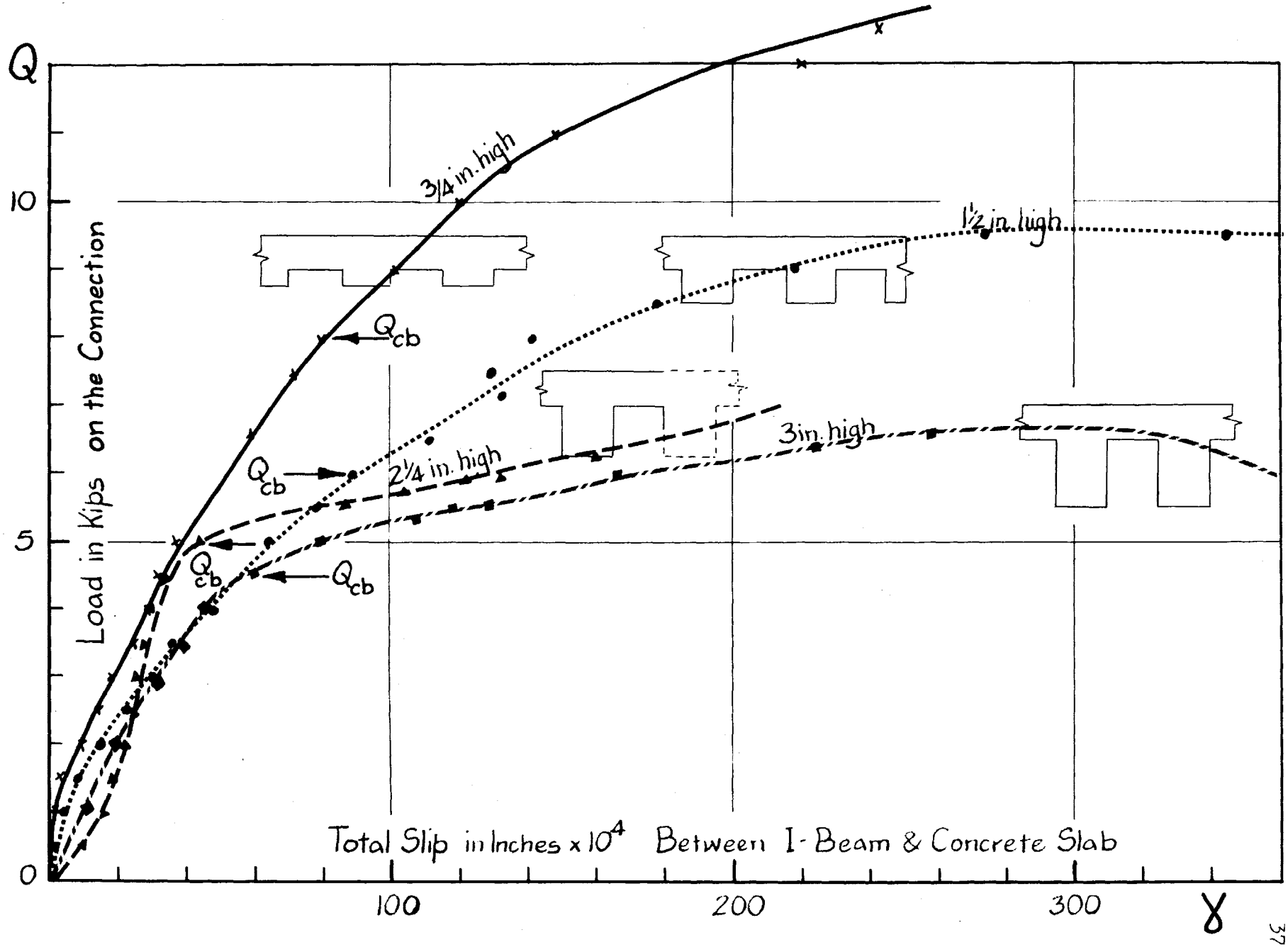

Figure 2.8 Load - Slip Curves for Specimens with Ribs 2 1/4 in. Wide

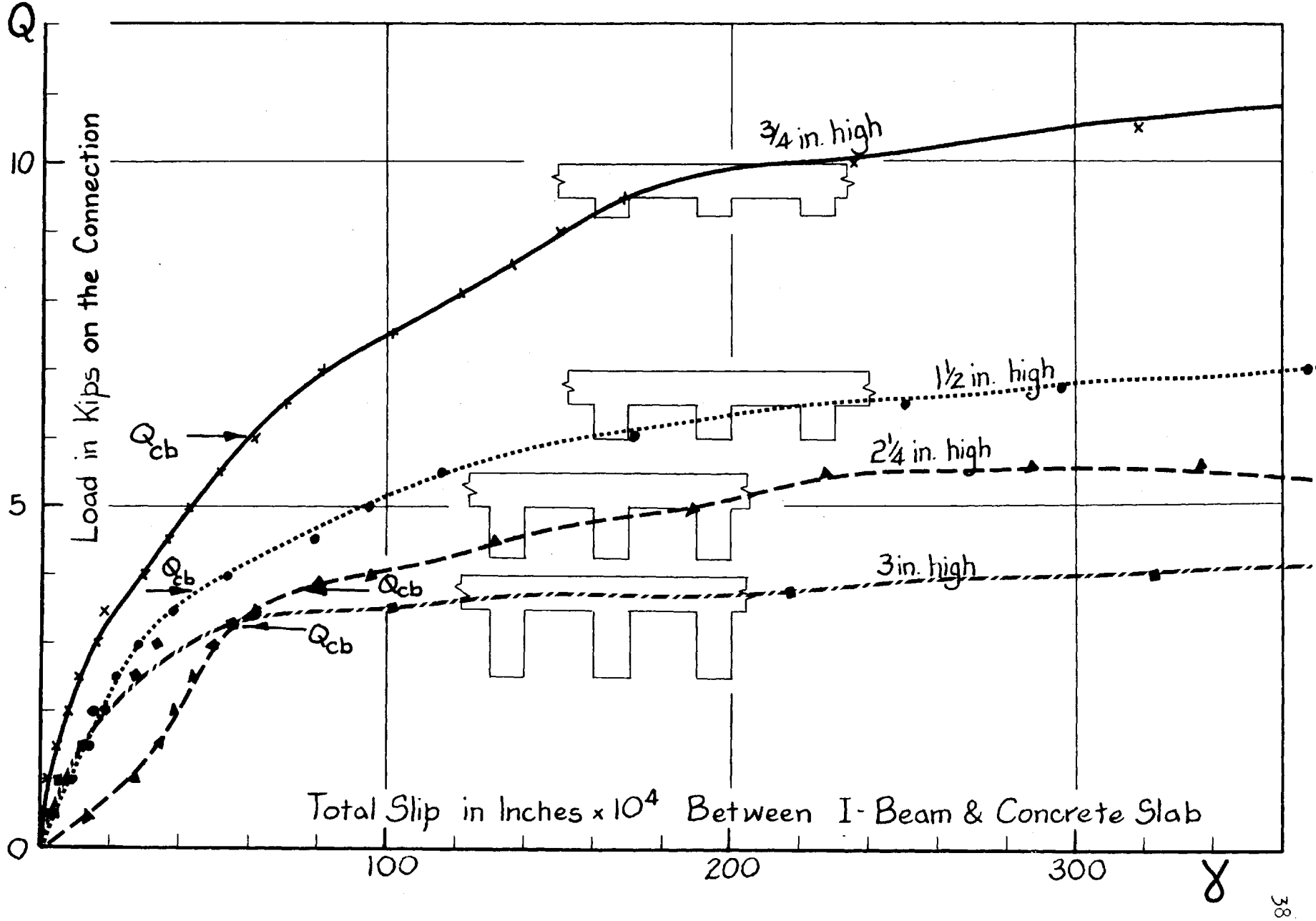

Figure 2.9 Load - Slip Curves for Specimens with Ribs 1 1/2 in. Wide

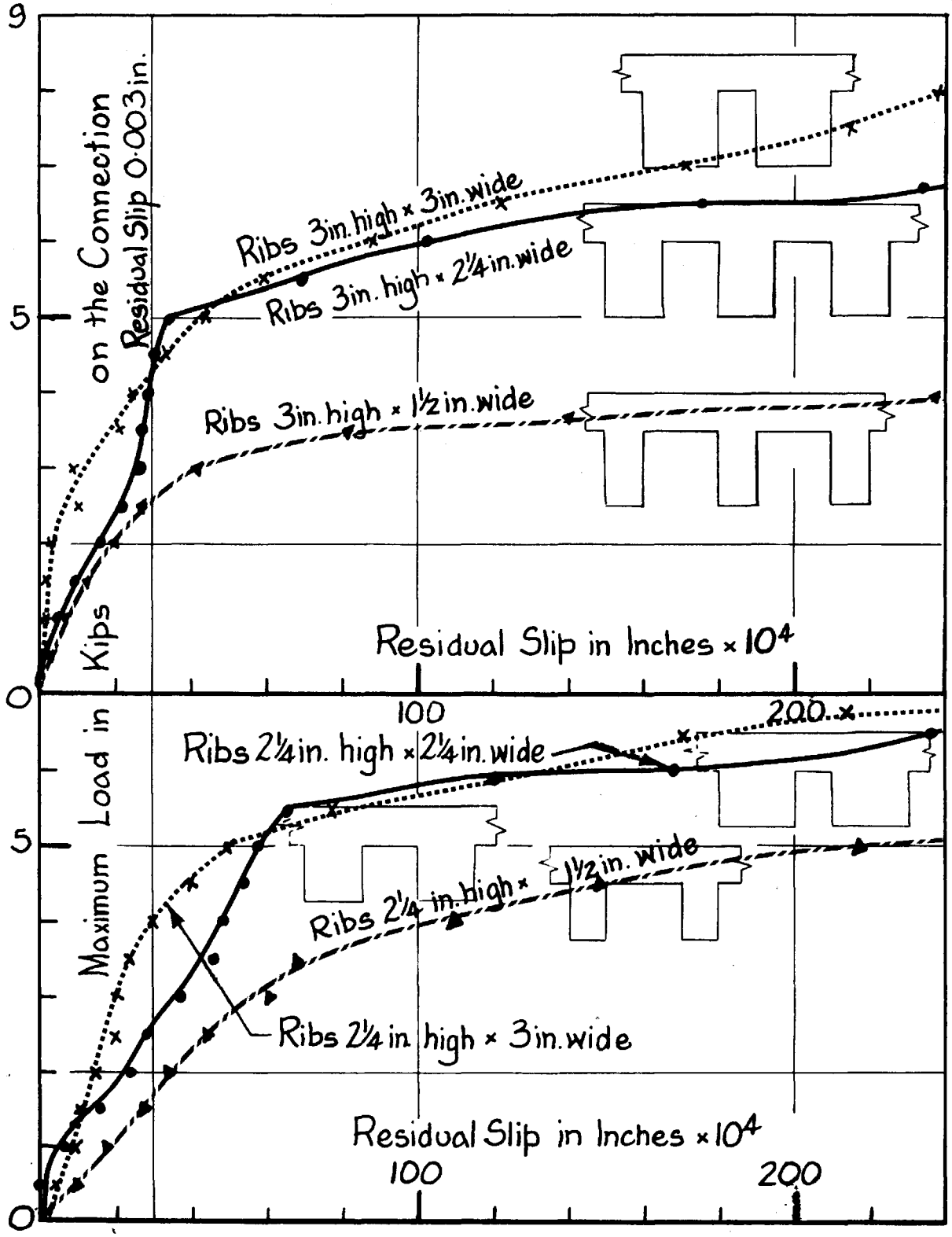

Figure 2.10 Residual Slip - Load Curves

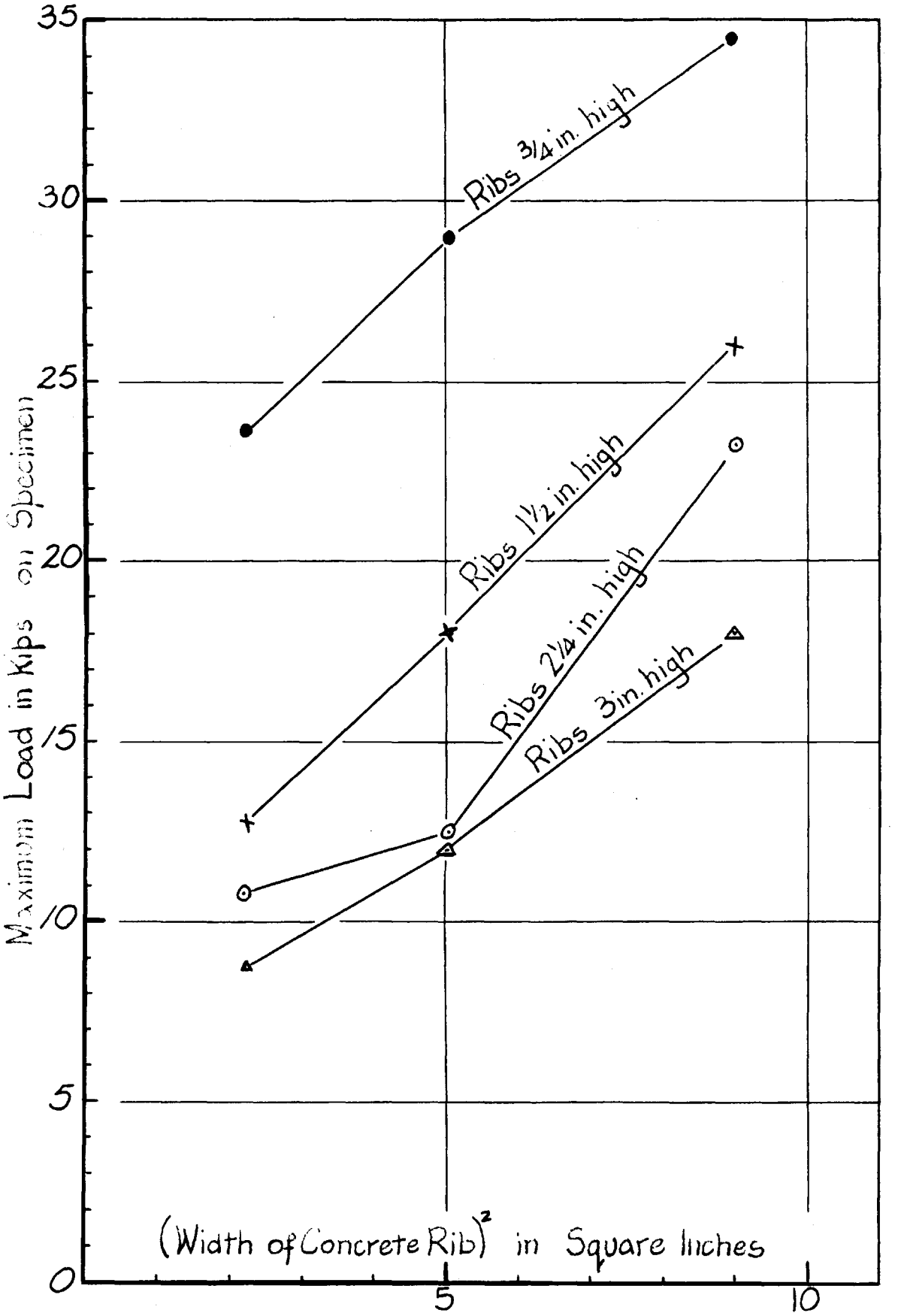

Figure 2.11 Effect of Width of Concrete Rib on Maximum Load

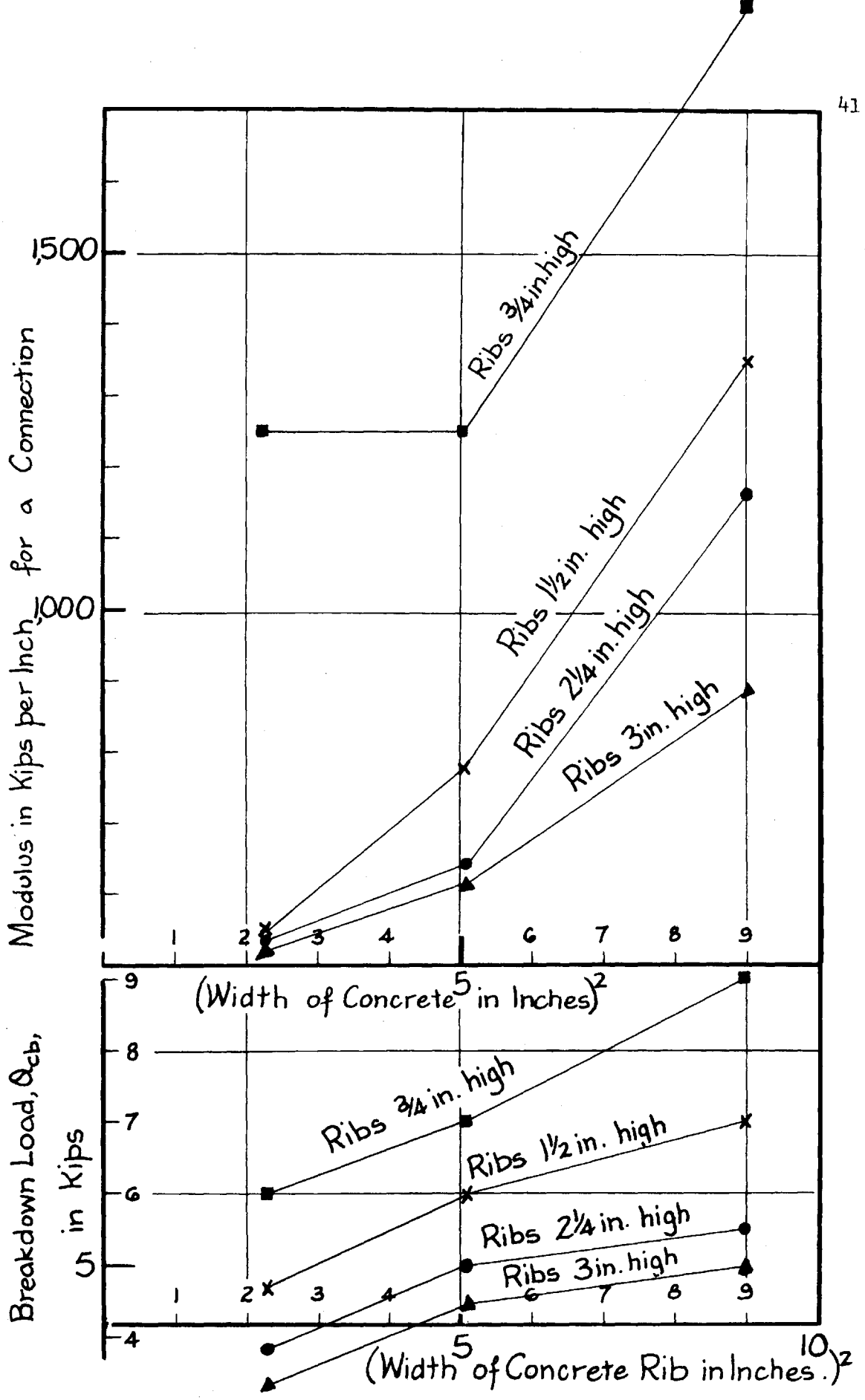

Figure 2.12 Effect of Width of Concrete Rib on Modulus and Breakdown Load

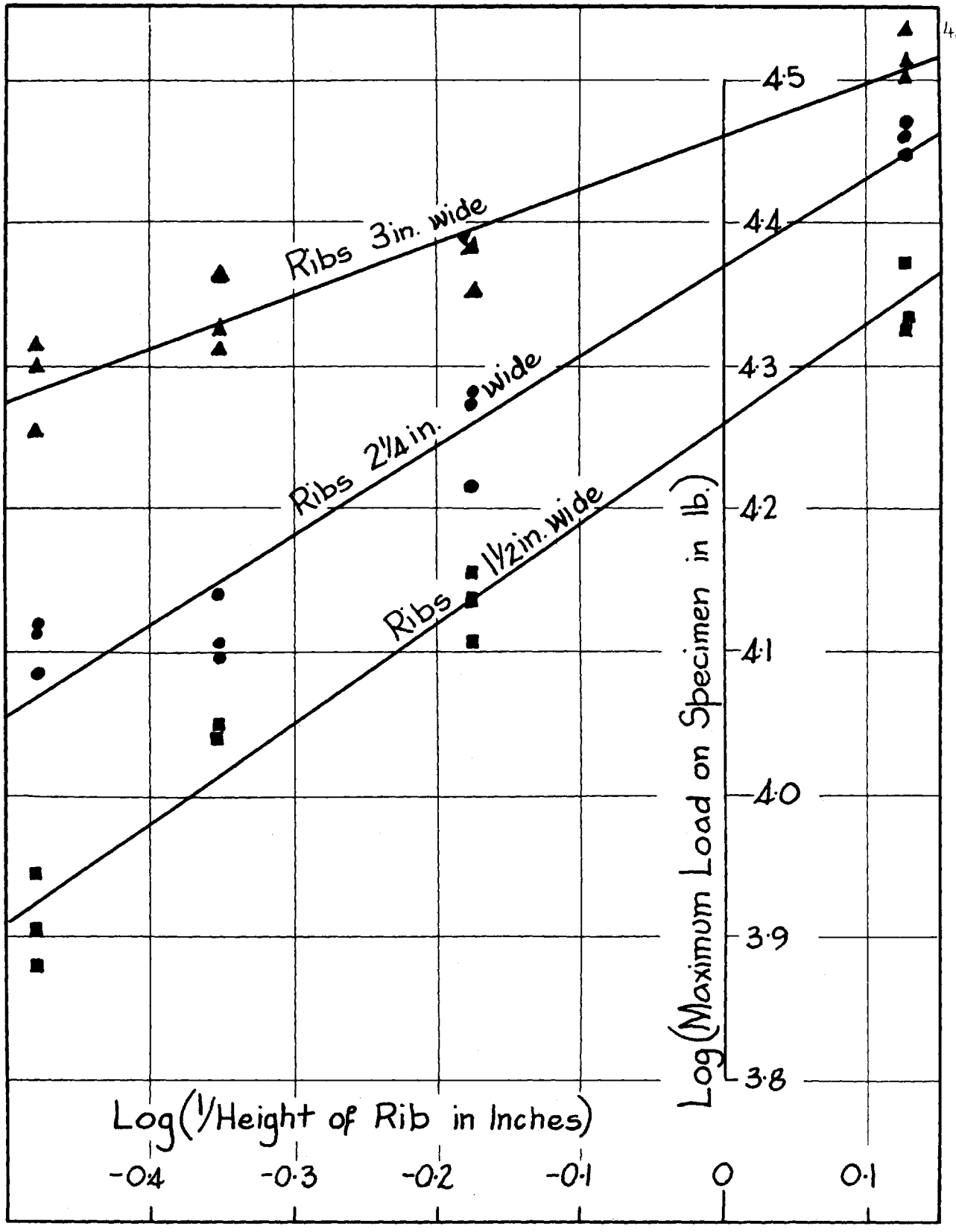

Figure 2.13 Effect of Height of Concrete Rib on Maximum Load

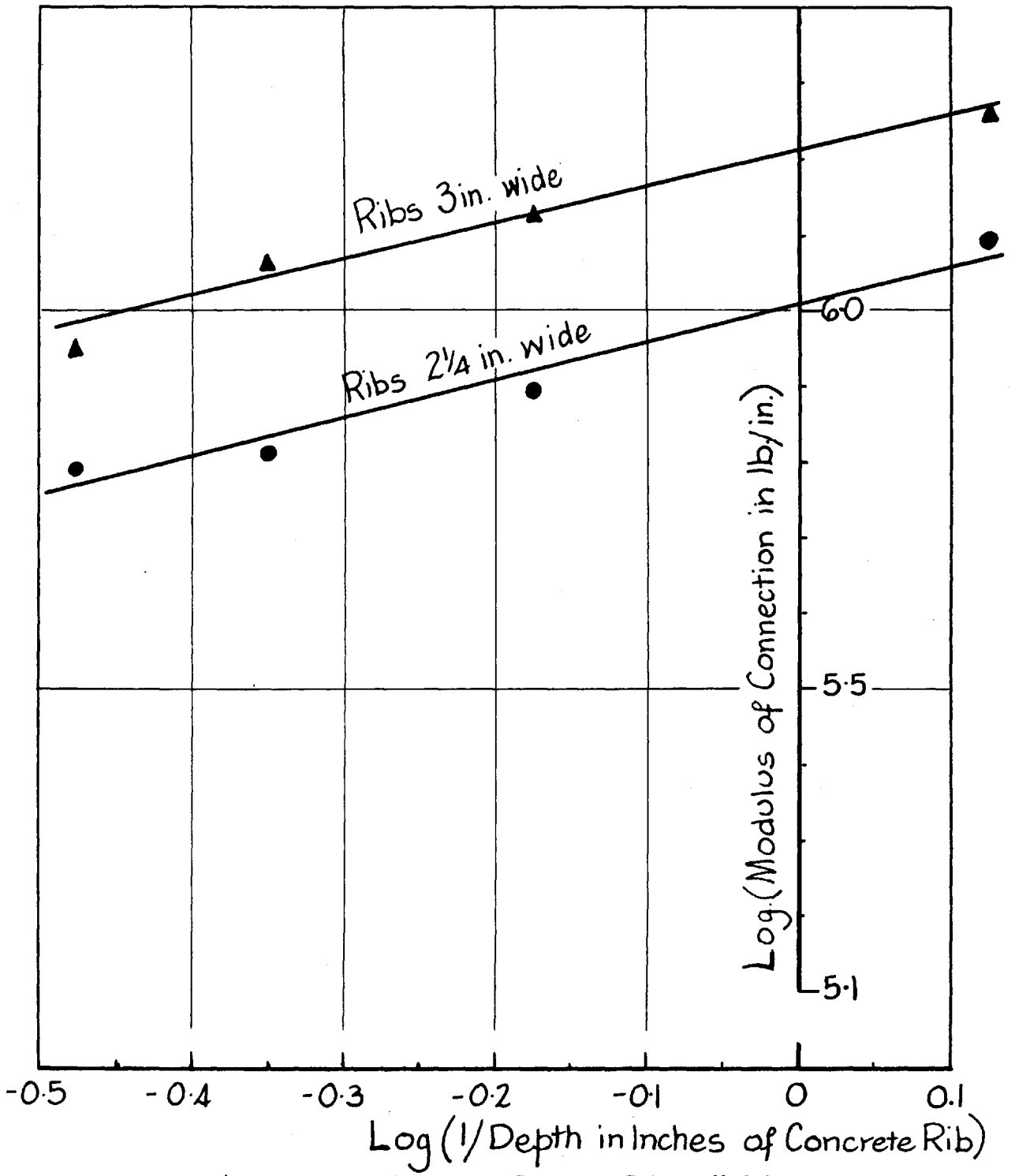

Figure 2.14 Effect of Height of Concrete Rib on Modulus

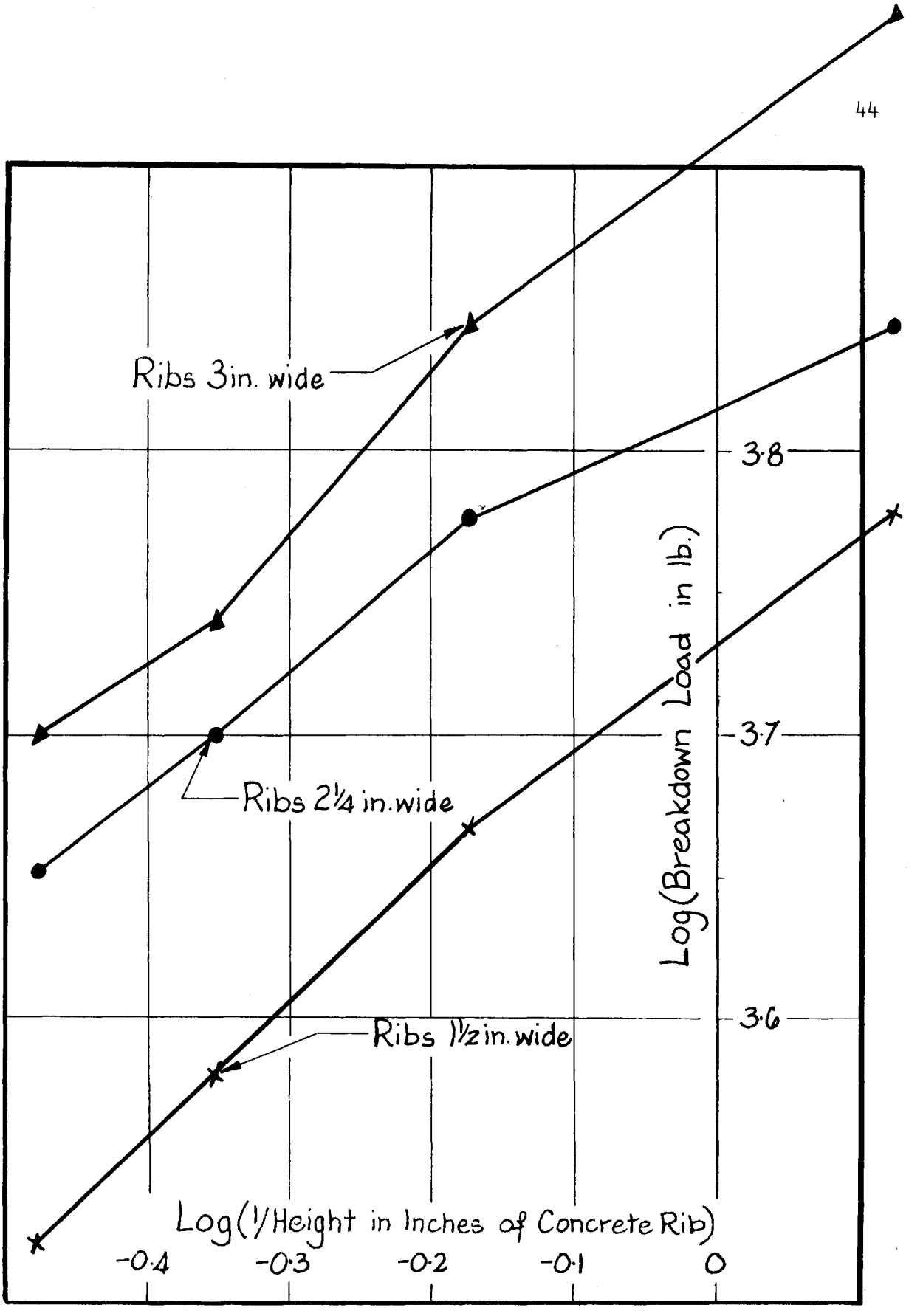

Figure 2.15 Effect of Height of Concrete Rib on Breakdown Load

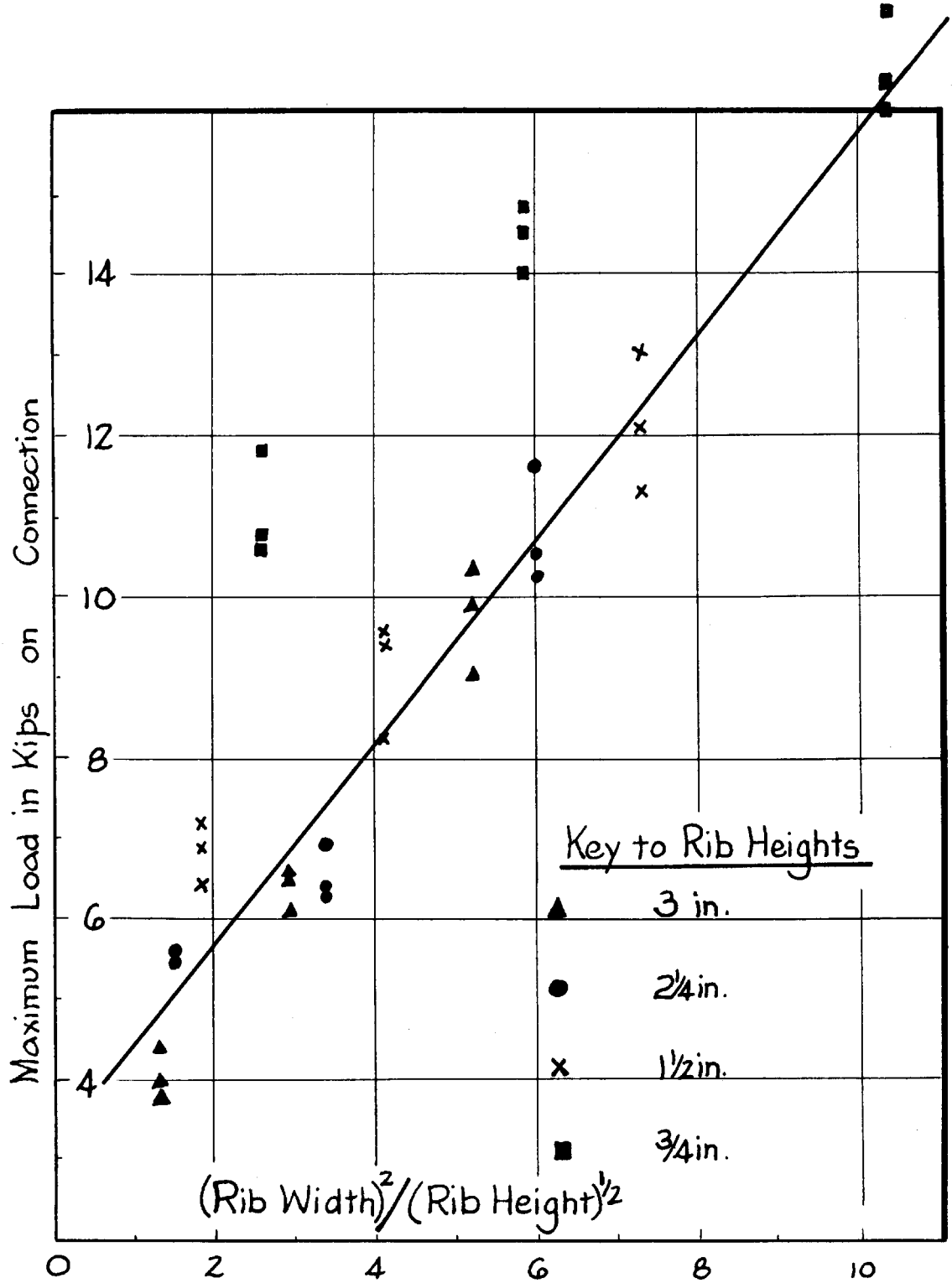

Figure 2.16 Combined Effect of Width and Height of Concrete Rib on Maximum Load

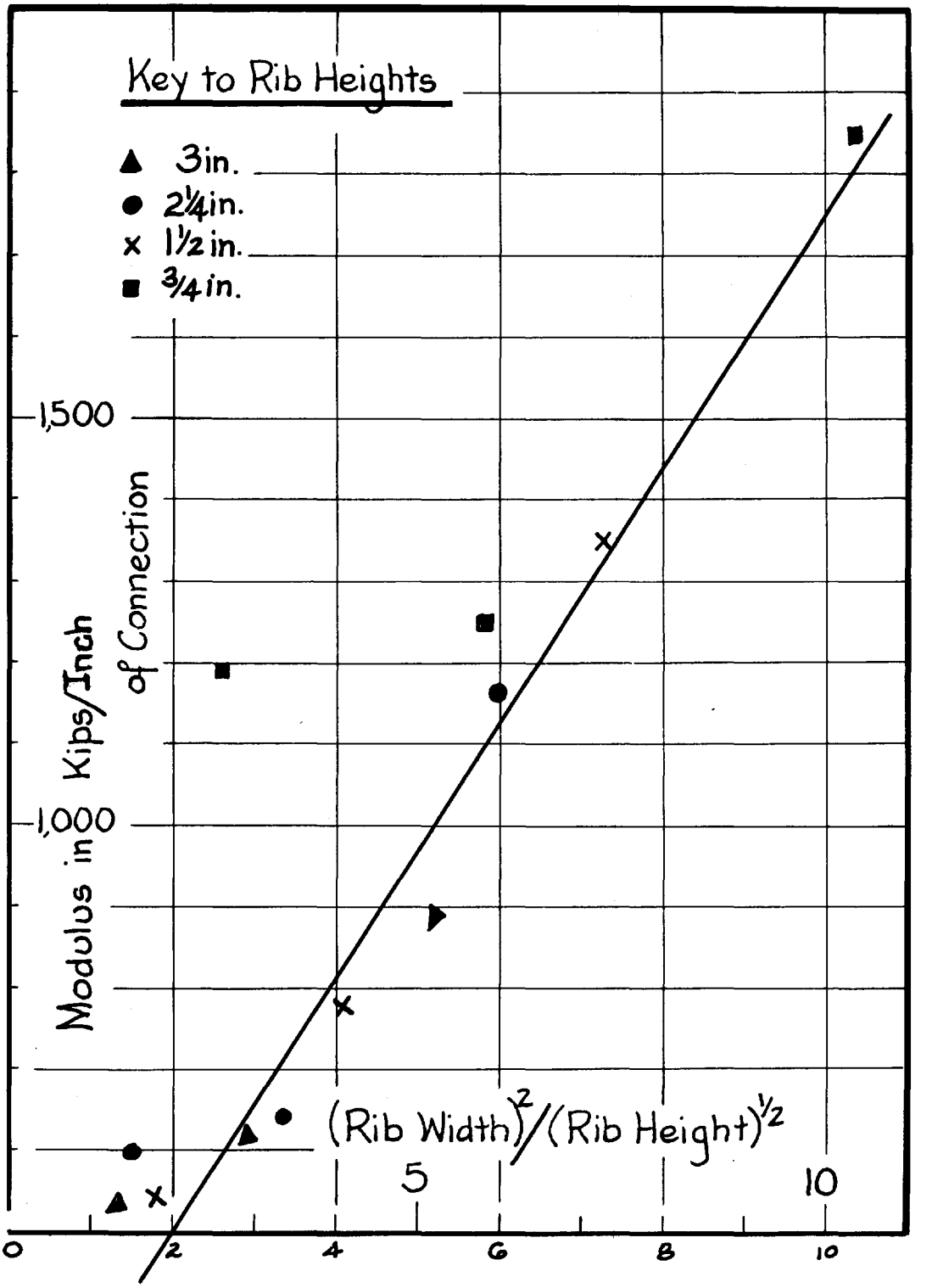

Figure 7.17 Combined Effect of Width and Height of Concrete Rib on Modulus

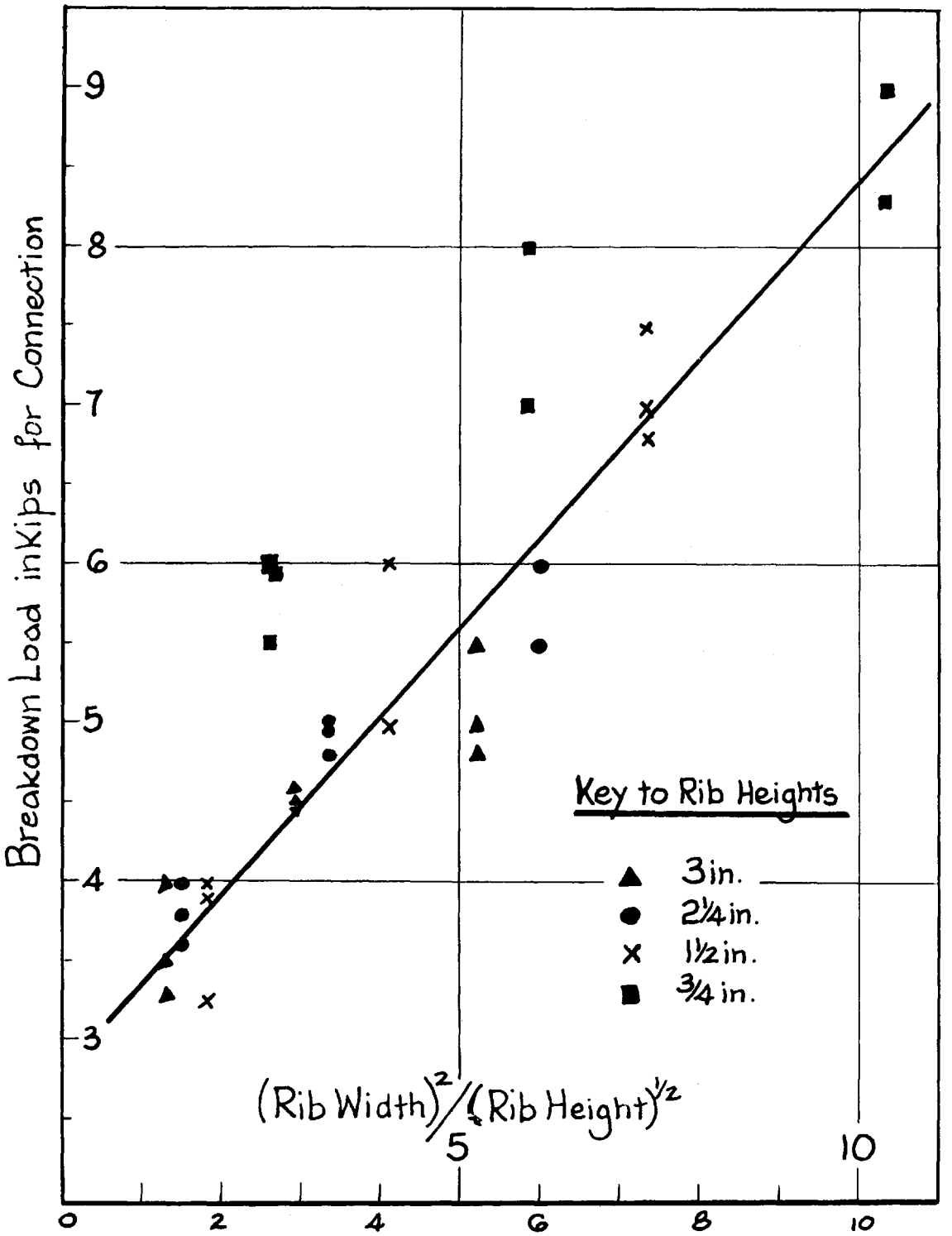

Figure 3.13 Combined Effect of Width and Height of Concrete Rib on Breakdown Load

CHAPTER 3

TESTS OF COMPOSITE CELLULAR T - Beams

3.1 Description of Specimens

Three composite cellular T - beams were tested for the purpose of investigating the influence of cell geometry on the behaviour of composite cellular beams. The principal variables in the T - beams were the cell and rib dimensions. These together with other beam details are listed in Table 3.1. The dimensions of the ribs were 2 1/4 in. high by 1 1/2 in. wide for the beam known as beam BI, 2 1/4 in. high by 2 1/4 in. wide for beam BII, and 3 in. high by 1 1/2 in wide for beam BIII.

The form, materials and manufacture as described for the push - out specimens applies to the composite beams. However, in the beams the cellular slab was connected through each rib to the flange of the I - beams by pairs of 3/8 in. diameter studs. The longitudinal spacing of the studs was 4 1/2 in. The slabs were 24 in wide and contained nominal shrinkage reinforcement. The longitudinal reinforcement was six bars of 1/8 in. diameter at 4 in. centres, placed symmetrically with respect to the centre of the slab. The lateral reinforcement was three bars of 1/8 in. diameter. All reinforcement had a minimum concrete cover of 3/8 in. The results of tests on the concrete test cylinders cast at the same time as the T - beams have already been listed in Tables 2.2 and 2.3. The average values for crushing strength and modulus of elasticity at the time of beam testing were 5780 psi and 4.25×10^6 psi respectively.

TABLE 3.1

DETAILS OF COMPOSITE T - BEAMS

Beam Identification	BI	BII	BIII
Overall Length	127.5 in.	127.5 in.	127.5 in.
Steel Beam	5 in. by 3 in. at 10 lb.- Standard Beam		
Slab Thickness	1 1/2 in.	1 1/2 in.	1 1/2 in.
Slab Width	24 in.	24 in.	24 in.
Cell Width	3 in.	2 1/4 in.	3 in.
Rib Width	1 1/2 in.	2 1/4 in.	1 1/2 in.
Cell and Rib Height	2 1/4 in.	2 1/4 in.	3 in.
Connectors	Pairs of 3/8 in. diameter studs at 4 1/2 in. centres		
Length of Studs	3 3/8 in.	3 3/8 in.	4 1/8 in.

Tensile test coupons were cut from an additional length of the I - beam and the values of static yield stress and modulus of elasticity for the steel are shown in Table 3.2.

TABLE 3.2

PHYSICAL PROPERTIES OF STEEL

Location	Static Yield Stress psi	Ultimate Stress psi	Modulus of Elasticity psi
Web	40,660	62,200	28.6×10^6
Flange	38,280	62,050	28.3×10^6
Decking	40,450	62,100	28.0×10^6

3.2 Instrument and Loading Apparatus

The instrument and loading apparatus was the same for all beams. The load was applied by means of a hydraulic jack through a spreader beam and the magnitude of the load was measured by means of a load cell.

Electric strain gauges were fixed to the composite beam at six cross sections, and at four levels at each cross section. The cross sections were at 18 in. 31.5 in., and 45 in. from the beam supports. These locations of the cross - sections corresponded to points of application of load as described later. The positions of the strain gauges are indicated in Figure 3.1. Budd 1/4 in. CG - 141 - B Metal film strain gauges were used on the I - beam and the decking, and 2 in. SR - 4 A - 12 filament gauges on the concrete. Strains in the steel and decking were recorded by a Datran Digital Recorder and in the concrete by a Pico

Strain Gauge Indicator.

Longitudinal end - slip between the centre of the 1 1/2 in. slab and the top flange of the steel beam was measured at each end of the composite beam, by a dial gauge reading to 0.0001 in.

Vertical deflections were measured at the supports, at mid - span, and at distances of 45 in. from the beam supports, by dial guages reading to 0.001 in.

3.3 Test Procedure

The general procedure described below applies to beams BI, BII and BIII.

A beam was simply supported over a span of 121.5 in. with 3 in. overhangs, and loaded with a two-point load system placed symmetrically with respect to the centre of the beam. Initially, the positions of the point loads were 45 in. from the nearest supports. This loading position is referred to as LP1 and is shown in Figure 3.1. The load was applied in increments of 2 kips. Loading was increased until first yielding was recorded in the extreme fibre of the bottom flange of the beam under at least one of the load points. Loading was continued beyond this stage, until the fibre strain was at least 140% of the yield strain. The load was then released gradually. At each load increment, and at intervals during the load release, readings were taken for strain, deflections and end - slips.

The load points were then moved to new positions (LP2) which were closer to the end supports. The loading procedure described above was repeated before the load points were again moved towards the supports to position LP3. The loading cycle was repeated, after which the load

positions were returned to the previous position, LP2; to distinguish this post - yield loading from the previous one it was designated LP4. The beam was loaded continuously at LP4 until plastic hinges were formed below the load positions in the whole depth of the I - beam.

Figure 3.2 shows the beam BIII prior to testing in the position LP1. Figure 3.3 shows the same beam in the later stages of loading in the position LP4.

3.4 Test Results

A composite beam is most effecient if no slip is permitted between the slab and the beam. This represents the upper limit for the capacity of a composite beam and is known as complete interaction. At the other extreme, the beam is weakest if there is no interaction i.e. if slip can take place freely. Between these two extremes lies the behaviour of an actual composite structure. It is virtually impossible to provide shear connectors that prevent slip completely and so actual composite beams are intermediate between the two extremes and this is known as incomplete interaction. In order to compare the actual performance of a composite structure with these extremes, the measured figures are shown along side curves for no - interaction and complete interaction.

Theoretical curves for strain and deflection for incomplete interaction are also given for pusposes of comparison. These curves were computed by the theoretical solution obtained by Newmark in 1943 and fully reported by SIESS, VIEST, and NEWMARK in 1952. This theory is presented in the Appendix, with the solution for the case of a beam subjected to a two point load system. In brief, the experimental observations

for end - slips and corresponding loads, are used to evaluate for the end - connections the value of 1/C, a coefficient indicating the degree of interaction present. This is assumed to be constant throughout the beam so that the calculations can be extended to determine the theoretical deflection at the centre of the beam and the strains at various positions within the beam.

TABLE 3.3

COMPARING THE BEHAVIOUR OF BEAMS TESTED WITH TWO - POINT LOADING AT POINTS 45 INCHES FROM EACH SUPPORT (LP1)

	Beam BI (Ribs 1 1/2" wide by 2 1/4" high)		Beam BII (Ribs 2 1/4" wide by 2 1/4" high)		Beam BIII (Ribs 1/1/2" wide by 3"(high)	
Theoretical yield moment for complete Interaction (Kip Inches) M_{yf}	438.9		437.5		503.0	
Load causing cracking of ribs in shear span (Kips)	13.70	15.25	-	21.45	11.65	12.19
∴ Moment at cracking of ribs M_{yf}	0.70	0.78	-	1.09	0.52	0.55
Load causing steel in bottom flange to yield (Kips)	14.35+	14.15+	19.65	19.65	15.65	16.65
∴ Moment at yield M_{yf}	0.74	0.73	1.01	1.01	0.70	0.74
	South shear span	North shear span	South shear span	North shear span	South shear span	North shear span

+ The yielding of the steel occurred after the cracking of the concrete ribs, (see Section 3.6).

It is hoped to illustrate that the Newmark approach gives an adequate, though conservative, description of the behaviour of composite T - beams with cellular slabs.

All theoretical calculations for complete, incomplete or no interaction are based on a T - beam cross section which makes no allowance for the concrete ribs and the steel decking.

South end and north end are used to distinguish between the ends of a beam.

The test data for composite T - beams with cellular slabs are presented in Figures 3.4 to 3.20 and Tables 3.3 and 3.4. The results were consistent in that they showed general agreement with the Newmark theory. It is considered sufficient to present results illustrating the salient features.

Table 3.3, which compares the performances of the three beams, indicates that beam BII had the highest degree of interaction. The tests of beam BII are presented in more detail than the other tests.

3.5 Beam BII

Beam BII, under test at loading position LP1, developed the theoretical yield moment for complete interaction without any signs of external cracks in the concrete ribs. The total load applied at this point was 19.65 kips. The load was increased to 21.45 kips and cracks formed in seven ribs of the north shear span but in only two ribs of the south shear span. In the north end, the ribs between the north support and up to and including the eighth rib from the support, were separated from the slab by cracks at the junctions of the ribs and the slab. In the south end, the eleventh rib from the south support was partly severed from the

slab by a diagonal crack in the slab starting from the top of the rib on the side nearest to the south support, and spreading upwards through the slab towards the load point; the third rib from the south support was completely severed from the slab by a crack at the top of the rib. Since most of the connections in the south shear span were undamaged, the south end gave a better performance than the north - end throughout the tests with load applied at positions LP2 and LP3. During tests at these positions it was evident that there was a higher degree of interaction in the south shear span than in the north shear span, because the strains and end - slips in the south end were lower than those in the north end.

Previous tests on beams with shallow ribs (e.g. ribs 1 1/2 in. high by 2 1/4 in wide) had indicated that it was possible in such beams to attain first yield of the steel in the lower flange without cracking the concrete slab; this had been demonstrated with the load first at position LP1, and then despite any deterioration in the performance of the beam due to previous load application, it had been possible to achieve the same condition with the load applied at positions LP2 and LP3.

The test on beam BII at position LP1 indicated that first yield of the steel could be achieved without the slab cracking, but when the magnitude of the load was increased by five percent above that load causing first yield, the beam was in a critical condition because the increased load together with the yielding of the steel induced cracking in the ribs. It was demonstrated that in each loading sequence at positions LP1, and LP2, definite yielding of the lower steel fibre below the corresponding load point was achieved without cracking the ribs in the south

shear span, (except for the ribs previously indicated). The ribs in the south shear span cracked during loading sequence LP3 when the extreme steel fibre strain at the load point was 1055 micro-inches per inch.

The end - slips for the beam at various stages of loading at position LP1 are listed in Table 3.4 and shown graphically in Figure 3.15. These measurements are used in the incomplete interaction theory to determine the interaction coefficient, 1/C, for the end-connections, and hence to evaluate the theoretical strains, deflections, and loads on the end - connections.

The moment - steel strain curves for beam BII are shown in Figures 3.5 and 3.6. The steel strains are those for the extreme fibre of the bottom flange at the load points. The theory for incomplete interaction indicates that the maximum steel strains will occur at this location. From the measured steel strains, it may be inferred that, in the initial stages of loading the beam functions better than a beam with complete interaction. This is theoretically impossible, and suggests that the assumption, that the effective cross - sectionmay be considered as the solid part of the slab above the ribs, is inaccurate but conservative.

Since most of the connections in the south shear were intact for load applications at positions LP2 and LP3, a good degree of interaction was anticipated in the south end. This was confirmed by the measured steel strains and is shown in Figure 3.6 where the measured strains are much smaller than the no - interaction strains.

For the test at load position LP4, the beam had damaged connections and a lower steel flange which had yielded at points below load points in previous tests. Therefore, agreement with the Newmark theory,

an elastic theory, is not to be expected. Nevertheless, it can be seen, even at this stage, that the measured steel strains are considerably less than those strains for no interaction.

The moment - concrete strain curves are shown in Figures 3.7 and 3.8. The measured strains again imply that complete interaction was achieved initially; but here, during the later stages of loading, the strains became greater than strains for complete interaction, even though at the same loads the steel strains were less than complete interaction strains. (This may be the result of assuming a constant modulus of elasticity for the concrete in the theoretical calculations.) The concrete strains shown in Figure 3.8 do not show the same agreement with the theory for incomplete interaction as the steel strains do.

In Figure 3.4, the measured deflections at midspan are compared with the theoretical deflections at midspan for complete and incomplete interaction. The deflections during loading sequence at position LP1 are greater than and within 10 percent of the measured deflections. The curves for application of load at positions LP2, LP3, and LP4 include residual deflections and the theoretical curves for incomplete interaction allow for residual slips. For these tests, the measured deflections are greater than the theoretical values; but with residual effects deducted, the incomplete interaction theory gave a conservative estimate for deflections.

3.6 Beam BI

Figures 3.9, 3.10 and 3.11 show the moment - deflection, moment - steel strain and moment - concrete strain curves for beam BI under test at loading position LP1. During this test, the concrete ribs cracked

before the lower steel fibre had yielded. The ribs cracked in the south shear span when the total load on the beam was 13.70 kips; then the load fell to 12.15 kips when the lower steel fibre strain was 1060 micro-inches per inch compared with 800 micro-inches per inch at the same load before the concrete had cracked. This indicated that due to cracking of the ribs the degree of interaction had decreased considerably. The load was increased to 14.35 kips and the lower steel fibre strain reached its yield value. With a further small increase in the magnitude of the applied load, to 15.25 kips, the ribs in the north shear span cracked. Again the load supported by the beam fell to 12.65 kips, giving a lower steel fibre strain at the north load point of 1160 micro-inches per inch compared with 865 micro-inches per inch at the same load before the north ribs had cracked. When the load was increased again to 14.15 kips, the lower steel fibre strain below the north load point reached its yield value. With further increase of load to 15.35 kips, the strains in the lower steel fibre became 1950 and 1720 micro-inches per inch below the south and north load points, respectively. The load was removed slowly and preparations made for test with the load applied at position LP2.

Since the connections of beam BI suffered extensive damage during the first test, the subsequent tests at positions LP2, LP3 and LP4 showed only small signs of composite action, but in all cases the performance was better than for no interaction.

The results of the test at position LP1 for steel strains and mid-span deflections are in good agreement with the Newmark theory for incomplete interaction. The concrete strains, as indicated in Figure 3.11, are not as satisfactory. However, for design considerations, the magnitudes of the concrete strains are generally not excessive.

3.7 Beam BIII

The moment - deflection, moment - steel strain and the moment - concrete strain curves for beam BIII under test at loading position LP1 are shown in Figures 3.12, 3.13, and 3.14, respectively.

The behaviour of this beam was similar to that of beam BI, in that the concrete ribs cracked before the steel in the lower flange of the I - beam yielded. The ribs in the south shear span cracked when the magnitude of the applied load was 11.65 kips; those in the north shear span cracked, when the magnitude of the applied load was 12.19 kips. The applied load was increased until the steel below the load points in the bottom flange yielded. This occurred at 15.65 kips and 16.65 kips for yield below the south and north load points, respectively.

The test results for application of load at position LP1 are in good agreement with the incomplete interaction theory.

3.8 Comparison of Performances of Beams

Figures 3.15 to 3.20 and Tables 3.3 to 3.6 compare the relative performances of the three beams.

The slips for the end - connections at various stages of loading at position LP1 are listed in Table 3.4, and shown graphically in Figure 3.15. Each curve in Figure 3.15 exhibits the same characteristic form, including an extended flat portion in which the load remains constant for large increases in end - slips. The curves clearly indicate the level at which the composite action is dissipated.

The figures listed in Table 3.4 are those used in the incomplete interaction theory to determine the value of the interaction coefficient 1/C. Knowing the interaction coefficient, the theoretical strains,

TABLE 3.4

MEASURED END - SLIPS FOR BEAMS BI, BII AND BIII - LOADING APPLIED AT POSITION LP1

Load (Kips)	End-Slip in Inches x 10^4 Beam BI		End-Slip in Inches x 10^4 Beam BII		End-Slip in Inches x 10^4 Beam BIII	
	North	South	North	South	North	South
0.65	1	1	0	1	2	0
2.65	7	3	2	5	5	5
4.65	12	7	5	9	9	9
6.65	18	11	8	12	$13\frac{1}{2}$	15
8.65	27	16	11	16	18	21
10.65	47	34	15	21	27+	43
12.65	76	59	20	29	382	302
14.65	109	369*	31	50	490	519
15.25	300	418	-	-	-	-
16.65	-	-	52	69		
18.65	-	-	81	89		
20.65	-	-	128	115		
21.45	-	-	250(a)	128		
21.45			336	126		

*At this stage of the loading, there was considerable cracking of the concrete ribs in the south shear span, causing load fluctuation; finally a load of 15.25 kips was applied which resulted in failure of concrete ribs in the north shear span.

(a) This corresponded to failure of the ribs in the north shear span; but the steel in the bottom flange, below the south load point, yielded before any extensive cracking was evident in the concrete of the south shear span.

+Due to slight increase in load, to total load of 11.65 kips, the concrete ribs of the south shear span cracked; at 12.19 kips, the ribs in the north shear span also failed.

deflections, and loads on the end - connections can be determined. The computed values of 1/C for each beam, are given in Table 3.5. A value of 1/C greater than 10, indicates a comparatively high degree of interaction; as the value of 1/C approaches zero the degree of interaction falls off, until at a value of zero there is no interaction. It can be seen from Tables 3.4 and 3.5 that there was a large increase in end - slips when the ribs cracked, and that at this stage the interaction coefficient dropped to a value less than 10. The computed values of 1/C denote the stage at which the connections breakdown.

There is a marked similarity between the load - slip curves of the push - out specimens as shown in Figures 2.7, 2.8, and 2.9 and the curves shown in Figure 3.15 for the load versus end - slip of the beams. It should be noted that in the latter curves, the ordinates represent load on the beam and not load on the end - connections.

Figure 3.16 shows, for each beam, the distribution of strains throughout the depth, for the same load applied to each beam at LP1. Figure 3.17 shows similar cases for applied load at LP2. Since the ribs of beam BIII have an extra height of 3/4 in. over the other beams, beam BIII is stiffer than beams BI and BII, and the measured strains are correspondingly lower in magnitude. Similarly, beam BII because of its wider ribs gives smaller strains than beam BI. Despite these small differences, the measured lower fibre strains for all beams are less than the theoretical strains for incomplete interaction.

Figure 3.16 shows clearly the effect of slip (or loss of interaction) on strains. For complete interaction the distribution is linear. Slip causes a difference in strain at the junction of the two elements, and the theoretical lines for incomplete interaction indicate this

TABLE 3.5

VARIATION OF COMPUTED INTERACTION COEFFICIENT (1/C) WITH INCREASING LOAD

Load (kips)	Beam BI - Value(1/C) North	South	Beam BII - Value (1/C) North	South	Beam BIII - Value (1/C) North	South
0.65	70.4	70.4	∞	70.4	40.0	∞
2.65	41.0	95.7	143.6	57.4	65.3	65.3
4.65	42.0	72.0	100.8	56.0	63.6	63.6
6.65	40.0	65.5	90.1	60.1	60.7	54.6
8.65	34.7	58.6	85.2	58.6	59.2	50.7
10.65	24.5	33.9	76.9	55.0	48.6	30.5
12.65	17.9	23.2	68.5	47.3	3.5+	4.7+
14.65	15.0	3.8*	51.2	31.7	3.1	2.9
15.25	5.0	3.4				
16.65			36.1	26.9		
18.65			24.9	22.6		
20.65			17.3	19.3		
21.45			9.0(a)	18.0(a)		

*Concrete ribs in the south shear span already damaged; the concrete ribs in both shear spans were damaged at 15.25 kips.

(a)Cracking of the concrete ribs in the north shear span followed, and was induced by, yielding of lower flange steel below south load point.

+Cracking of the concrete ribs in the south and north shear spans occurred when the load was 11.65 kips and 12.19 kips, respectively.

difference at the interface. As the interaction breaks down, this difference at the interface increases until strains of the magnitude of no interaction strains result. Figure 3.17 indicates that beam BIII has a low degree of interaction and the magnitudes are approaching those of no - interaction. Here the steel strain distributions for beams BI and BIII fall between the limits of complete and no interaction, and the values based on the incomplete interaction theory give the best agreement with the measured strains. The steel strains in beam BII are very close to the complete interaction line.

If the performances of the beams, with uncracked concrete ribs, are compared simply by strains or deflections under the same load, then the beam BIII is the best because it is deepest; and the beam BI is the weakest since it has narrower ribs than the beam BII. In order to draw a more equitable comparison, account must be taken of the higher potential of beam BIII, and of the influence of change of cell geometry. This is done in Figures 3.18, 3.19 and 3.20. The ordinates of the graphs are the ratios of the applied moment to the theoretical yield moments for complete interaction (i.e. the denominator of the ratio, is that moment which the beam with complete interaction would theoretically support before the steel in the lower flange yields). As anticipated, the beam BII is superior at all stages of loading. In the early stages of loading, beam BIII despite having narrower ribs than beam BII shows deflections and strains of similar magnitudes to those for beam BII. After the concrete ribs crack it can be seen that the curves deviate from the complete interaction curves. This deviation occurs earliest in the case of beam BIII. This trend is consistent and illustrates that beam BIII is the least practical design proposition.

Beam BI shows itself initially as the weakest beam because the measured deflections were greater than those for complete interaction as indicated in Figure 3.9. This suggests that a lower degree of interaction was attained in beam BI initially, possibly because of absence of bond. This feature is also indicated in the curves for strain.

Table 3.6 shows a comparison of the theoretical yield moments for complete interaction, the theoretical ultimate moments, and the maximum moments applied to the beams.

It is possible that tests prior to that at position LP4 may have caused the ultimate strength of the beam in the final test to be reduced. Nevertheless, it is concluded from Table 3.6 that, even if a composite cellular T - beam has strong connections, the optimum moment for design pusposes, which a beam could be expected to resist, should be the theoretical yield moment for complete interaction. It is highly improbably that a composite cellular beam could be designed on the basis of ultimate moment.

3.9 Summary

The significant conclusions from the T - beam tests are summarized below:

(a) In all of the beams tested, the shear connections allowed slip at even small loads. As a result complete interaction was not possible.

(b) The decking and ribs were neglected in estimating the effective slab cross section, which probably resulted in the Newmark theory giving a conservative estimate for steel fibre strains and mid - span deflections.

TABLE 3.6

MAXIMUM MOMENTS FOR BEAMS BI, BII AND BIII

	Maximum Moment Applied During Test at LP1 (Kip Inches)	Applied Moment Causing First Yield (Kip Inches)	Maximum Moment Applied in Tests LP2 - LP4 Moment (Kip Inches)	Load Position	Theoretical Yield Moment For Full Interaction (Kip Inches)	Theoretical Ultimate Moment (Kip Inches)
BI	345.4	322.9	339.4	LP4	438.9	600.0
BII	482.6	442.1	451.2	LP4	437.5	600.0
BIII	374.6	352.1	421.3	LP4	503.0	678.0

(c) The computations based on the Newmark theory gave better agreement with steel fibre strains than with the concrete slab strains. The steel fibre strains are the more important, since they are the strains which will probably control the design of this type of beam.

(d) The theoretical yield moment for complete interaction is a practical upper limit for calculations to assess design moments. Beam BII supported this moment before cracking of the concrete ribs occurred and with such a beam the theoretical yield moment for complete interaction would be a satisfactory starting point for calculating design moments. Composite cellular beams, which incorporate slender ribs, such as in beams BI and BIII, could not attain this moment, and in such cases allowance must be made for the effects of rib geometry, which weaken the connections.

(e) Beams, with connections similar to those in beams BI, BII and BIII, will not reach theoretical ultimate moment.

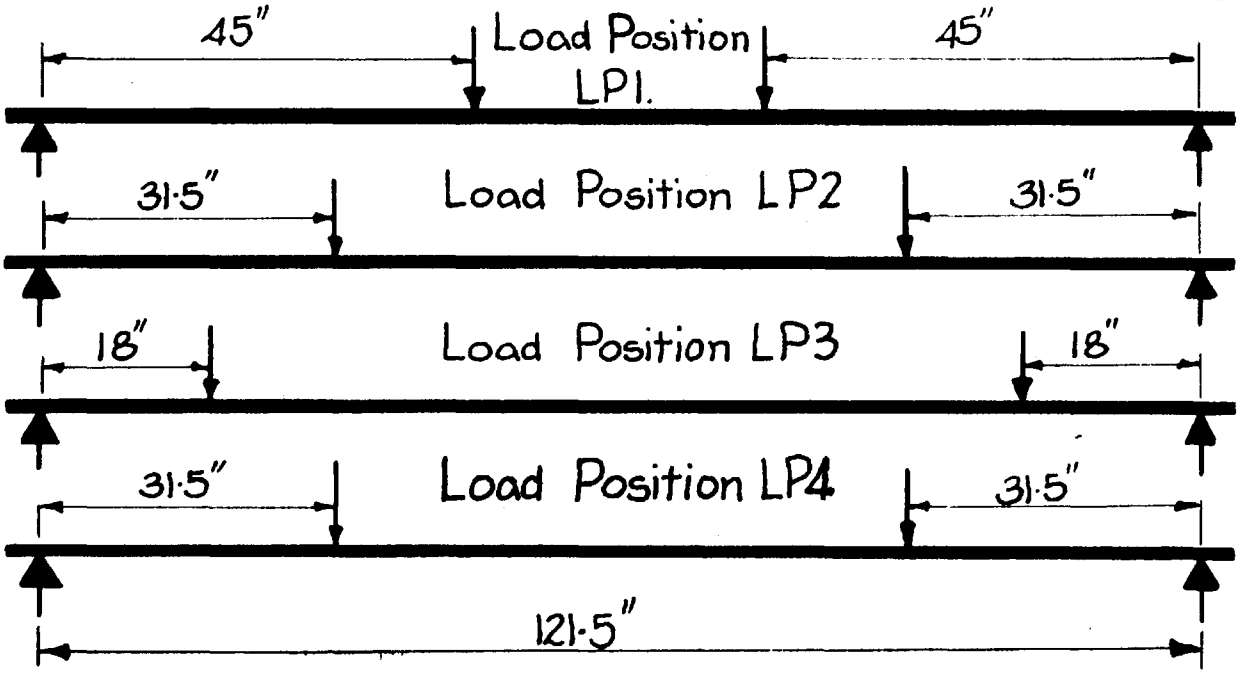

Loading Positions

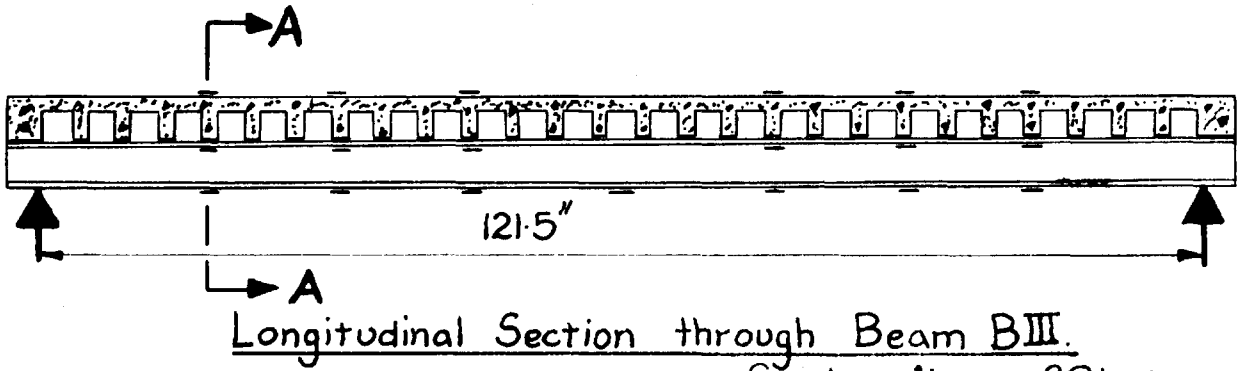

Longitudinal Section through Beam BIII.

Scale:- 1inch = 20inches

Strain Gauges shown as ⊥ & —

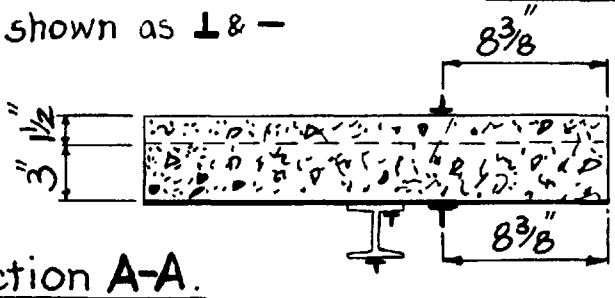

Section A-A.

Scale:- 1inch = 10inches

Figure 3.1 Strain Gauge and Loading Positions

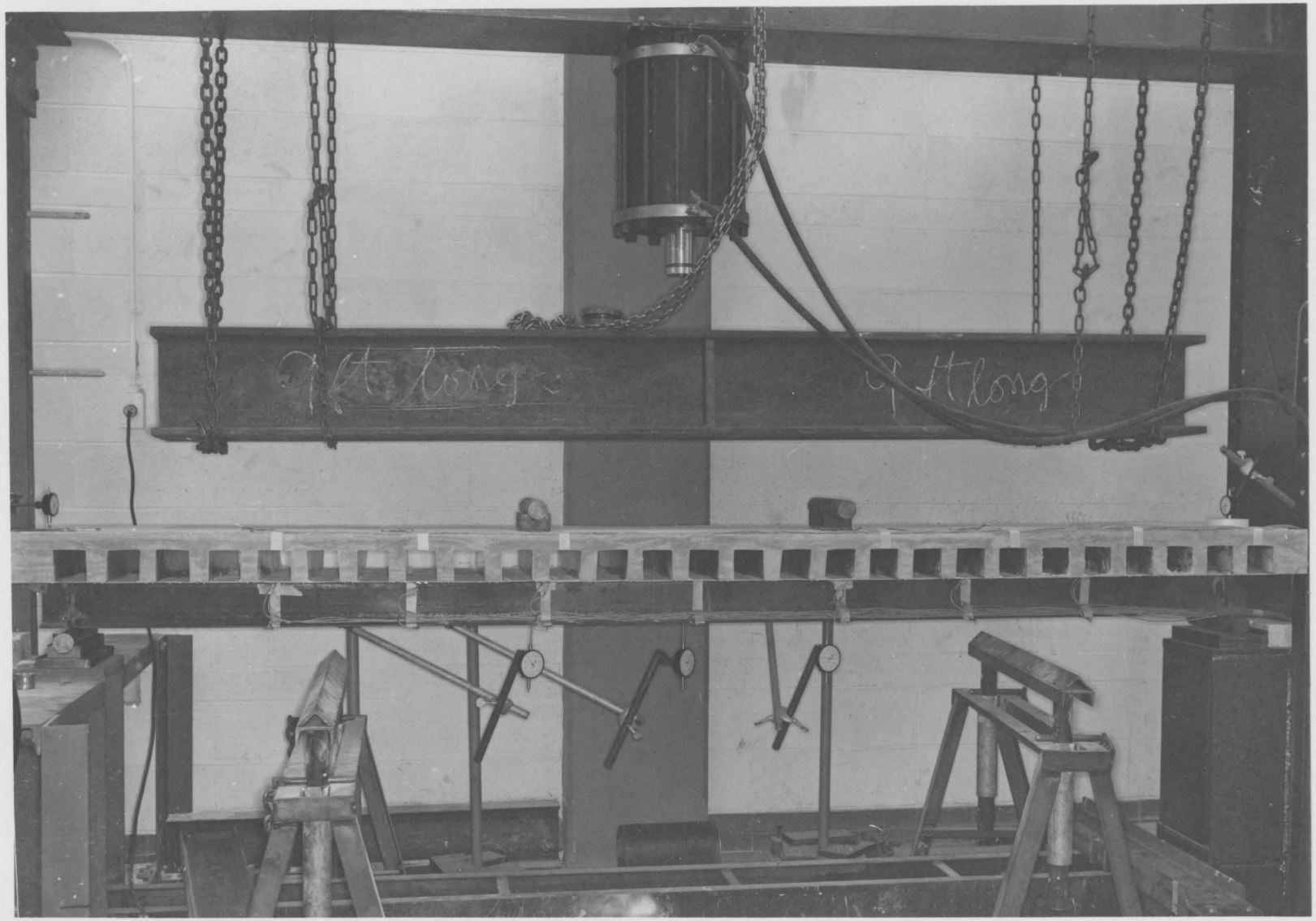

Figure 3.2 Beam BIII Ready for Testing

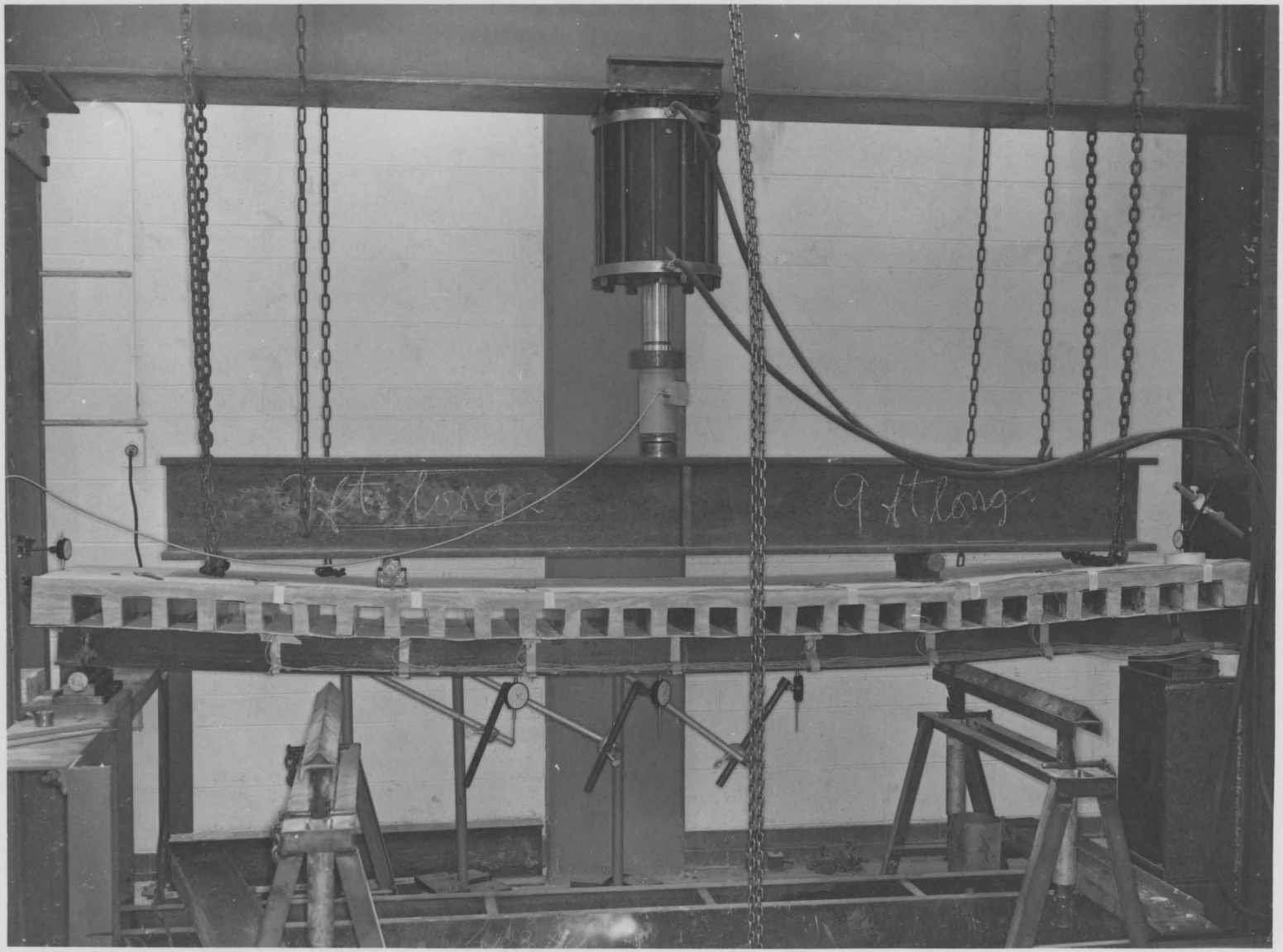

Figure 3.3 Beam BIII Under Test at Loading Position LP4

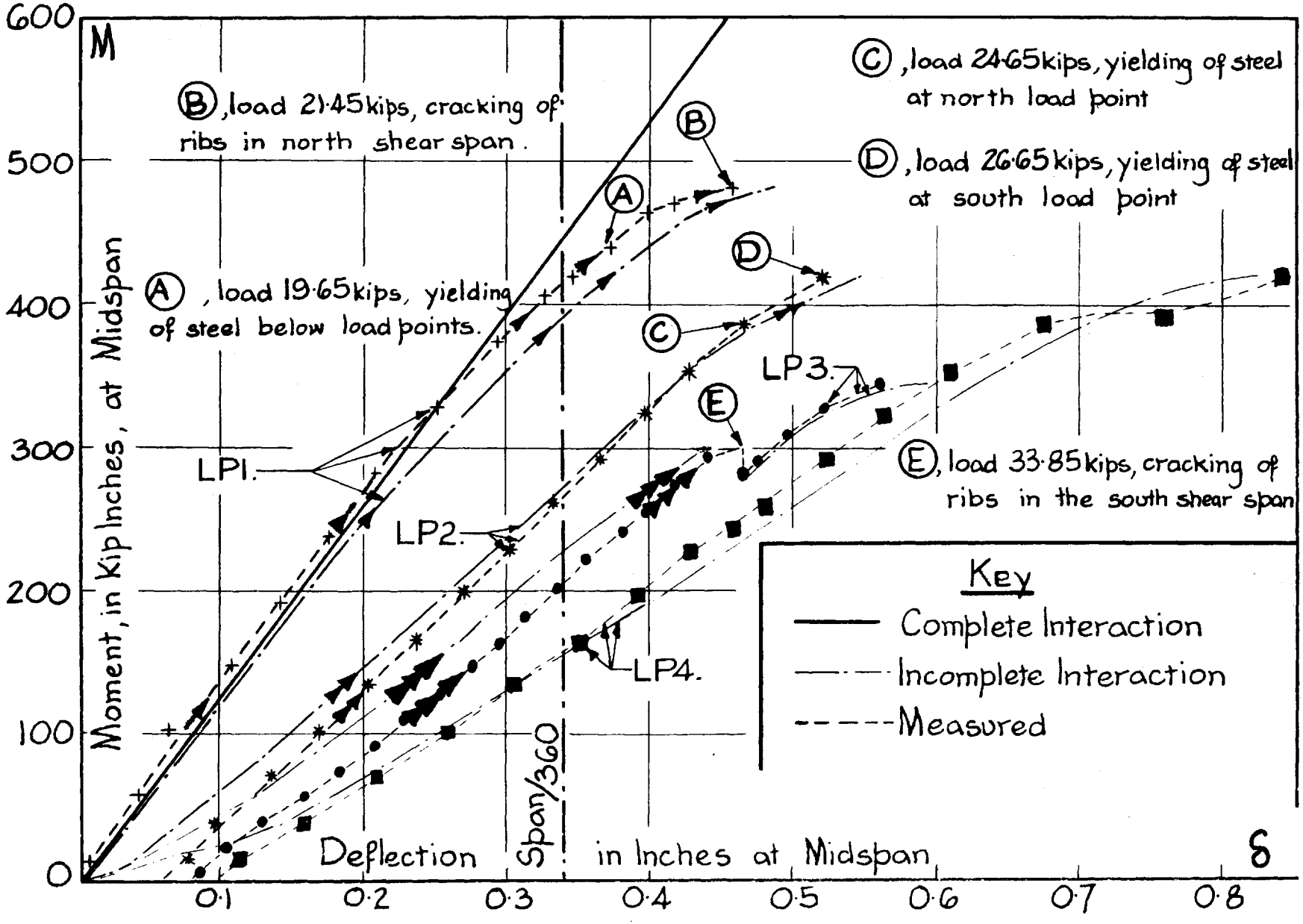

Figure 3.4 Moment - Deflection Curves for Beam BII

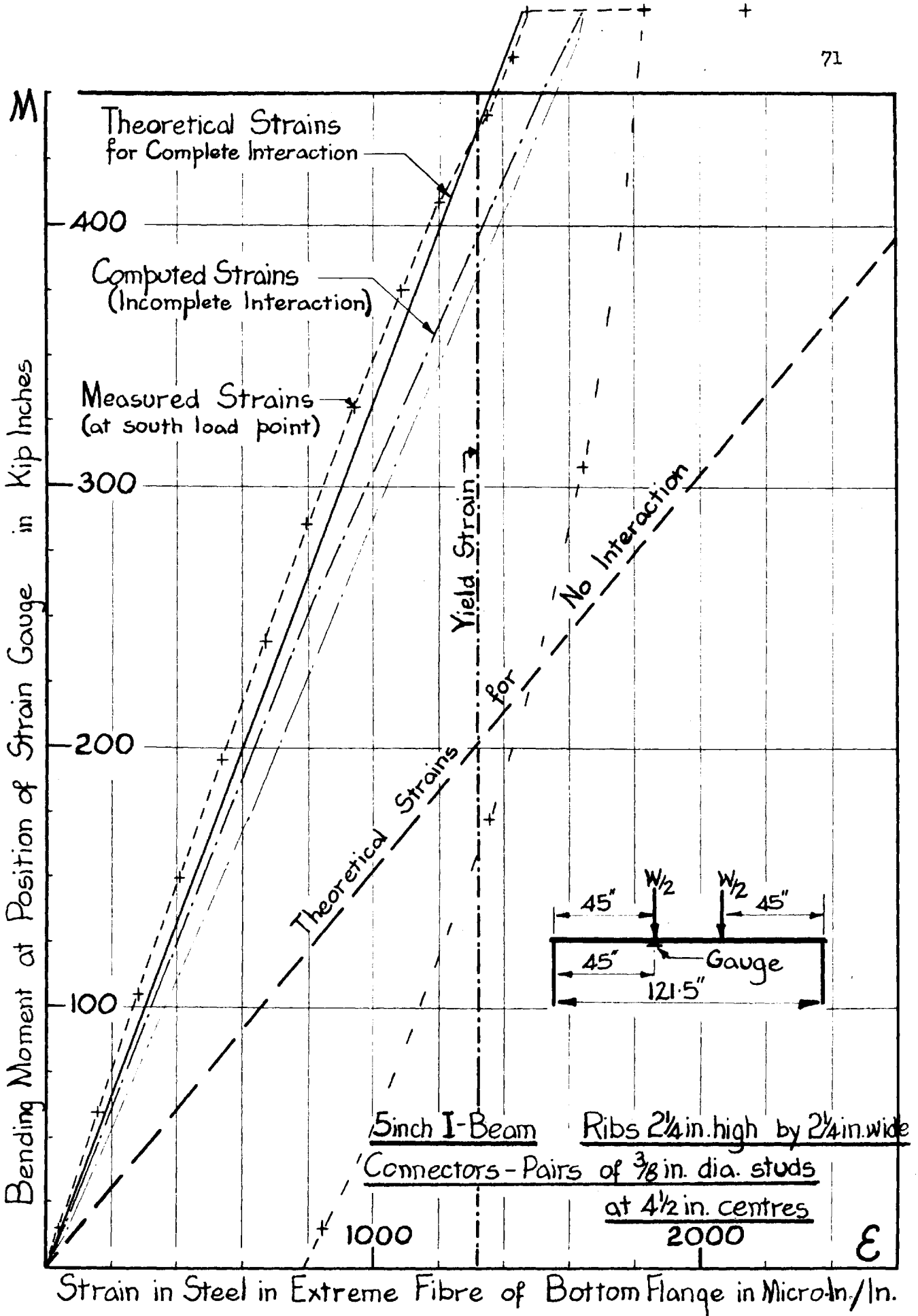

Figure 3.5 Moment - Steel Strain Curves for Beam BII (Loading Position LP1)

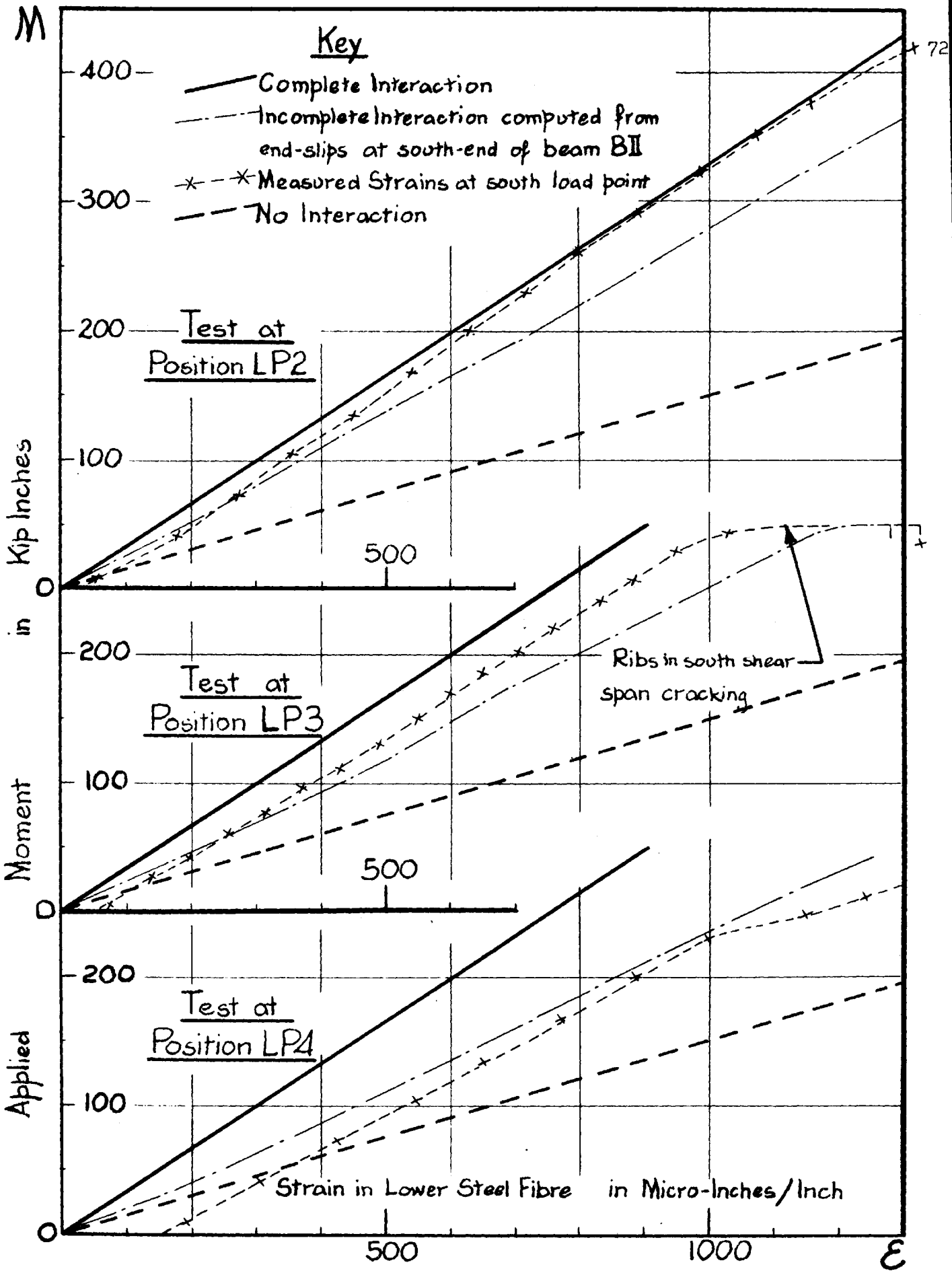

Figure 3.6 Moment - Steel Strain Curves for Beam BII (Loading Position LP2, LP3, LP4)

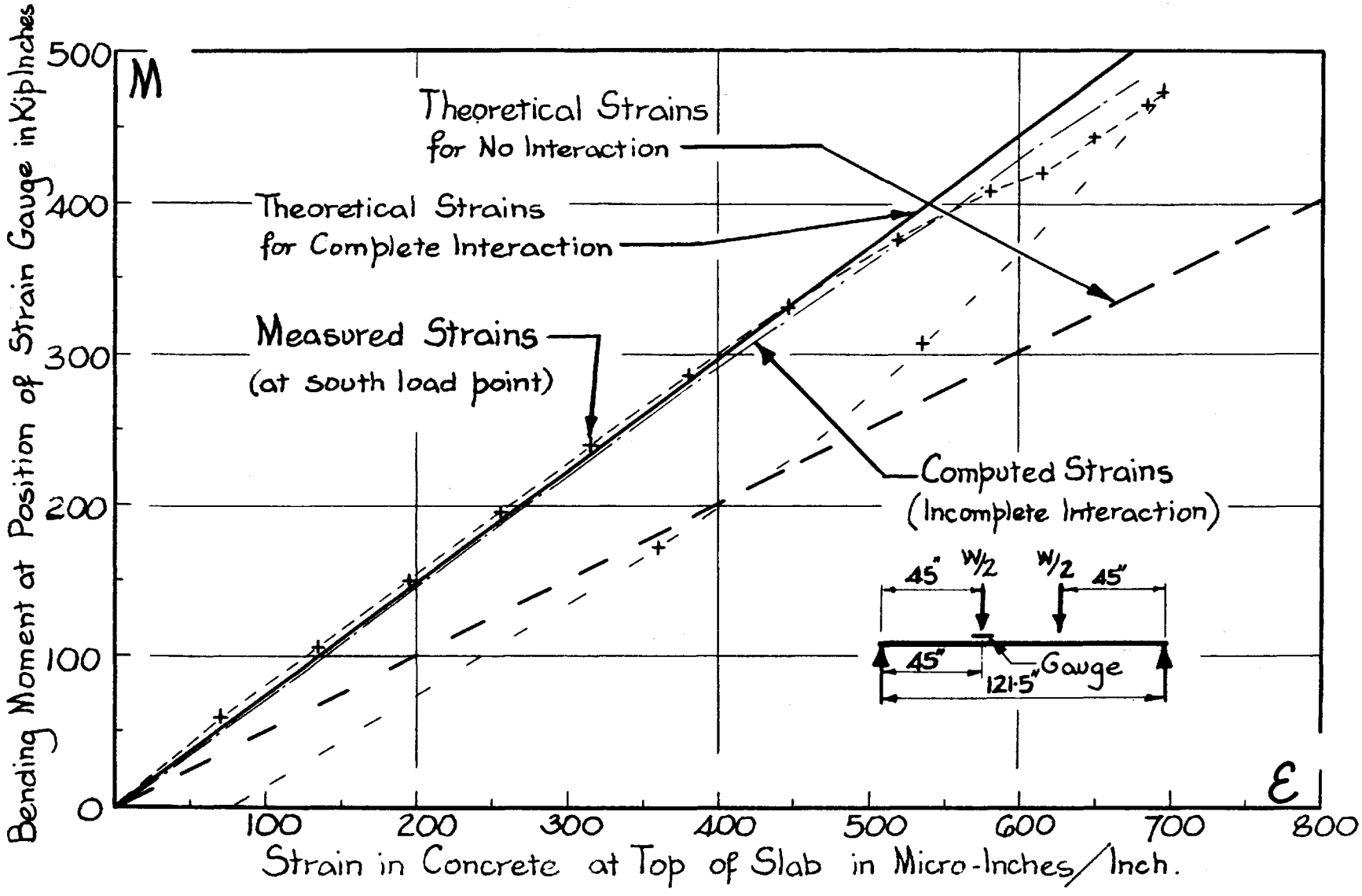

Figure 3.7 Moment - Concrete Strain Curves for Beam BII (Loading Position LP1)

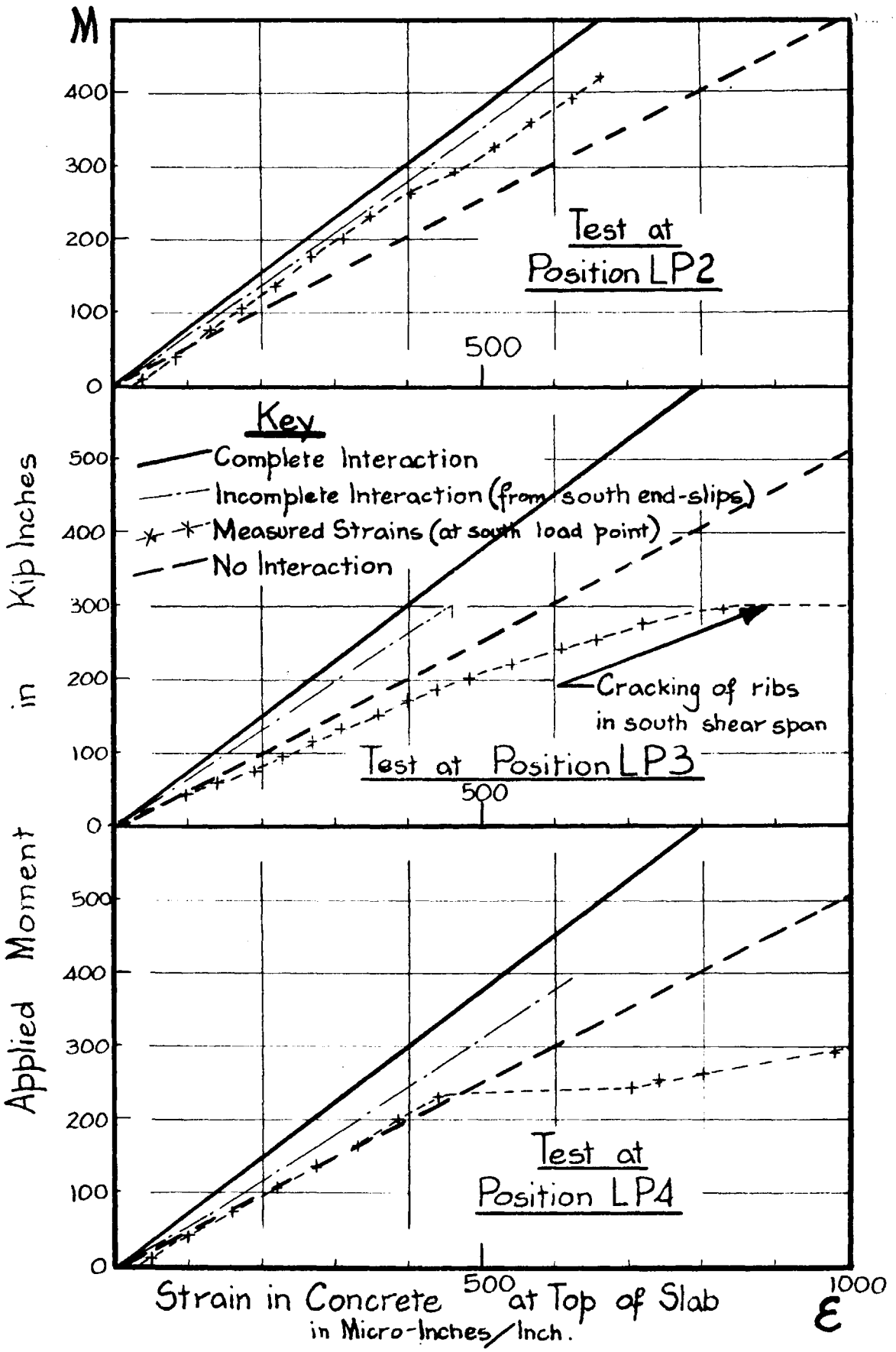

Figure 3.8 Moment - Concrete Strain Curves for Beam BII
(Loading Position LP2, LP3, and LP4)

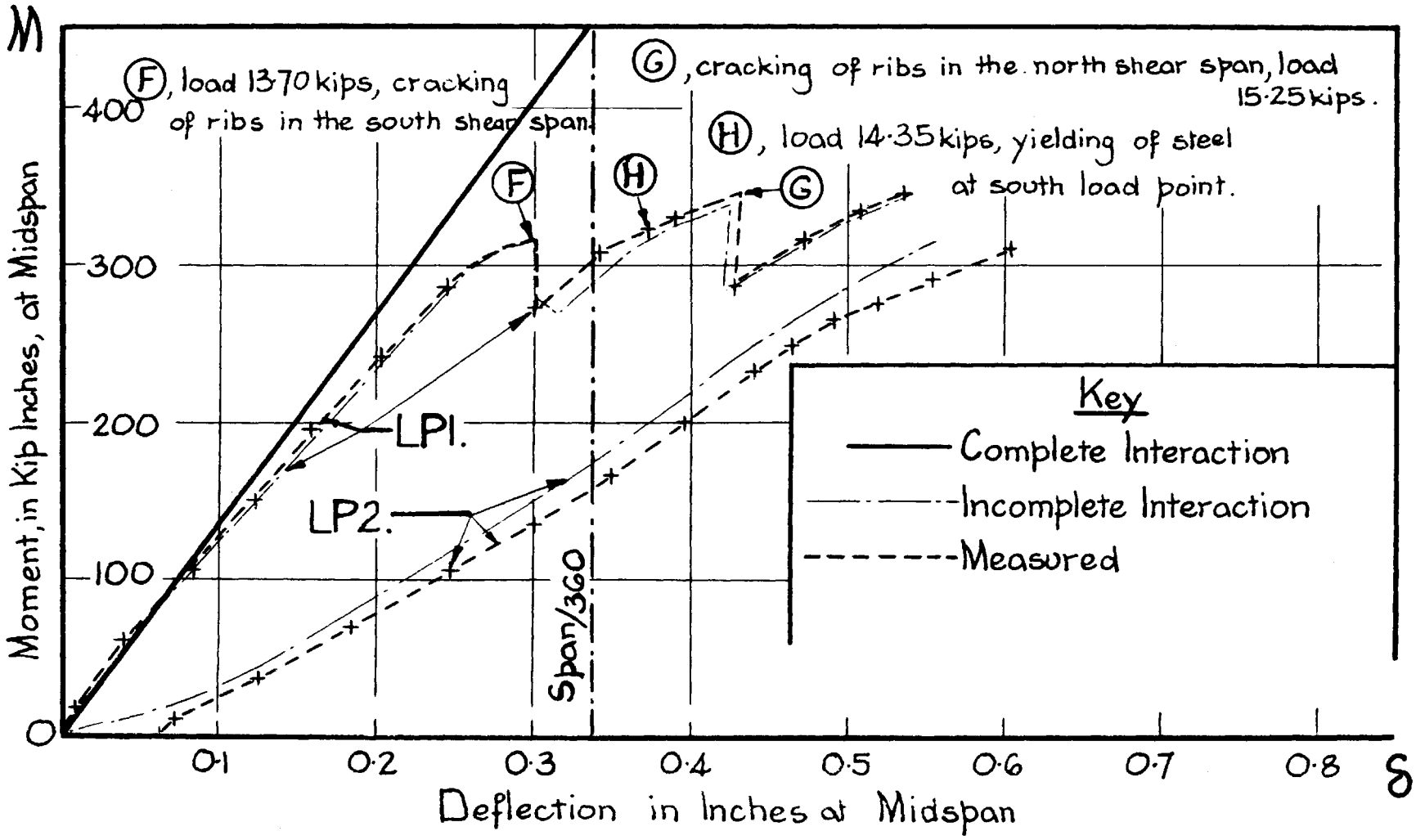

Figure 3.9 Moment - Deflection Curves for Beam BI

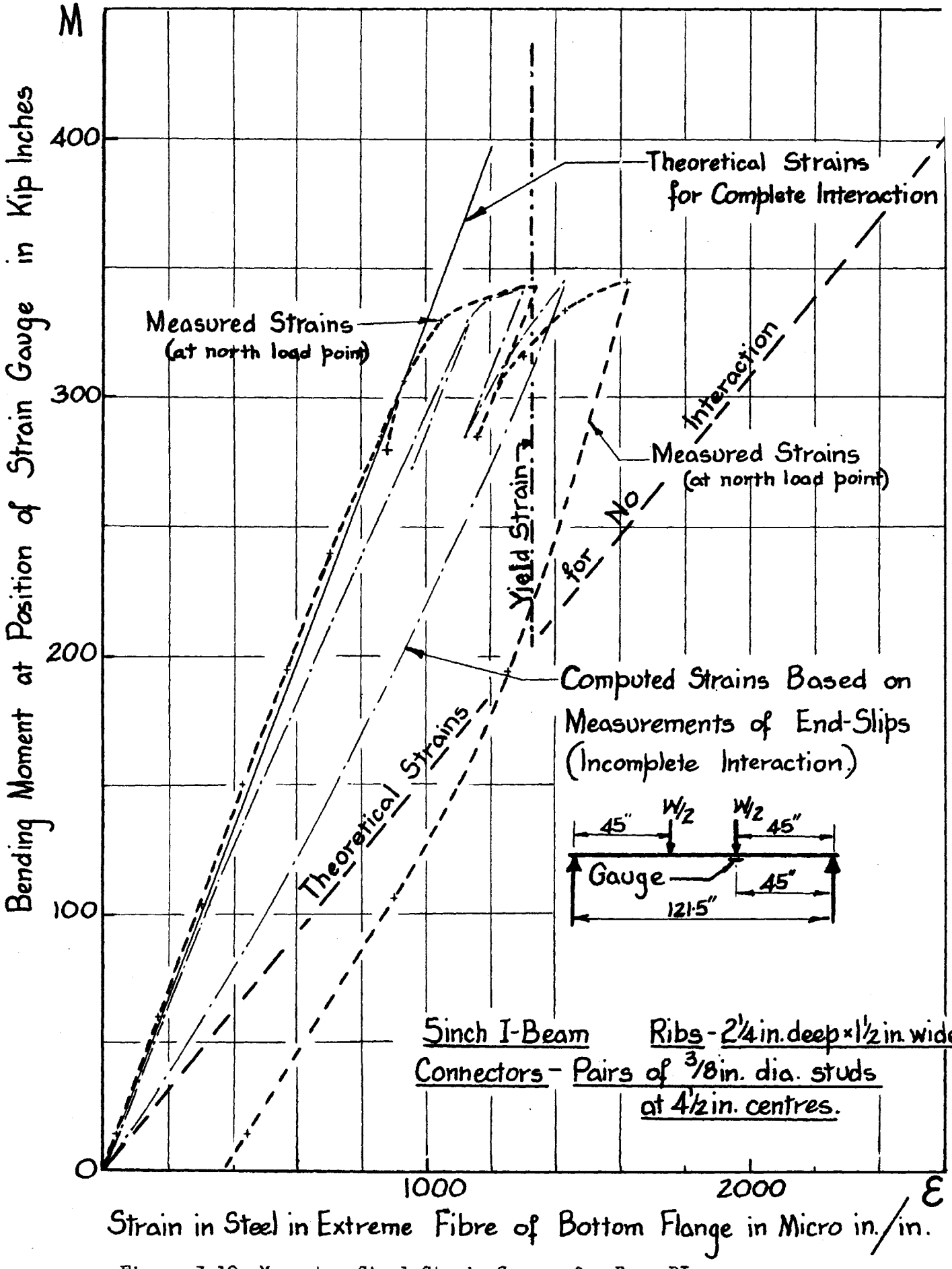

Figure 3.10 Moment - Steel Strain Curves for Beam BI

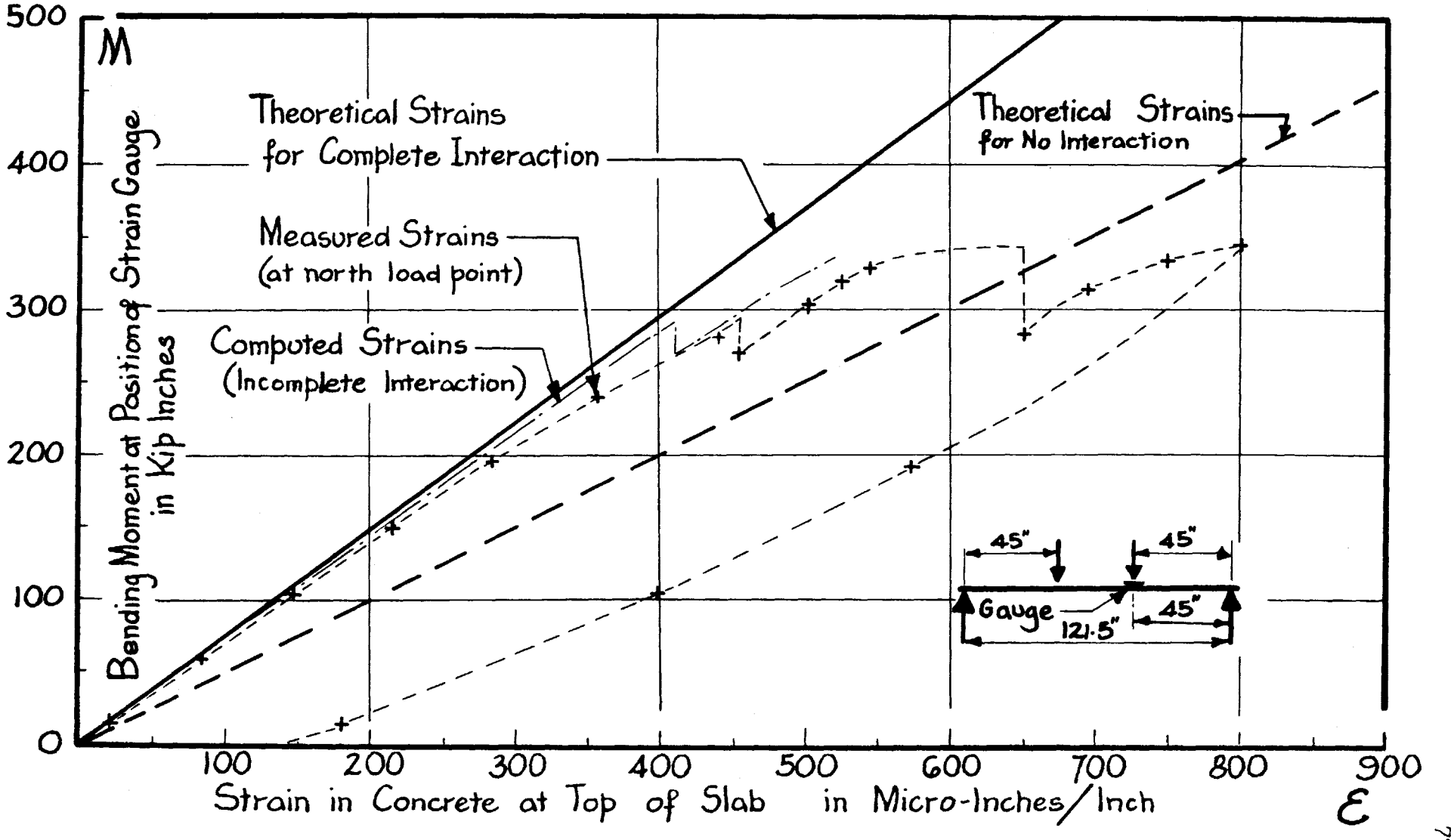

Figure 3.11 Moment - Concrete Strain Curves for Beam BI

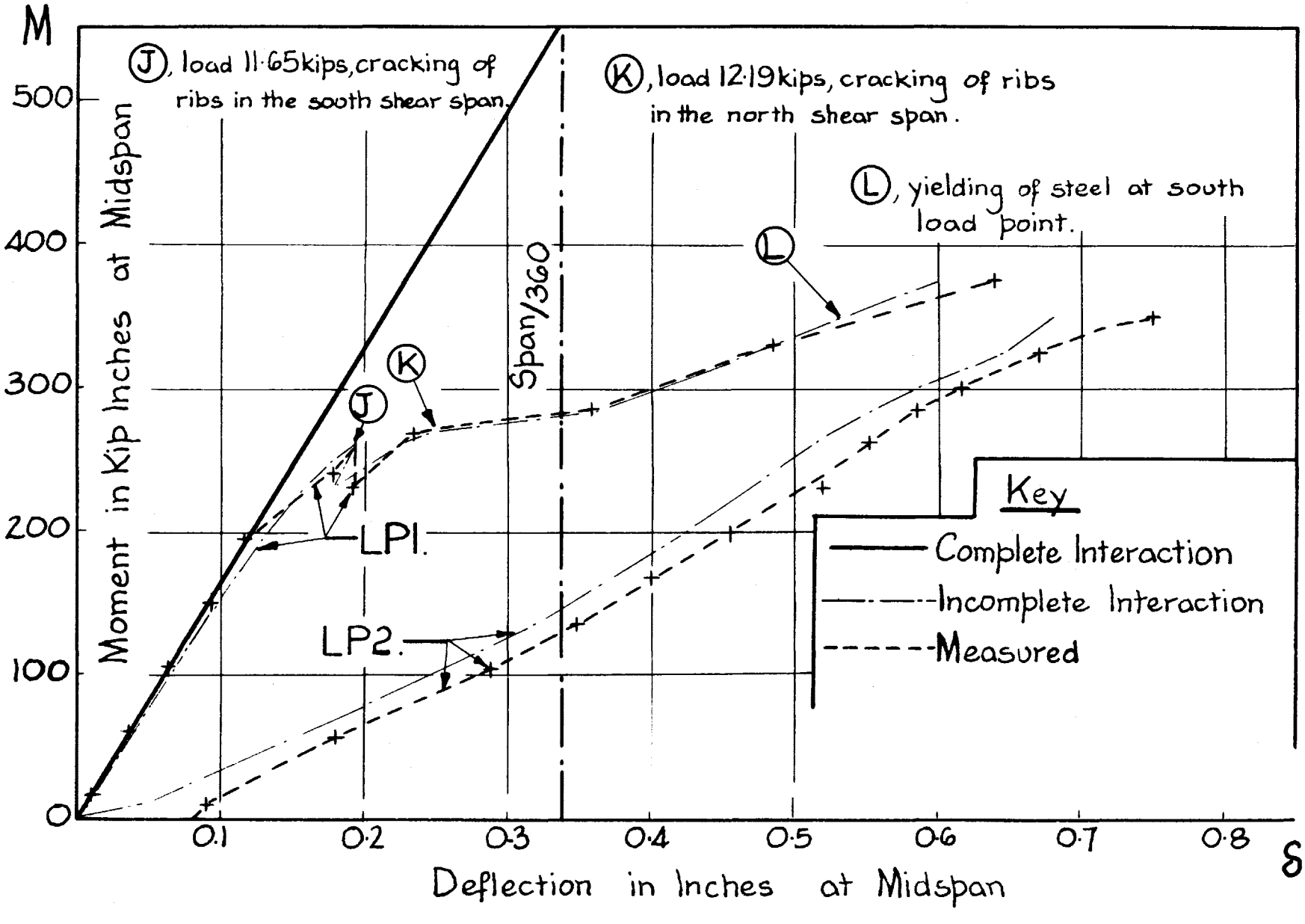

Figure 3.12 Moment - Deflection Curves for Beam BIII

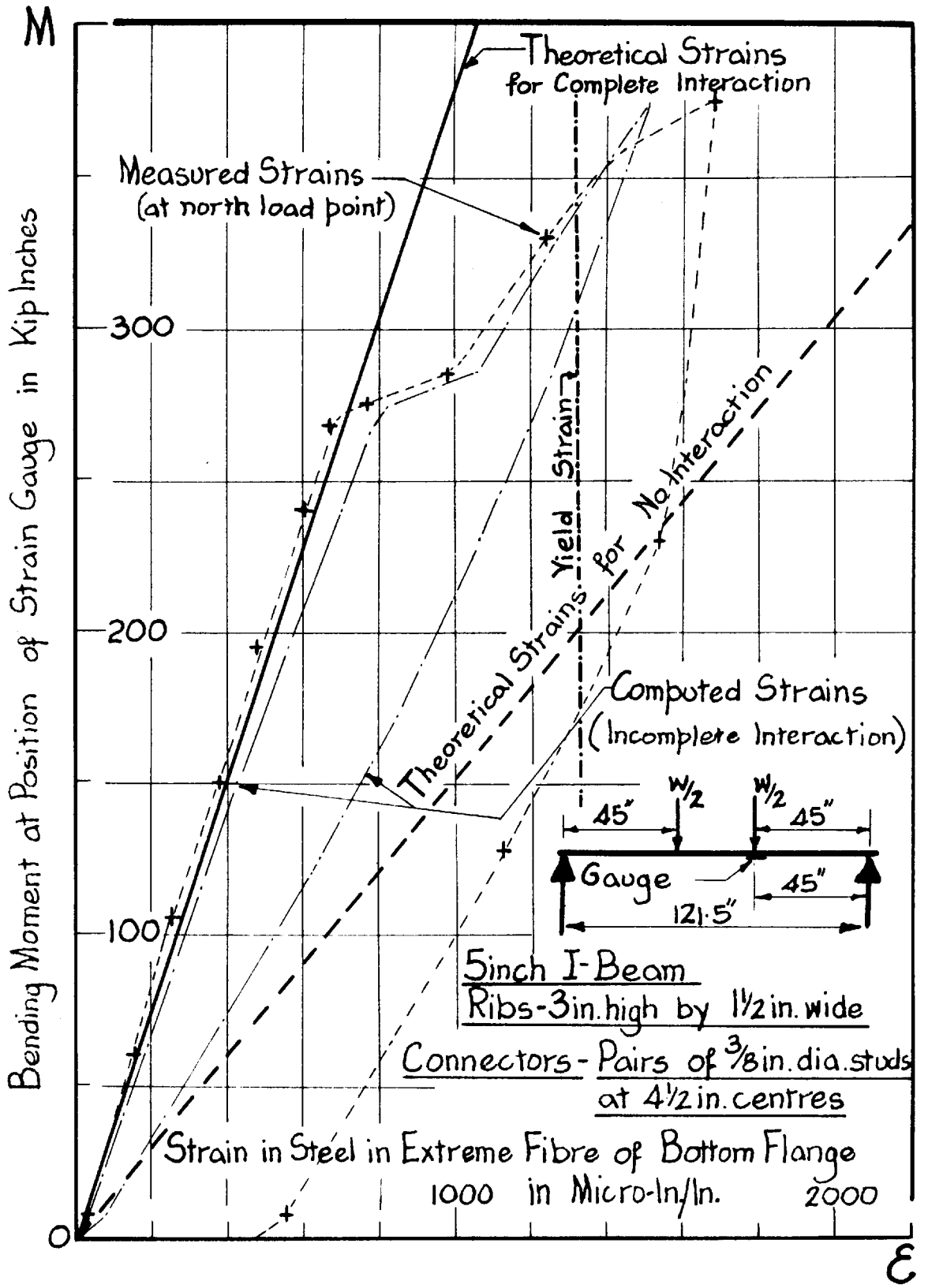

Figure 3.13 Moment - Steel Strain Curves for Beam BIII

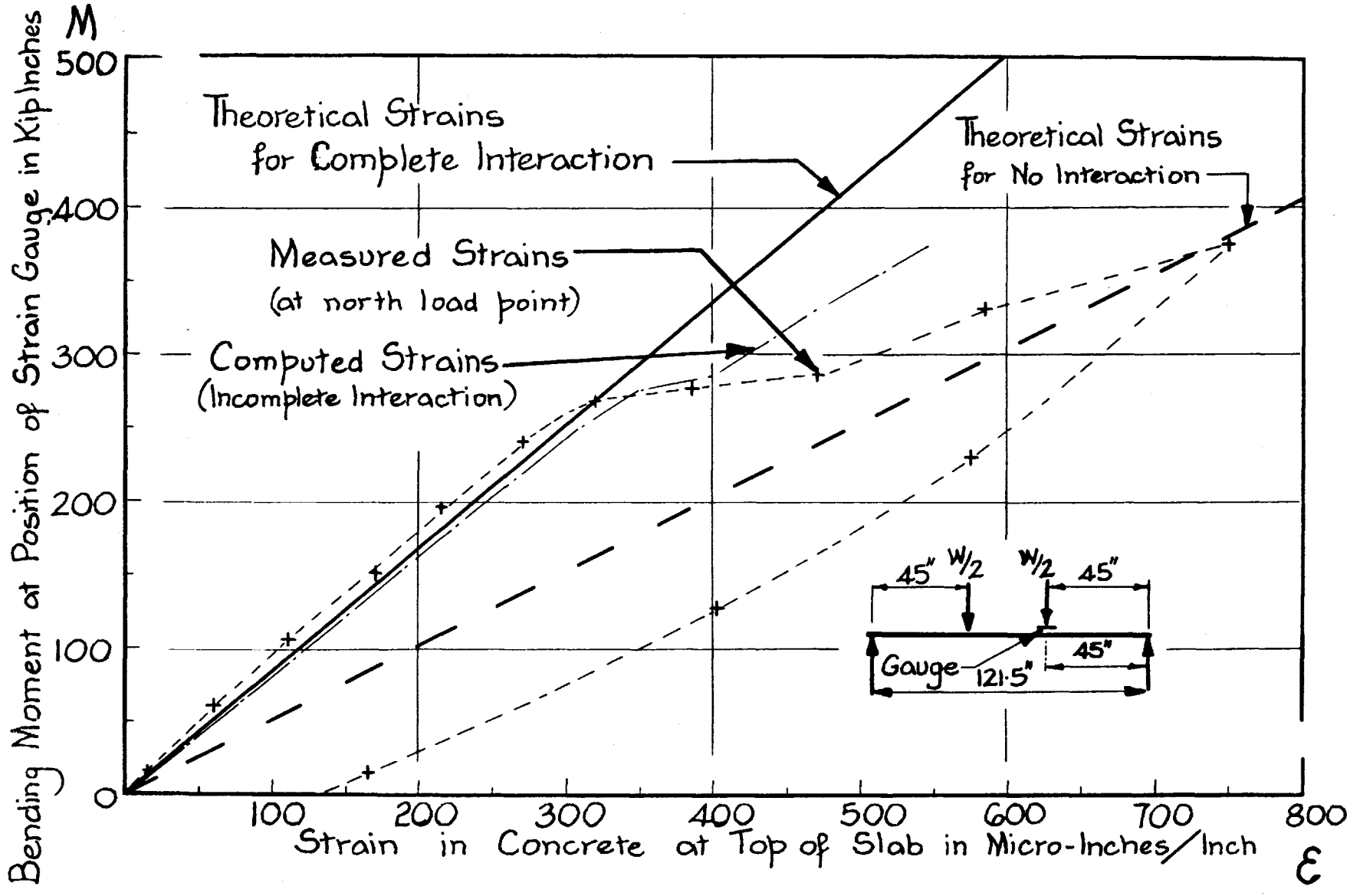

Figure 3.14 Moment - Concrete Strain Curves for Beam BIII

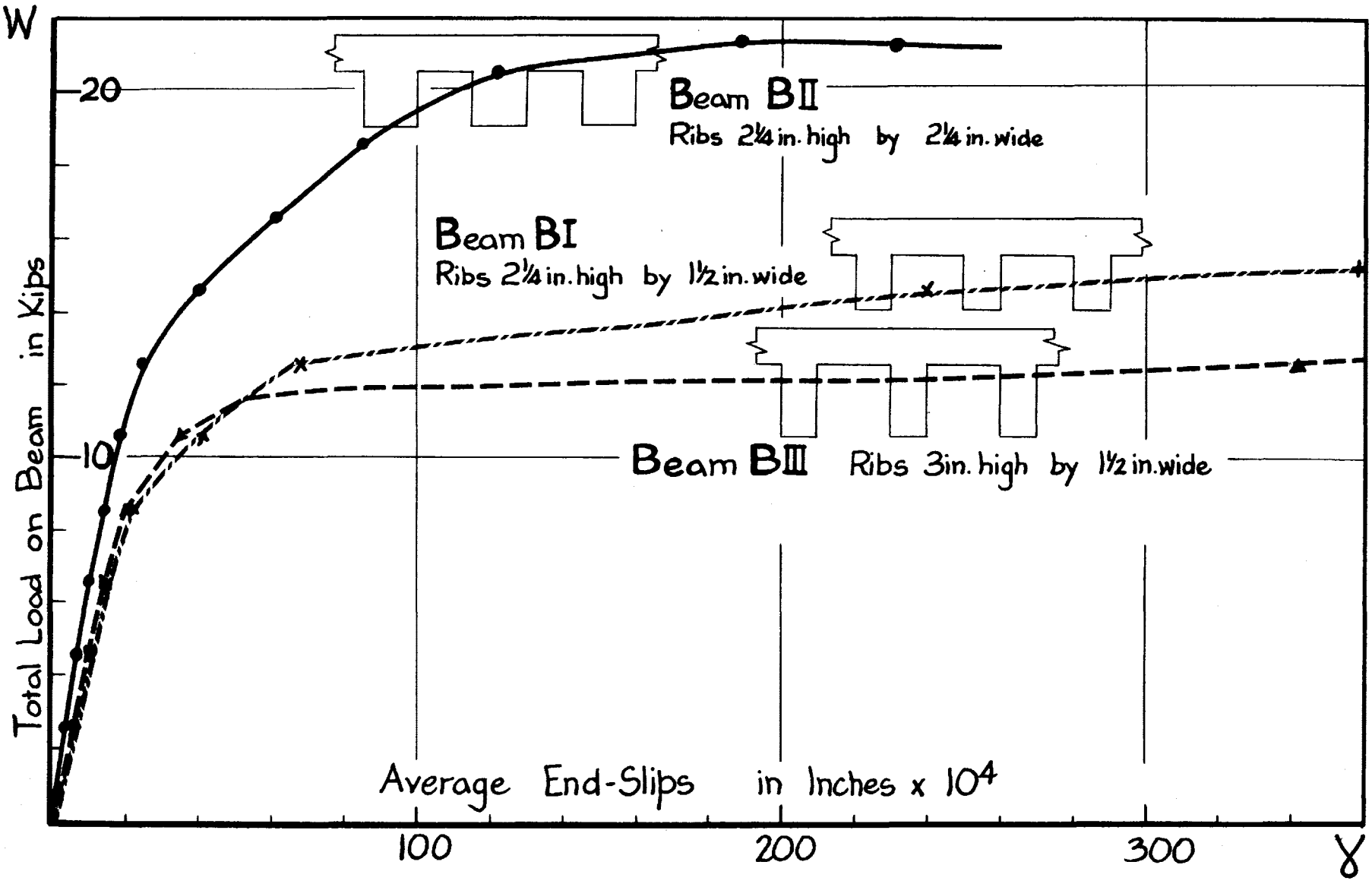

Figure 3.15 Comparison of End - Slips for Beams BI, BII and BIII

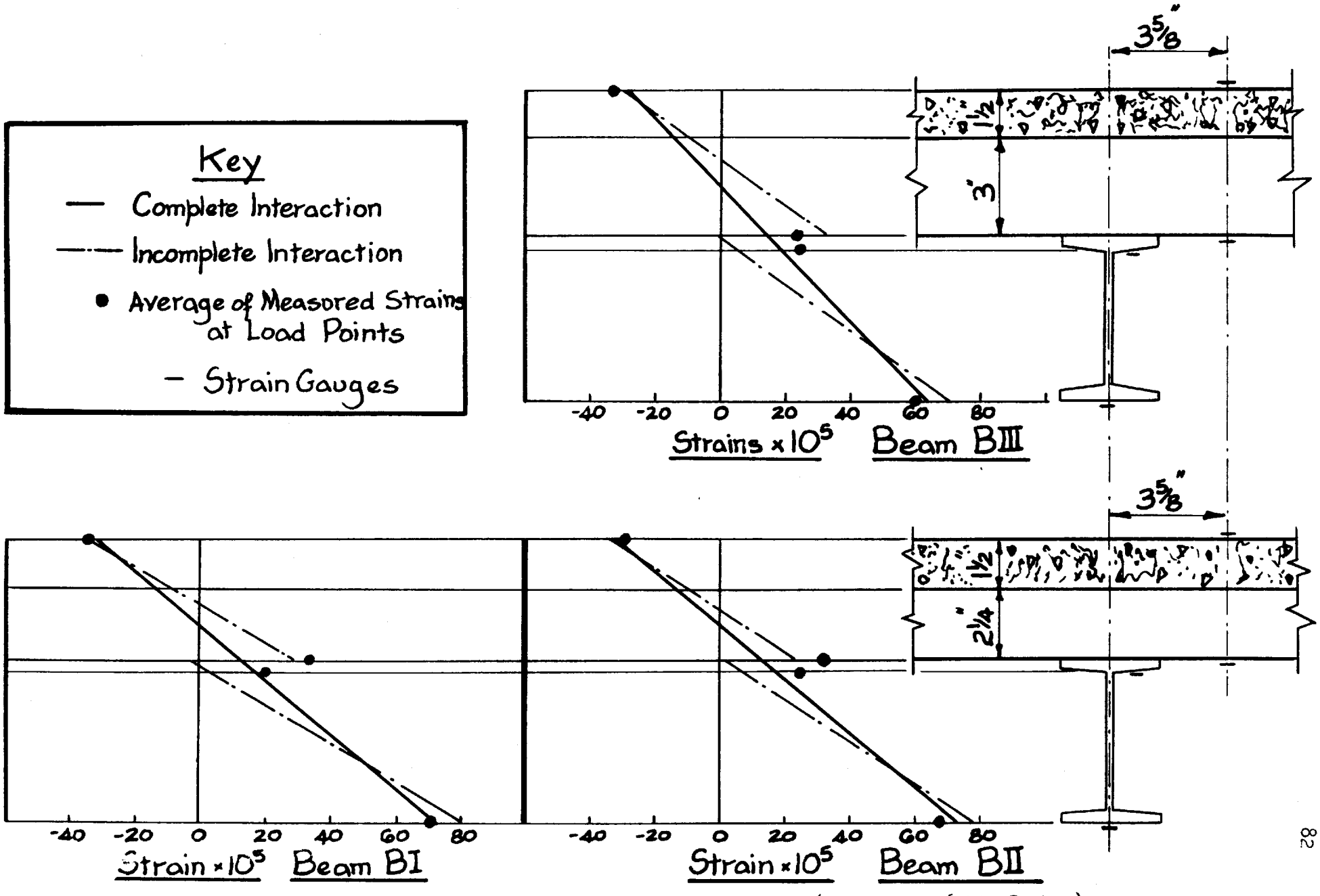

Figure 3.16 Strain Distribution Applied Load 10.65 kips in Position LP1 (Moment 239.6 kip Inches)

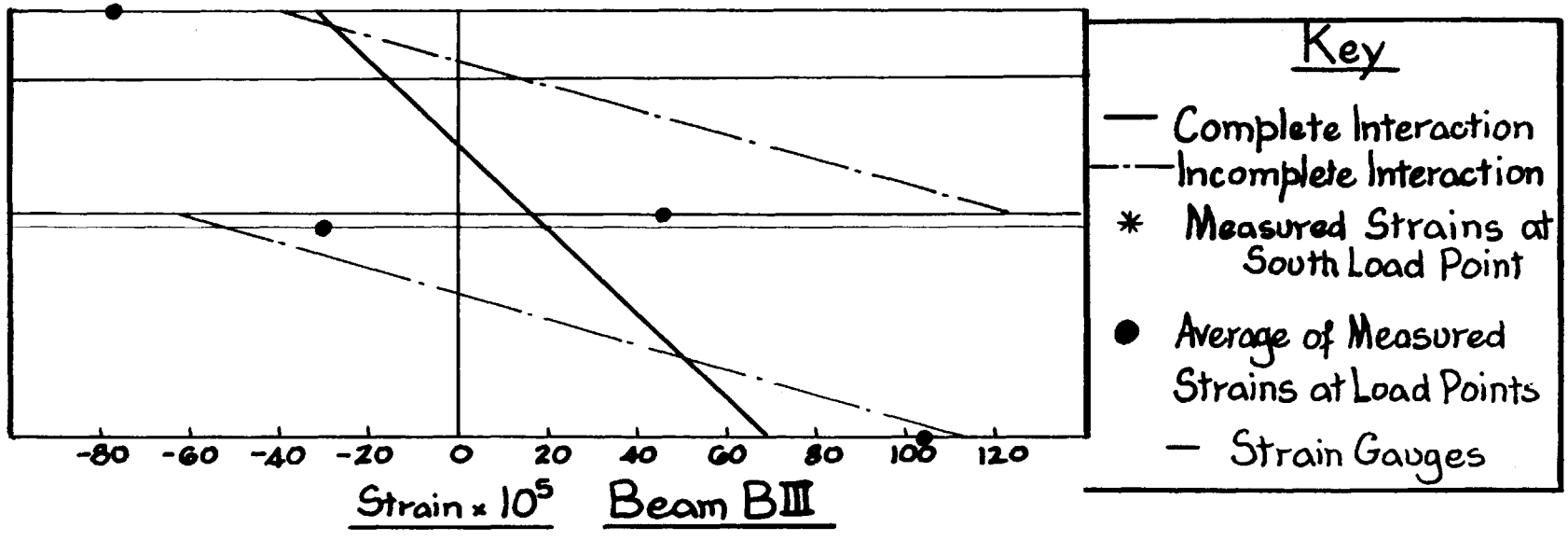

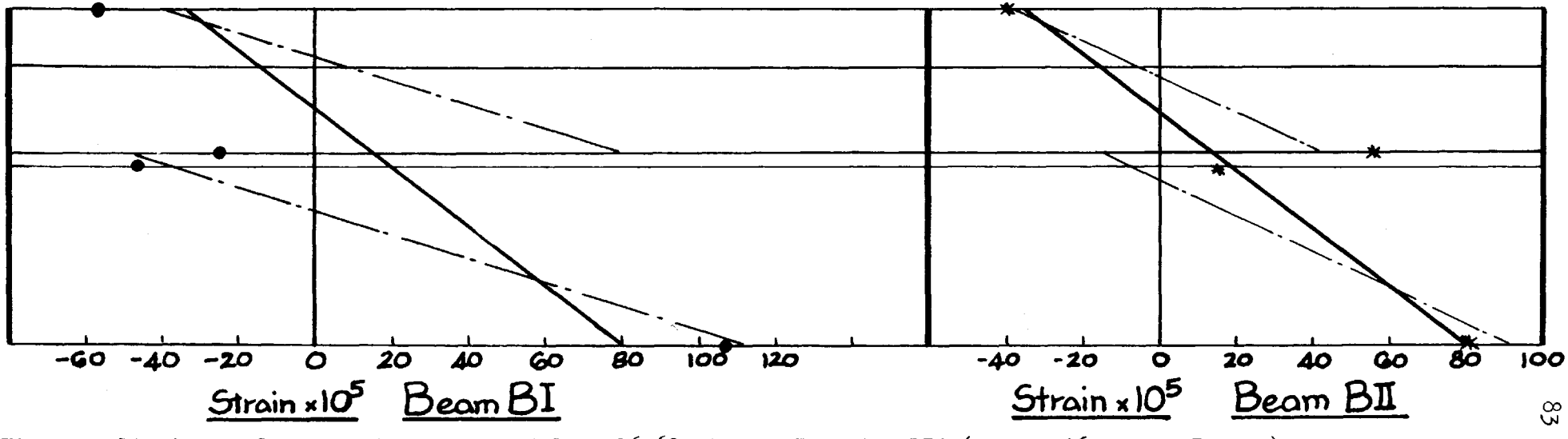

Figure 3.17 Strain Distribution Applied Load 16.65 kips in Position LP2 (Moment 262.2 kip Inches)

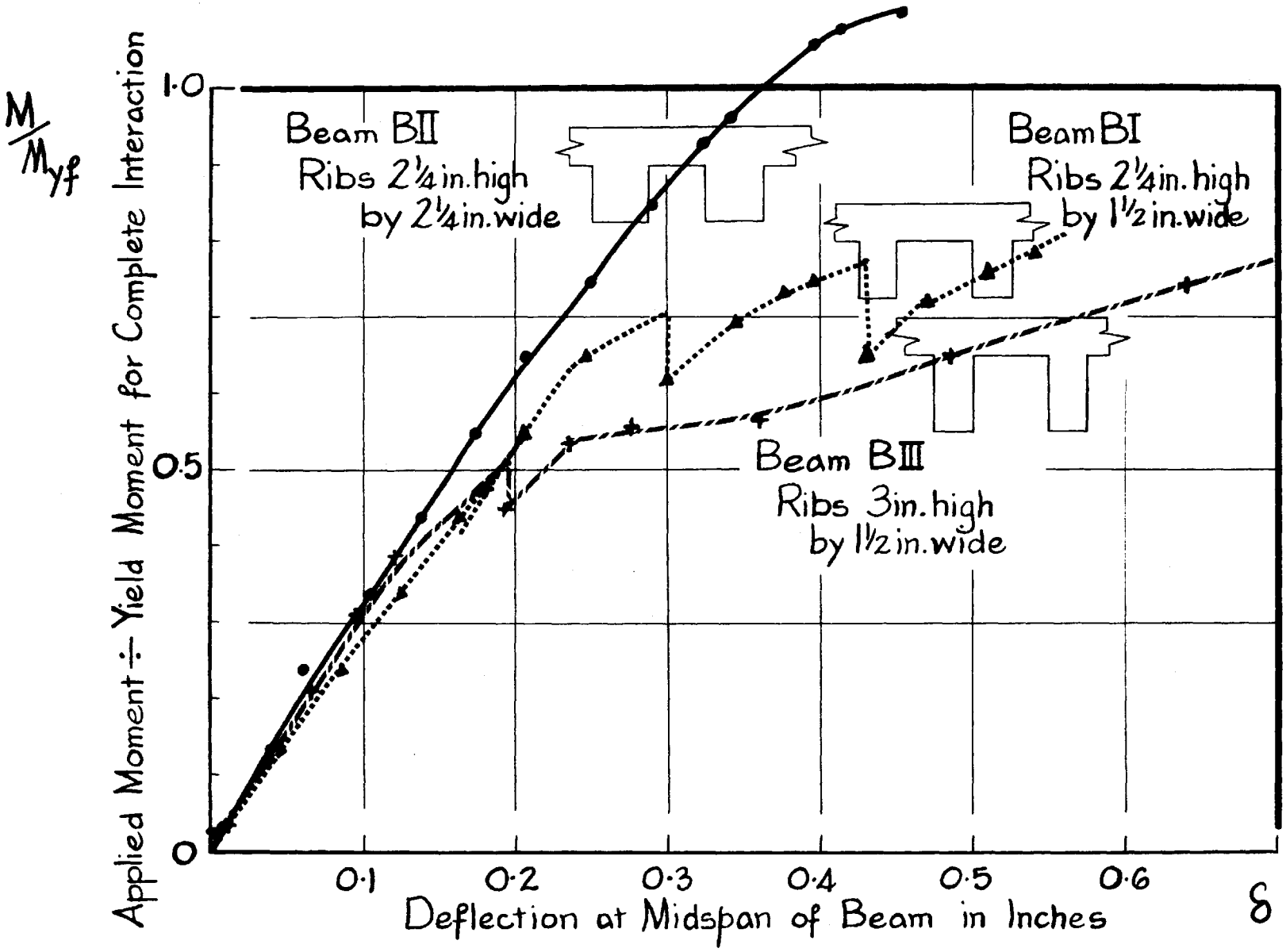

Figure 3.18 Comparison of Deflections for Beams BI, BII and BIII Under Test at Position LP1

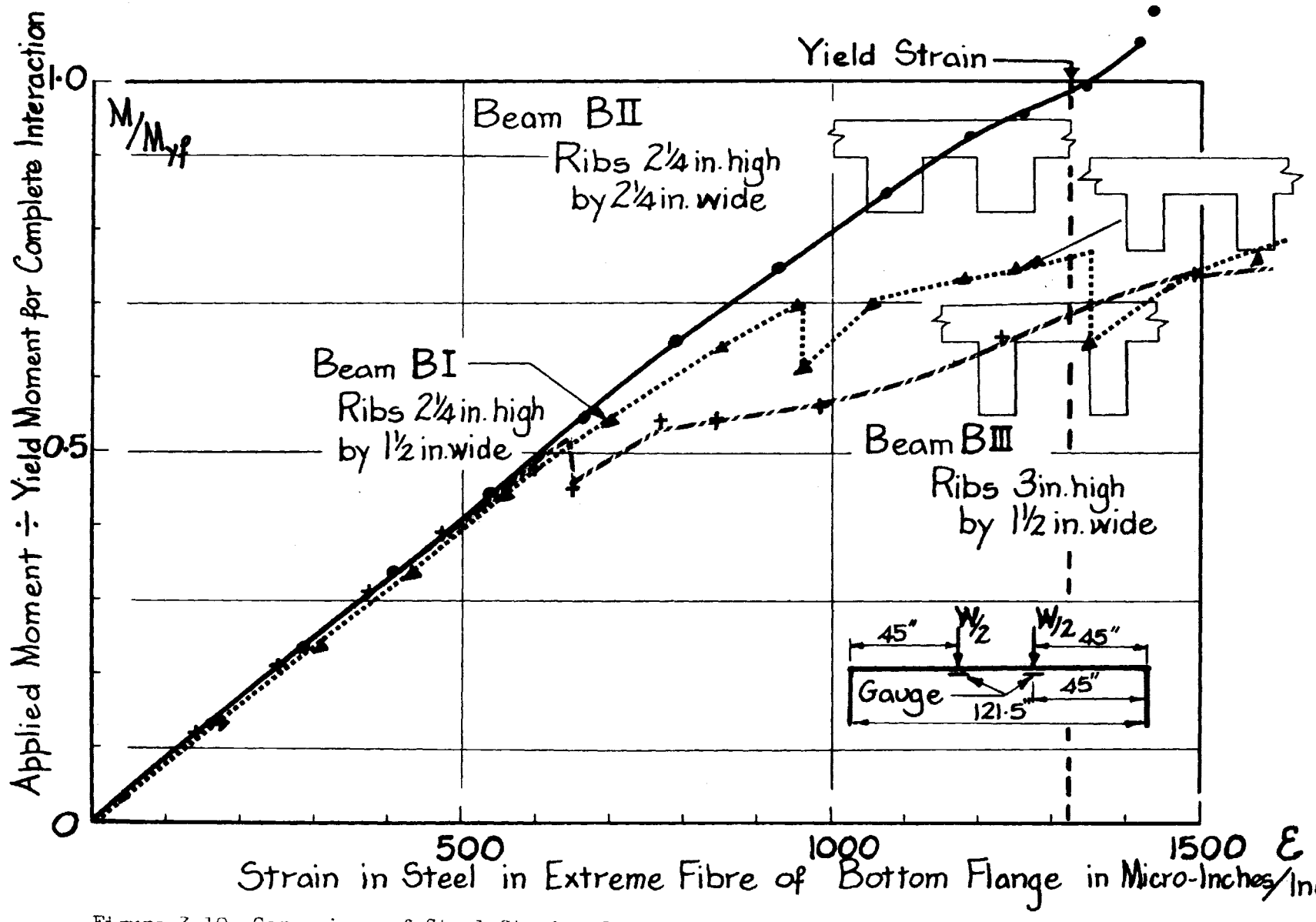

Figure 3.19 Comparison of Steel Strains for Beams BI, BII and BIII Under Test at Position LF1

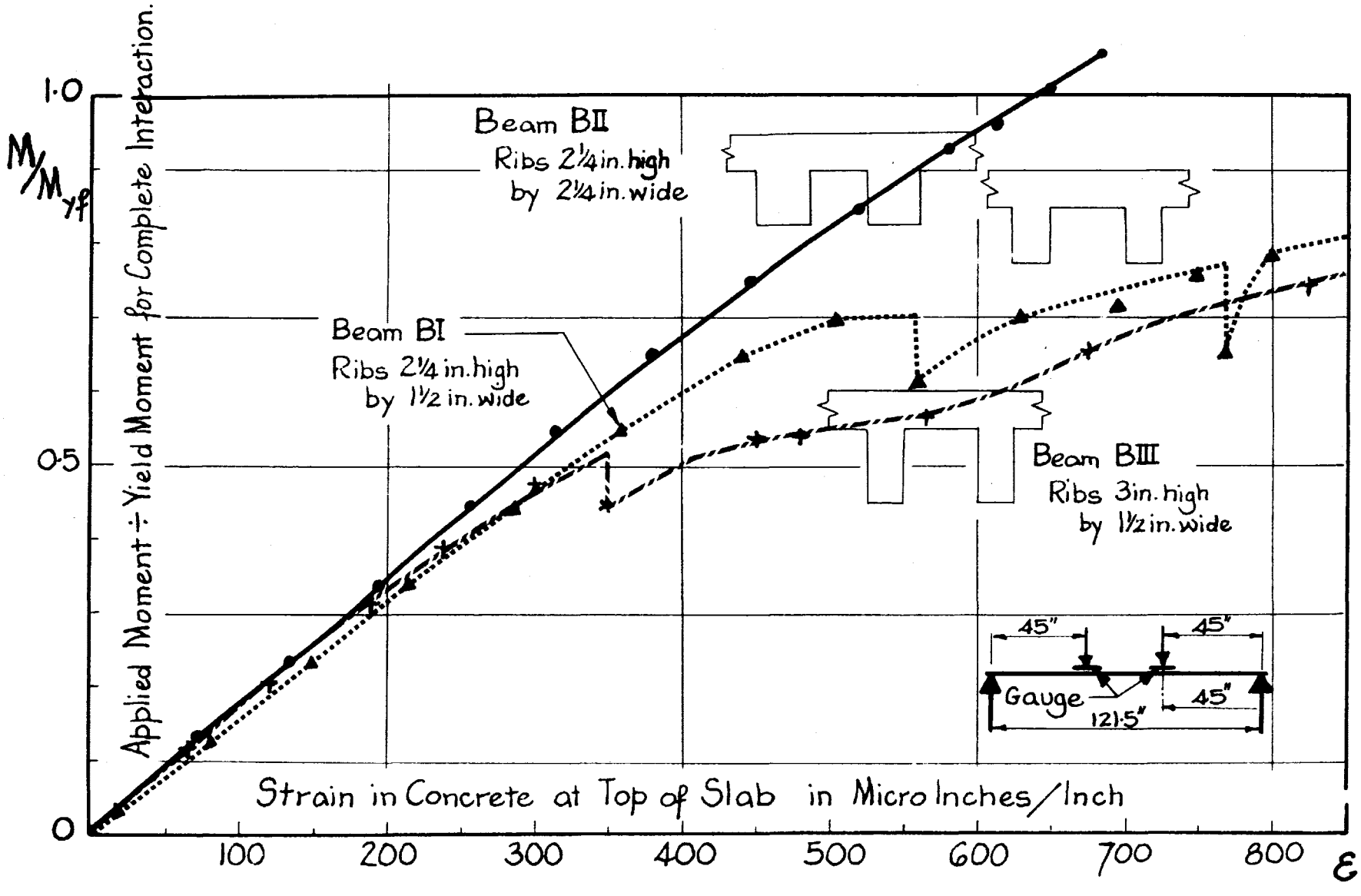

Figure 3.20 Comparison of Concrete Strains for Beams BI, BII and BIII under Test at Position LP1

CHAPTER 4

RATIONAL APPROACH FOR DESIGN PROCEDURE

4.1 Introduction

The aim of this chapter is to derive idealized and simplified criteria, in order to establish a rational approach for the design prodecure for composite cellular beams which will take into account the influence of cell geometry on the performance of composite beams.

It has already been established that the Newmark theory for incomplete interaction describes satisfactorily the behaviour of the test beams. This theory can be applied to any beam if a comprehensive load - slip curve is known for the connections of the beam. This load - slip curve must take into account any change in interaction coefficient (1/C) with change in load on the beam or load on the connection. This characteristic curve is best found by tests on a beam but for reasons of economy the results of push - out tests may be accepted. In both cases, the load - slip curve in its intrinsic form is not suitable for design purposes because it will give rise to complex computations. For this reason, it is considered that for design purposes it is necessary to idealize the load - slip curve. If this is possible, the theory for incomplete interaction can be used to obtain families of design curves for different cell geometries and for different spacings of studs.

In order to illustrate a possible basis for design procedure, predictions will be made in section 4.3 for the behaviour of beams BI, BII and BIII from simplified load - slip characteristics for the

connections. The characteristic curves for the connections have been derived from:

(a) data obtained from push - out tests on specimens having cell geometry identical with that of the beams, and

(b) data from the beam tests.

4.2 Comparison of Behaviour of Connections in T - beams and Push - Out Tests.

As discussed in section 3.8, the calculations based on end - slip measurements and corresponding loads on T - beams give theoretical values for load on the end - connection. These theoretical loads on the end - connection are plotted in Figures 4.1 and 4.2.

Figure 4.1 which shows the load - slip curve for the end - connections of beam BII also shows the load - slip curves for the push - out specimen with ribs 2 1/4 in. high by 2 1/4 in wide from Series 1 and Series 2. Likewise, Figure 4.2(a) shows the load - slip curves for beam BI, and for the push - out specimens with similar cell geometry from Series 1 and Series 2; and Figure 4.2(b) the load - slip curves for beam BIII and for the two corresponding push - out specimens from Series 1 and Series 2.

In attempting to compare the results of beam and push - out tests, it should be remembered that in the T - beam the slab is subjected to bending as well as compression, whereas in the push - out specimen the slab is essentially in compression, and that perfect agreement is not to be expected.

It may be concluded from Figures 4.1 and 4.2 that:

(a) the results of the tests on push - out specimens from Series 2,

with slabs laterally free, are preferable to those from Series 1, with slabs laterally restrained, since the results of tests on push - out specimens in Series 2 show better agreement with the results from the beam tests.

(b) the load - slip curves for the push - out specimens of Series 2 are of the same form as those from the beam tests, but percentage differences are large, particularly in the early stages of loading.

(c) the slips observed in the push - out tests are greater than those in the beam tests (this may be partly explained by the fact that friction as a direct result of the applied load is present in beam tests, whereas in the case of push - out tests there is a tendency for the beam and slab to separate).

(d) as a consequence of (c), the modulus of the connection is higher in the beam tests than in the push - out tests.

(e) the maximum loads and the breakdown loads for the end - connections in beams BI and BIII are of the same order of magnitude as the maximum loads and breakdown loads calculated from the load - slip curves for the corresponding push - out specimens.

(f) the maximum load and the breakdown load for a connection taken from results on a beam test are functions of the loading position, if the connection is sufficiently strong, to cause the lower steel fibre to yield before the concrete ribs crack (this is illustrated in Figure 4.1) and

(g) an idealized load - slip curve might be taken as the modulus of the connection followed by a range where the modulus of the connection might be considered to be zero, as shown in Figure 4.3(a).

4.3 Idealized Load - Slip Curve

An idealized load - slip curve was used by DAI and SEISS in 1963 for the purposes of making an analytical study of conventional composite T - beams with inelastic shear connection. Their idealized curve was formed by three straight lines. The load - slip curves for connections in composite cellular T - beams have a form intrinsically different from those considered by Dai and Seiss. It was considered that an idealized curve as shown in Figure 4.3 would accurately describe the load - slip curves for connections in composite cellular T - beams.

This idealized curve for a connection consists of an initial linear part, OA, having a modulus which is constant for increase in load up to a critical load. At this critical load, it is assumed that the connection has become plastic in behaviour or has zero modulus. The initial modulus varies with the rib arrangement of the connection as indicated in Chapter 2 and Figures 4.1 and 4.2. The load on the connection at which the idealized curve changes gradient is also a function of the geometry. It will be assumed that this change of gradient takes place when the load on the connection is the breakdown load Q_{cb}. Therefore to idealize the load - slip curves obtained from the push - out tests shown in Figures 2.6, 2.7, and 2.8, and the load - slip curves obtained from the beam tests, it is necessary to know the appropriate values for:

(a) the modulus of the connection, and

(b) the breakdown load of the connection.

These will give idealized curves which envelope the load - slip curves obtained from tests such as those on beams BI and BIII; see Figure 4.3(b). For many of the load - slip curves obtained from push - out tests, the idealized curve will form only part of the full load - slip

curve and will not envelope the zone of maximum load; see Figure 4.3(c).

Table 4.1 lists the moduli and the breakdown loads for the connections of beams BI, BII and BIII, obtained from the analysis of the beam test results and from the load - slip curves of the corresponding push - out specimens. The values obtained from the push - out results are less than those from the beam computations. In particular, the moduli from the push - out test results are as low as one third of the moduli from the beam tests. This is partly explained by the fact that the tangent modulus was used to interpret the beam tests, whereas the secant modulus was taken from the push - out load - slip curves; and is partly explained as a normal occurrence as suggested in section 4.2(d).

4.4 Predicted Behaviour of Beams Using Idealized Load - Slip Curves.

The quantities for modulus and breakdown load listed in Table 4.1 were used to predict the behaviour of beams BI, BII and BIII. An outline of the method employed to compute the predicted performance of a beam is given below.

Stage 1: The load on the beam is increased in small increments and calculations are made for:

(1) deflections at midspan

(2) strains in the lower steel fibre beneath the load points, and

(3) end - slips

at each load increment. For each step, checks are made to ensure that:

(a) the strain in the lower steel fibre below the load is less than the yield strain

TABLE 4.1 PREDICTED BEHAVIOUR OF BEAMS BASED ON IDEALIZED LOAD - SLIP CURVES

	Beam	Modulus* k (kips/in.)	Breakdown* Load Q_{cb} (kips)	Theoretical Yield + Moment M_{yf} (Kip Inches)	Breakdown Load on Beam (kips)	Load at Applied Moment M_{yf}	Yield of Steel in Bottom Flange At Load (Kips)	Moment (Kip In.)	Applied Moment M_{yf}
Measured					13.70	0.700	14.35	322.9	0.735
Predicted (based on beam computations)	BI	1628	4.82	438.9	14.4	0.738	16.3	366.7	0.835
Predicted (based on push - out tests)		600	3.80		11.5	0.586	14.5	326.0	0.744
Measured					21.45	1.104	19.65	442.1	1.01
Predicted (based on beam computations)	BII	2409	6.86	437.5	20.60	1.060	18.25	410.6	0.939
Predicted (based on push - out tests)		640	5.0		15.0	0.772	16.10	363.0	0.829
Measured					11.65	0.521	15.65	352.1	0.700
Predicted (based on beam computations)	BIII	1534	3.53	503.0	11.50	0.514	15.49	348.6	0.693
Predicted (based on push - out tests)		536	3.35		10.95	0.490	14.90	335.2	0.666

$+M_{yf}$ = Theoretical yield moment for complete interaction is that moment which the beam with full interaction would support theoretically, before the steel in the lower flange yields (allowance being made for dead loads).

* Moduli and breakdown loads obtained from load - slip curves.

and (b) the load on the end - connections is less than the breakdown load of the connection.

If the condition (b) is broken first, the calculations for Stage 1 are concluded and the computations continued as indicated below in Stage 2. If the condition (a) is broken first the calculations are terminated.

Stage 2: The load on the beam is increased beyond the level at the end of Stage 1. The load on the end - connections remains unchanged at the breakdown load.

Calculations are made for

(1) deflections at midspan

(2) strains in the lower steel fibre beneath the load points

and (3) end - slips.

All these values are caluclated on the basis of no - interaction, and are added to the deflections, strains and end - slips accumulated at the end of Stage (1).

For each load increase in Stage 2, a check is made to ensure that the total strain in the lower steel fibre below the load, is less than the yield strain. When this condition is broken, the calculations are terminated.

The predicted behaviour and the observed behaviour of each beam is compared in Tables 4.1 and 4.2 and in Figure 4.4.

4.5 Discussion

In the early stages of loading, the predicted values for strain based on idealized curves from beam tests, are better than those values based on idealized curves from push - out tests, because they have closer agreement with the observed measurements. This is simply a reflection of

TABLE 4.2 END - SLIPS AND DEFLECTIONS FOR IDEALIZED LOAD - SLIP CURVES

	Beam	End Slips at:- Breakdown Load (Inches x 10^4)	End Slips at:- Yield (Inches x 10^4)	Central Deflection at:- Breakdown Load (Inches)	Central Deflection at:- Yield (Inches)	Value of (1/C)
Measured*	BI	61 to 78	430	0.274	0.430	-
Predicted (based on beam computations)		30	543	0.262	0.431	53.2
Predicted (based on push - out tests)		63	898	0.237	0.505	19.6
Measured*	BII	128 to 250	100	0.396	0.370	-
Predicted (based on beam computations)		-	25	-	0.324	78.7
Predicted (based on push - out tests)		77	374	0.304	0.403	21
Measured*	BIII	47 to 75	600	0.234	0.520	-
Predicted (based on beam computations)		23	1255	0.171	0.528	62.0
Predicted (based on push - out tests)		62	1280	0.186	0.540	21.6

* The measured figures are obtained by interpolation from beam test data.

the higher moduli assumed from the beam tests. In the later stages of loading, just prior to yielding of the lower steel fibre, the predictions, based on push - out tests, are preferable since they always over-estimate the strain, whereas the predictions for the strains in beams BI and BIII, based on beam tests, underestimate the strains.

At all stages of loading, the predictions for slip from both sources are unsatisfactory. Fortunately, slip is not an important design criterion.

In general, the predictions are satisfactory for assessing the moment at which the lower steel fibre yields, but the prediction for beam BI based on computations on beam data is 13 percent higher than observed, and the prediction, based on push - out tests, for beam BII is 18 percent lower than observed.

The predicted deflections are smaller than the measured deflections at the load on the beam causing the end - connection load to be the breakdown load; this indicates that interpolation from the measured deflections is unsatisfactory because the modulus of the connection falls off continually as the load increases and there is no sudden change as assumed in the idealized condition. In later stages of loading, the predictions give reasonable agreement for deflection. The predicted deflection at midspan for beam BII, based on beam computations, is lower than the measured deflection. This is the only predicted case in which the calculations were completed without the load on the end - connections reaching the breakdown load, i.e. Stage 2 described in section 4.3 was not used. In all the other predictions (where the load on the end - connections reached peak load before the steel in the lower fibre

yielded) the predicted midspan deflections are larger than the corresponding measured deflections. However, the deflections at this point are not critical.

The curves of Figure 4.4 indicate that the push - out tests do not provide acceptable data for developing design curves if a cell arrangement as in beam BII is used, because the prediction is too conservative; the push - out tests provide acceptable data for beams incorporating slender ribs as in beams BIII and BI. The failure of the "weak connections" in beams BI and BIII, was a result of excess load being applied to the connections, whereas in beam BII, having comparatively "strong connections", the failure followed and was induced by yielding of steel in the lower flange. It is probable that results from beam tests with "weak connections" are preferable to results from beam tests with "strong connections", because they will be more reliable for predicting beam behaviour and will show better agreement with results from push - out tests.

The push - out data used in the idealized load - slip curve is the modulus and the breakdown load. SIESS, VIEST and NEWMARK in 1952, stated that if the connections in a beam are such that the interaction coefficient has a value greater than 10, the steel strains and the midspan deflections change only slightly for large variations in the value of the interaction coefficient (Figure 4.4 confirms this for strains). This indicates that the modulus is less important than the breakdown load. The breakdown load must be accurately ascertained, otherwise poor predictions result. The breakdown loads derived from push - out tests are lower than those from computations on beam data. Therefore, the predictions from push - out tests are more conservative than predictions

based on beam tests. This holds true at the working level; to illustrate this, the predicted and observed working moments for beams BI, BII, and BIII are listed in Table 4.3.

The predicted working design moments based on the results of push - out tests are one percent larger, 18 percent smaller, and five percent smaller than indicated by the tests on beams BI, BII, and BIII, respectively. The best agreement is given for the narrow ribs, (i.e. for weak connections.).

TABLE 4.3 WORKING MOMENTS AND STRAINS

		Beam BI	Beam BII	Beam BIII
Working Moments Kip Inches)	Observed	193	264	210
	Predicted (based on Beam Computations)	220	246	208
	Predicted (based on Push - Out Results)	195	217	200
Strains at Working Moments (Micro Inches /Inch)	Observed	600	745	512
	Predicted (based on Beam Computations)	710	784	593
	Predicted (based on Push - Out Results)	660	728	600

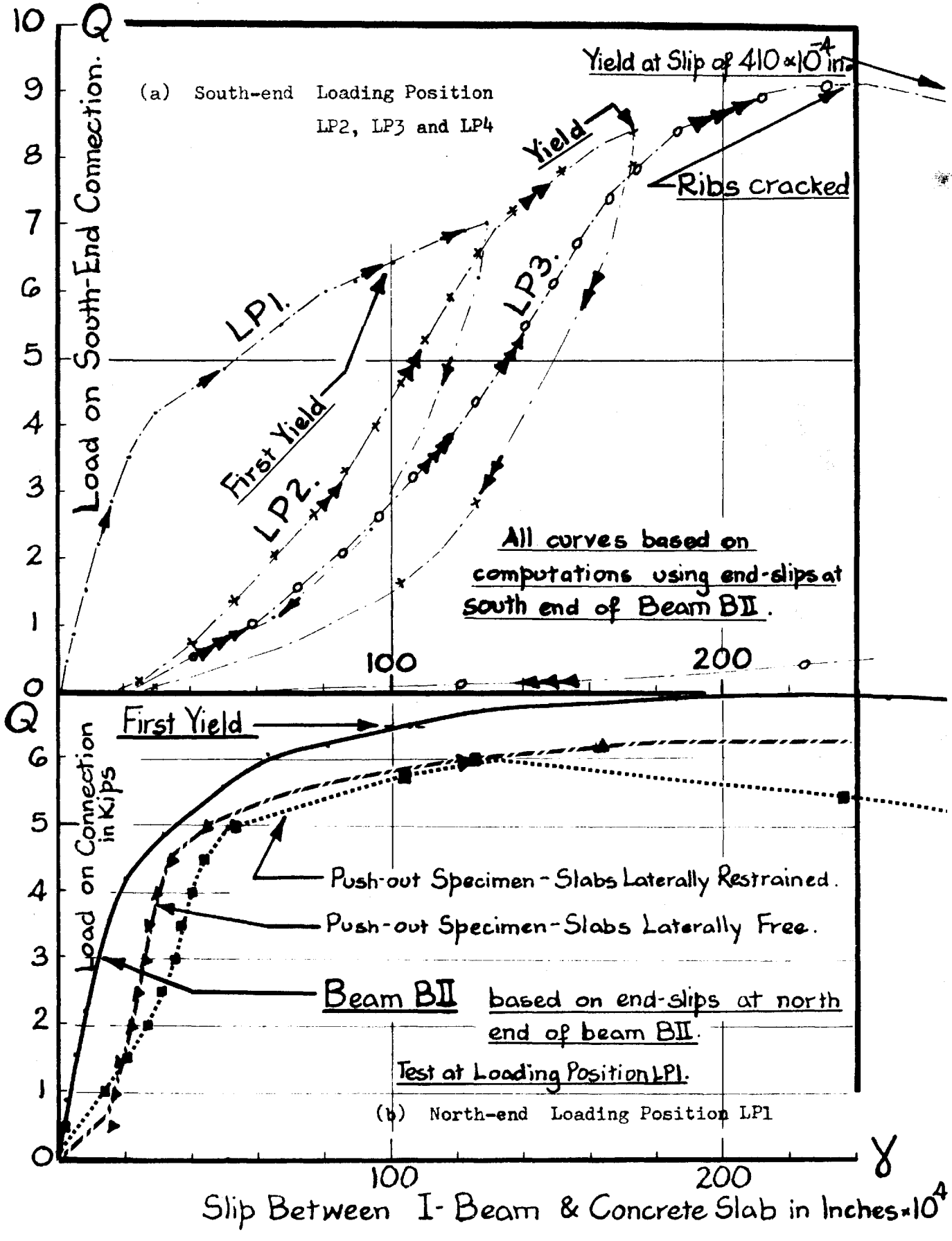

Figure 4.1 Load - Slip Curves for End - Connections of Beam BII

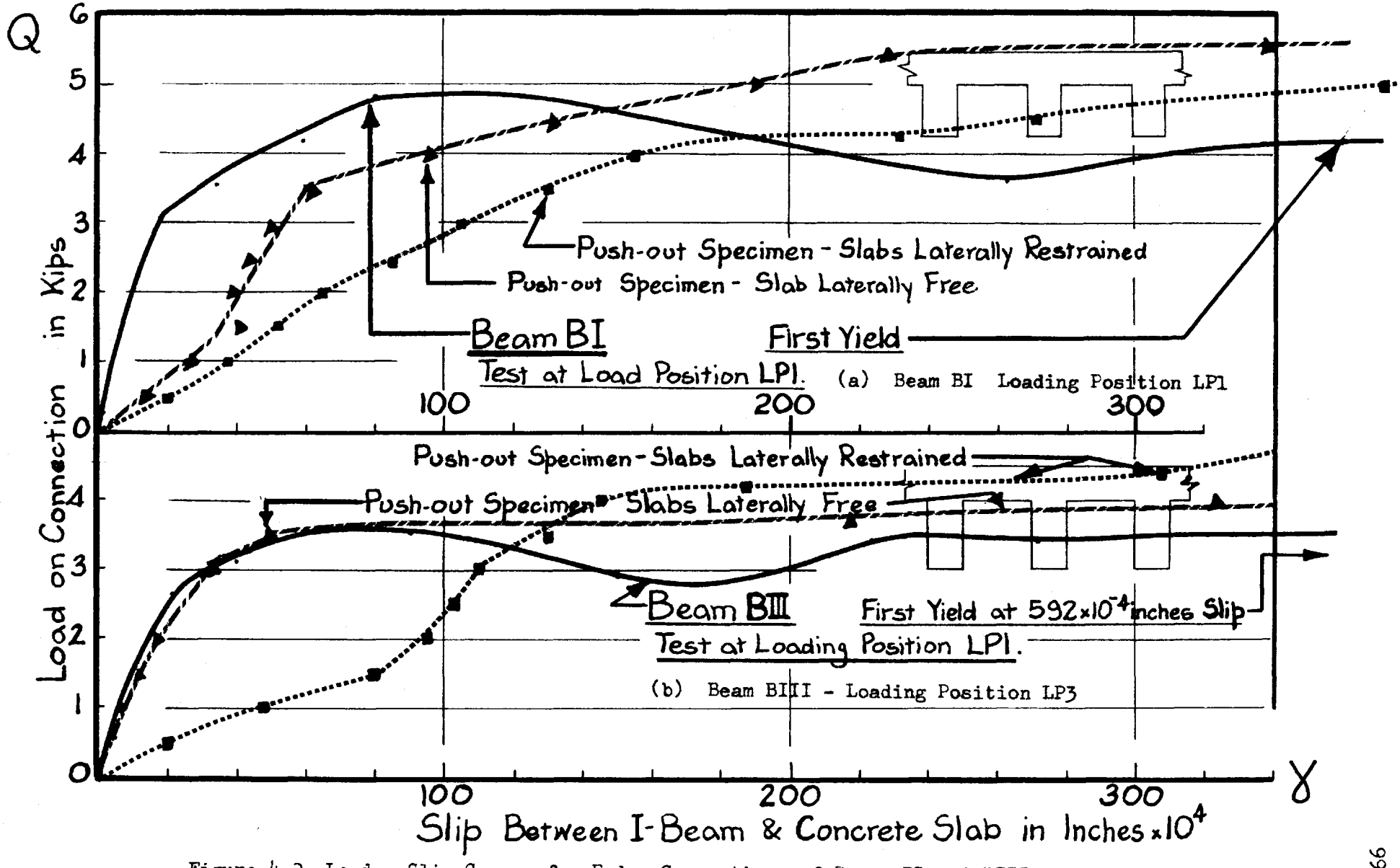

Figure 4.2 Load - Slip Curves for End - Connections of Beams BI and BIII

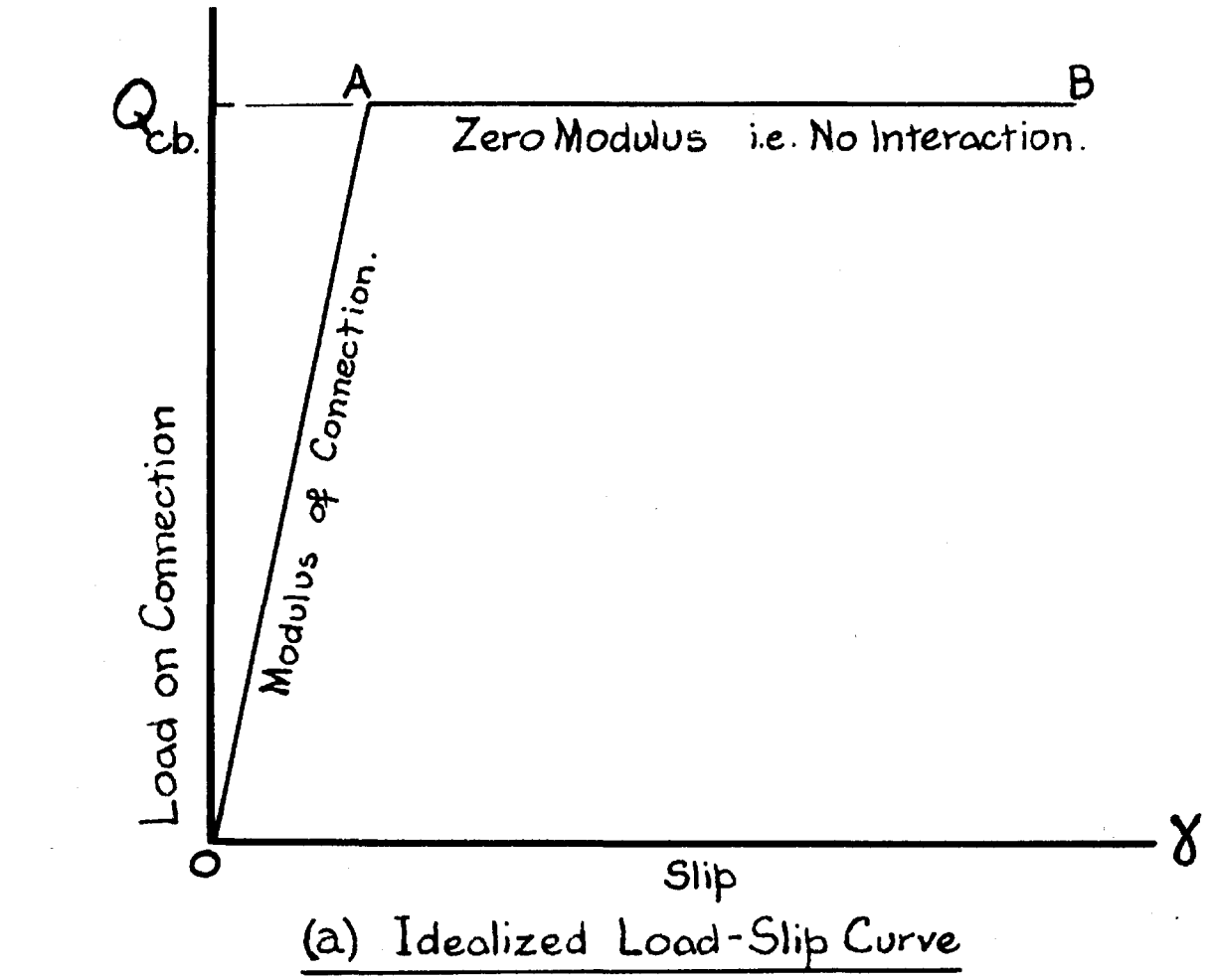

(a) Idealized Load-Slip Curve

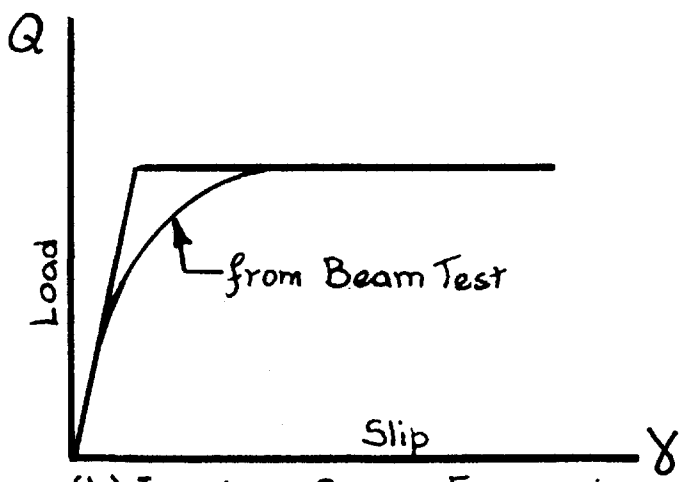

(b) Idealized Curve Enveloping Beam Result.

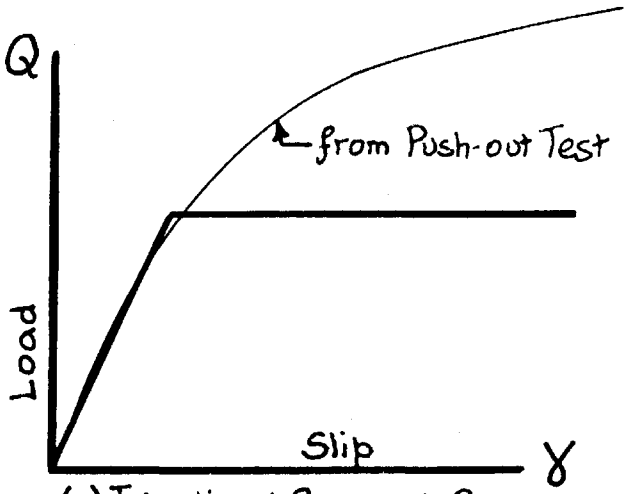

(c) Idealized Curve & Curve from Push-out Test

Figure 4.3 Idealized Load - Slip Curve

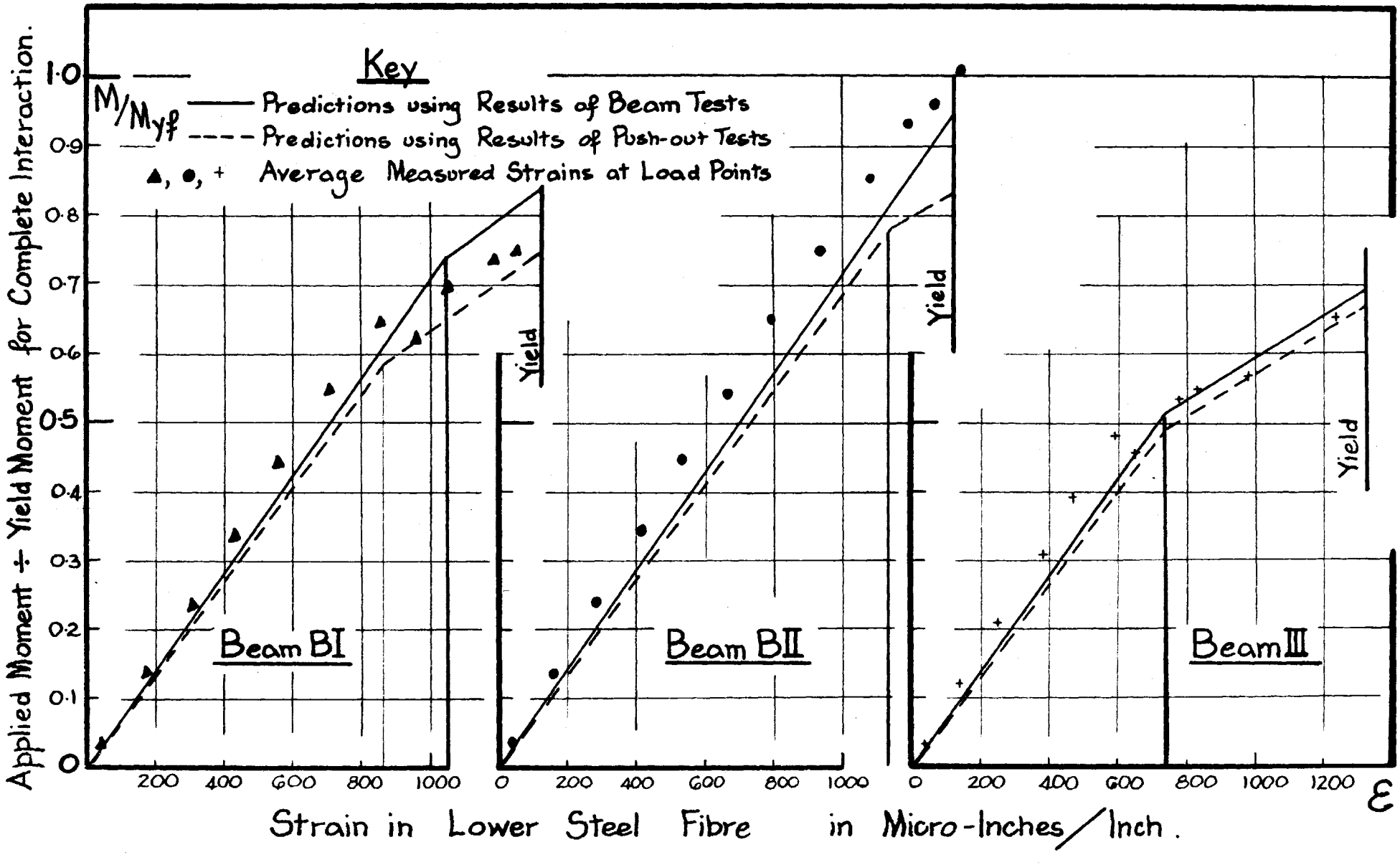

Figure 4.4 Comparison of Measured and Predicted Steel Strains

CHAPTER 5

CONCLUSIONS AND RECOMMENDATIONS

5.1 Effect of Cell Geometry

A main objective of this investigation was to examine the influence of variation of cell geometry on the behaviour of composite cellular structures. The following effects of cell geometry are concluded from the results of tests on push - out specimens:

(a) The characteristics of behaviour of shear connections change with change in cell geometry.

(b) The strength and modulus of a connection vary:

(i) directly with variation of (width of conrete rib)^2, and

(ii) inversely with variation of (height of concrete rib)$^{1/2}$.

The results of tests on composite cellular T - beams were in agreement with finding (a) above, for the push - out tests, but it was not possible to establish that the parameters, width and height of the concrete ribs, had the same influence on the behaviour of the connections in the beams as in the push - out specimens because only the results of a few tests on T - beams are available in which the failure of the connections was free of affects due to yielding of the steel.

5.2 Conclusions From Tests on T - Beams

The connections of all the composite cellular T - beams tested included 3/8 in. diameter stud connectors. In all cases, attempts were

made to destroy bond between the cellular slab and the I - beam before testing was started. The beams were tested on simple spans of 121.5 in. by applying a two - point load system. Within the bounds of these limitations the following conclusions apply:

(a) A composite cellular T - beam is far superior to a similar beam without connection between the beam and the slab.

(b) In all of the beams tested, perfect interaction between the slab and the I - beam was not achieved because the connections allowed slip.

(c) The Newmark theory for incomplete interaction gives a satisfactory qualitative and quantitative description of the behaviour of composite cellular T - beams despite the fact that the composite cellular T - beam does not have a distinct interface.

(d) A composite cellular T - beam has little reserve strength after first yielding; theoretical ultimate moment is not achieved.

(e) The upper limit for the moment of resistance of a composite cellular T - beam is the theoretical yield moment for full interaction.

5.3 Design Method

It was hoped that the test programme described in this thesis would provide insight into the behaviour of composite cellular structures and lead to a rational approach for design procedure. The tests demonstrated that the behaviour of composite cellular T - beams can be analysed satisfactorily by the Newmark theory and an attempt has been made to develop a rational design method based on this theory. Although perfect agreement was not obtained between the predicted behaviour and

the test data, sufficient agreement was found to warrant the extension of the method to full - size beams.

In order to predict beam behaviour it is necessary to have the characteristics of the beam connections. The best means of assessing these characteristics and of obtaining other information for design purposes is to test full - size beams which incorporate the connections under consideration. Such a procedure might entail the testing of many beams with different spacings of studs, and may not be possible economically. Therefore, it may be expedient to base design curves on results of push - out tests.

5.4 Suggestions for Future Studies

The properties and dimensional relations of the small - scale specimens were not exact models of possible full - scale beams. Therefore, it would be advantageous if future tests are carried - out on a number of full - size beams. The basic problems which require further investigation are:

(a) the effect of cell geometry, and

(b) the influence of spacing of the shear connectors, on the behaviour of full - size composite cellular T - beams.

The connection characteristics in many of the small - scale beam tests were affected by yielding of the steel. Therefore, if a full - size beam test is carried out to obtain information about the characteristics of a connection, it is advisable to ensure that a weak total connection is used (by increasing the spacing of the shear connectors when using stiff ribs) so that connection failure occurs before yielding of the lower steel fibre.

Consideration might also be given to more economical use of the composite cellular T - beam by making the lower flange of the I - beam larger than the upper flange and by taking into account the steel decking and/or the concrete ribs in the effective cross - section.

Further tests are also needed to investigate the effect of the following factors on the behaviour of a connection:

(a) the concrete strength

(b) the length of the shear connectors, and

(c) the diameter of the shear connectors.

It would seem that push - out tests of full - scale connections would be adequate for these purposes.

APPENDIX

INCOMPLETE INTERACTION ANALYSIS OF COMPOSITE BEAMS

A.1 Introduction

The type of structure considered is shown in Figure A.1. It is a T - beam made by an I - beam and a ribbed slab formed by the inclusion of cellular sheet steel decking. These are tied together by a shear connection which transfers horizontal shear from one element to the other.

The Newmark theory for incomplete interaction was developed for conventional composite T - beams in which the flat slab was in direct contact with the upper flange of the I - beam. This contact surface is the interface. In the composite cellular beam the flat slab and the beam are separated by a zone of ribs and cells, so that there is no distinct interface. In order to apply the Newmark theory, it is necessary to assume that the junction of the ribs and the slab is a pseudo-interface and that slip at a point on the beam, consists of two components due to:

(1) slip between the upper flange surface of the I - beam and the bottom of the concrete ribs, and

(2) relative displacement between the top of the beam and the bottom of the slab due to rotation of the rib.

Any contribution by the decking or the concrete ribs to the strength of the composite section has been neglected in the analysis.

A.2 Nomenclature

The subscripts used have the following meaning:

s = slab

b = beam

L = section between point load on left and left support

R = section between the point loads

Primed symbols indicate values for composite beam with complete interaction.

The following symbols have been used:

A_s, A_b = cross - sectional areas of the slab and beam respectively.

C_s, C_b = distances between the respective centroidal axes of the slab and the I - beam and their respective extreme fibres.

E_s, E_b = moduli of elasticity of slab and beam respectively.

$\frac{1}{\overline{EA}} = \frac{1}{E_s A_s} + \frac{1}{E_b A_b}$

$\sum EI = E_s I_s + E_b I_b$ and $\overline{EI} = \sum EI + \overline{EA}\, z^2$

$\frac{1}{C} = \frac{k}{s} \frac{L^2 \overline{EI}}{\pi^2 \overline{EA} \sum EI}$

F, F_L, F_R, F' = horizontal direct forces acting at the centroids of the slab and the beam.

I_s, I_b = second moments of area of slab and beam respectively.

k = modulus of shear connection (in lb./in.).

L = span length of composite beam.

M = external moment applied to composite beam.

M_s, M_b = moment of flexural stresses in slab and beam respectively.

P =	half of load on beam
q, q_L, q_R, q' =	horizontal shear per unit length of the beam at the interface of the I - beam and the slab.
Q =	load on connection.
s =	spacing of shear connectors.
u =	distance of either of the point - loads to the nearest support.
x =	distance of a cross - section from the left - hand support.
y, y_L, y_R, y' =	flexural deflections.
y_s, y_b =	vertical distances from the centroidal axis of the slab and the beam respectively.
z =	distance between centroidal axes of the slab and the beam
γ =	slip between the slab and the beam.
ε_s, ε_b,	strains in the slab and the beam respectively.

A.3 Assumptions

(a) The total shear connection between the I - beam and the slab is assumed to be continuous along the length of the beam. When individual shear connections are considered, the assumed condition is approximated only if the connections are equally spaced along the beam and are of equal capacity , i.e.

$$\frac{k}{s} = \text{constant} \qquad (1)$$

where k = the modulus of the connection

and s = the spacing between the connectors

(b) The amount of slip, γ, permitted by the shear connection is directly proportional to the load, Q, transmitted:

$$\gamma = \frac{Q}{k} \qquad (2)$$

For individual connections this requires that the load - slip curve for a connection be a straight line, the slope of which is called the modulus of the connection.

(c) The distribution of strains throughout the depth of the slab and the depth of the beam is linear.

(d) The slab and the I - beam are assumed to deflect equal amounts at all points along their lengths.

(e) The radius of curvature of the centroidal axis of the slab is equal to the radius of curvature of the centroidal axis of the beam.

A.4 Analysis

The load on a connection may be expressed in terms of the unit horizontal shear q and the spacing s as shown below:

$$Q = qs \tag{3}$$

Substituting Equation (3) in Equation (2) gives

$$\gamma = \frac{qs}{k} \tag{4}$$

Therefore:

$$\frac{d\gamma}{dx} = \frac{s}{k} \cdot \frac{dq}{dx} \tag{5}$$

The rate of change of slip along the beam is equal to the difference between the strain in the slab and the strain in the I - beam at the level at which slip occurs. Using the notation of Figure A.1, the rate of change of slip is given by:

$$\frac{d\gamma}{dx} = \varepsilon_b - \varepsilon_s \tag{6}$$

If the composite beam is subjected to a positive bending moment, the connections exert forces which produce compression in the slab and tension in the I - beam. These forces may be replaced by a couple and a

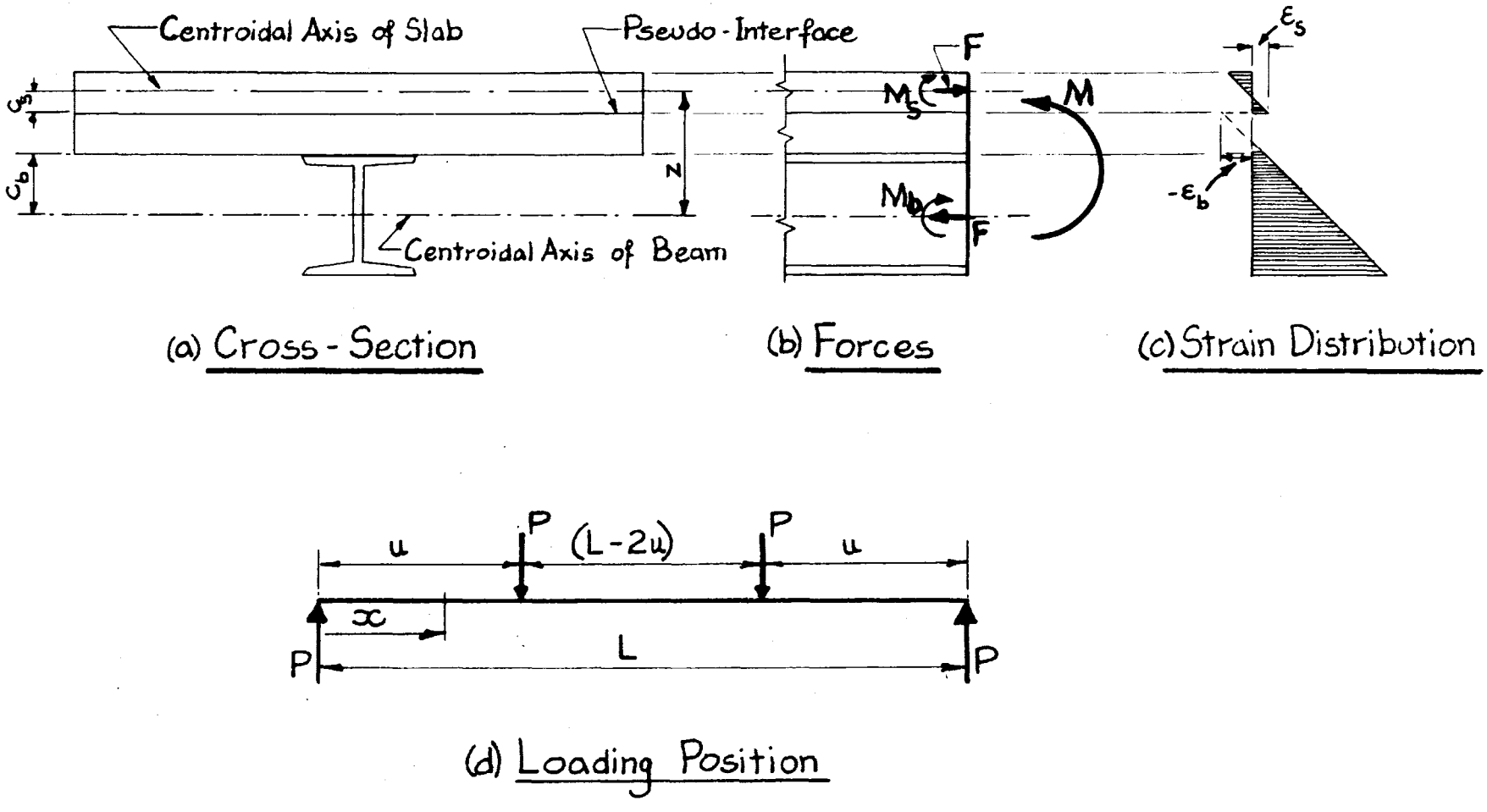

Figure A.1 Cellular Composite T - Beam With Incomplete Interaction

force acting at the centroid of each element as shown in Figure A.1(b)

From Assumption (C), it follows that:

$$-\varepsilon_b = -\frac{F}{E_b A_b} + \frac{M_b C_b}{E_b I_b} \tag{7a}$$

and

$$\varepsilon_s = -\frac{F}{E_s A_s} + \frac{M_s C_s}{E_s I_s} \tag{7b}$$

where E_b and E_s are the moduli of elasticity, I_b and I_s are the second moments of area, and A_b and A_s are the cross - sectional areas, of the I - beam and the slab respectively.

The rate of change of the force F, along the beam is equal to the load per unit length which is transmitted between the slab and the I - beam, that is:

$$q = \frac{dF}{dx} \tag{8}$$

which gives:

$$\frac{dq}{dx} = \frac{d^2F}{dx^2} \tag{9}$$

If Equations (5), (7), and (9) are substituted in Equation (6), the results is:

$$\frac{s}{k}\frac{d^2F}{dx^2} = F\left(\frac{1}{E_b A_b} + \frac{1}{E_s A_s}\right) - \left(\frac{M_b C_b}{E_b I_b} + \frac{M_s C_s}{E_s I_s}\right) \tag{10}$$

From Assumption (e), it follows that the moments M_b and M_s are related:

$$\frac{M_b}{E_b I_b} = \frac{M_s}{E_s I_s} \tag{11}$$

Since the beam is in equilibrium, the external moment applied to the beam is balanced in the following way:

$$M = M_b + M_s + Fz \tag{12}$$

Therefore, Equations (11) and (12) yield:

$$\frac{M_b}{E_b I_b} = \frac{M_s}{E_s I_s} = \frac{M - Fz}{\sum EI} \tag{13}$$

where

$$\sum EI = E_b I_b + E_s I_s \quad .$$

Substituting Equation (13) into Equation (10) gives:

$$\frac{s}{k}\frac{d^2F}{dx^2} = F\left(\frac{1}{E_b A_b} + \frac{1}{E_s A_s} + \frac{z^2}{\sum EI}\right) - \frac{Mz}{\sum EI}$$

or

$$\frac{d^2F}{dx^2} - F \cdot \frac{k}{s} \cdot \frac{\overline{EI}}{\overline{EA}\sum EI} = -\frac{k}{s}\frac{Mz}{\sum EI} \tag{14}$$

where

$$\overline{EI} = \sum EI + \overline{EA}\, z^2$$

and

$$\frac{1}{\overline{EA}} = \frac{1}{E_s A_s} + \frac{1}{E_b A_b}$$

If moment M is expressed as a function of the distance x, the following solution is obtained for a two point loading case as shown in Figure A.1(d).

The distance is measured from the left hand support.

If $x < u$, the moment is

$$M = Px$$

and the Equation (14) will have the form:

$$\frac{d^2F_L}{dx^2} - \frac{k}{s}\frac{\overline{EI}}{\overline{EA}\sum EI} F_L = -\frac{k}{s}\frac{z}{\sum EI} Px \qquad (14a)$$

If $u \ll x \ll (L - u)$, the moment is

$$M = Pu$$

and Equation (14) becomes

$$\frac{d^2F_R}{dx^2} - \frac{k}{s}\frac{\overline{EI}}{\overline{EA}\sum EI} F_R = -\frac{k}{s}\frac{z}{\sum EI} Pu \qquad (14b)$$

The differential equations (14a) and (14b) can be solved using the following end conditions:

at $x = 0$, $F_L = 0$

at $x = u$ $F_L = F_R$ and $\frac{dF_L}{dx} = \frac{dF_R}{dx}$

at $x = L/2$ $\frac{dF_R}{dx} = 0$

The solutions for the force F are:

for $x \ll u$

$$F_L = P\frac{\overline{EA}}{\overline{EI}} z\left[x - \frac{L\sqrt{C}}{\pi}\frac{\cosh\frac{\pi}{\sqrt{C}}\left(\frac{1}{2} - \frac{u}{L}\right)\sinh\left(\frac{\pi}{\sqrt{C}}\frac{x}{L}\right)}{\cosh\frac{\pi}{2\sqrt{C}}}\right] \qquad (15a)$$

and for $u \ll x \ll (L - u)$

$$F_R = Pz\frac{\overline{EA}}{\overline{EI}}\left[u - \frac{L\sqrt{C}}{\pi}\frac{\cosh\left(\frac{\pi}{\sqrt{C}}\left(\frac{1}{2} - \frac{x}{L}\right)\right)\sinh\left(\frac{\pi}{\sqrt{C}}\frac{u}{L}\right)}{\cosh\frac{\pi}{2\sqrt{C}}}\right] \qquad (15b)$$

where $$\frac{1}{C} = \frac{k}{s}\cdot\frac{L^2\,\overline{EI}}{\pi^2\,\overline{EA}\sum EI} \qquad (16)$$

The dimensionless $\frac{1}{C}$ is introduced for convenience.

If a perfect connection is considered, which allows no slip, the modulus of the connection is infinitely large and complete interaction is attained. The force, F', for complete interaction is given by setting C = 0:

$$\text{at } x \leq u \qquad F'_L = \frac{\overline{EA}}{\overline{EI}} zPx \tag{17a}$$

$$\text{at } u \leq x \leq (L - u) \qquad F'_R = \frac{\overline{EA}}{\overline{EI}} zPu \tag{17b}$$

Therefore the ratio of the horizontal force F for incomplete interaction to the horizontal force F' for complete interaction is:

for $x \leq u$

$$\frac{F_L}{F'_L} = 1 - \frac{\sqrt{C}}{\pi} \frac{L}{x} \frac{\cosh \frac{\pi}{\sqrt{C}} \left(\frac{1}{2} - \frac{u}{L}\right) \sinh \frac{\pi}{\sqrt{C}} \frac{x}{L}}{\cosh \frac{\pi}{2\sqrt{C}}} \tag{18a}$$

for $u < x < (L - u)$

$$\frac{F_R}{F'_R} = 1 - \frac{\sqrt{C}}{\pi} \frac{L}{u} \frac{\cosh \frac{\pi}{\sqrt{C}} \left(\frac{1}{2} - \frac{x}{L}\right) \sinh \left(\frac{\pi}{\sqrt{C}} \frac{u}{L}\right)}{\cosh \frac{\pi}{2\sqrt{C}}} \tag{18b}$$

The ratio F/F' gives a convenient indication of the degree of interaction present, at a specific section of a beam.

A.5 Load on Shear Connections

The load, Q, on any connection is given by:

$$Q = qs$$

where q is found from Equations (8) and (18)

The horizontal shear per unit length of the beam is:

for $x \leq u$

$$q_L = \frac{dF_L}{dx} = P \frac{\overline{EA}}{\overline{EI}} z \left[1 - \frac{\cosh \frac{\pi}{\sqrt{C}} (\frac{1}{2} - \frac{u}{L}) \quad \cosh (\frac{\pi}{\sqrt{C}} \frac{x}{L})}{\cosh \frac{\pi}{2\sqrt{C}}} \right] \quad (19a)$$

and for $u \ll x \ll (L - u)$

$$q_R = P \frac{\overline{EA}}{\overline{EI}} z \left[\frac{\sinh \frac{\pi}{\sqrt{C}} (\frac{1}{2} - \frac{x}{L}) \quad \sinh (\frac{\pi}{\sqrt{C}} \frac{u}{L})}{\cosh \frac{\pi}{2\sqrt{C}}} \right] \quad (19b)$$

The horizontal shear per unit length of the beam for complete interaction is given by:

$$q' = \frac{\overline{EA}}{\overline{EI}} z P$$

Therefore Equations (19a) and (19b) may be written in the form of ratios as follows:

for $x \ll u$

$$\frac{q_L}{q'_L} = 1 - \frac{\cosh \frac{\pi}{\sqrt{C}} (\frac{1}{2} - \frac{u}{L}) \quad \cosh (\frac{\pi}{\sqrt{C}} \frac{x}{L})}{\cosh \frac{\pi}{2\sqrt{C}}} \quad (20a)$$

for $u \ll x \ll (L - u)$

$$\frac{q_R}{q'_R} = \frac{\sinh \frac{\pi}{\sqrt{C}} (\frac{1}{2} - \frac{x}{L}) \quad \sinh (\frac{\pi}{\sqrt{C}} \frac{u}{L})}{\cosh \frac{\pi}{2\sqrt{C}}} \quad (20b)$$

A.6 Strains

The strains in the composite beam may be obtained from the relations

$$\varepsilon_b = \frac{F}{E_b A_b} + \frac{M_b y_b}{E_b I_b} \quad (21a)$$

and

$$\varepsilon_s = - \frac{F}{E_s A_s} + \frac{M_s y_s}{E_s I_s} \qquad (21b)$$

where y_b and y_s are the distances from the centroid of the I - beam or of the slab to the point at which the strain is required; y is positive when measured downwards. The force F is determined from Equations (15a) and (15b), and the moments M_b and M_s are obtained from Equation (13).

A.7 Flexural Deflections

The curvature of a composite beam is given by Equation (13) as:

$$\frac{d^2y}{dx^2} = - \frac{M}{\sum EI} + \frac{Fz}{\sum EI} \qquad (22a)$$

If Equation (14) is used to substitute for F in the above, the result is:

$$\frac{d^2y}{dx^2} = - \frac{M}{\overline{EI}} + \frac{s}{k} \frac{\overline{EA}}{\overline{EI}} z \frac{d^2F}{dx^2} \qquad (22b)$$

This equation can be solved for the deflection due to flexural deformations by using the following end conditions:

at $x = 0$ $y = 0$, and $F = 0$

at $x = L$ $y = 0$, and $F = 0$

at $x = L/2$ $\frac{dy}{dx} = 0$.

The solution for the deflection due to flexural deformation is:

$$y = y' + \frac{s}{k} \frac{\overline{EA}\, z}{\overline{EI}} F$$

where y' is the flexural deflection of a composite beam with complete interaction.

A.8 Interpretation of Tests of Composite Beams

The modulus k may be determined from the tests of composite beams. This method is based on the slip data obtained in the tests.

For any particular section of a composite beam and for a particular location of the two - point loading system, Equations (20) give the ratio (q/q') as a function of $1/C$:

$$\frac{q}{q'} = f\left(\frac{1}{C}\right) \qquad (20a,b)$$

If Equations (4) and (16) are combined, the ratio of (q/q') is given as a function of $1/C$ by:

$$\frac{q}{q'} = \frac{\pi^2 \overline{EA} \sum EI}{C \; L^2 \; \overline{EI}} \; \frac{Y}{q'} \qquad (23)$$

In the two relations above, the slip is taken from beam tests, and therefore the only unknowns in these expressions are C and (q/q').

The solution is found analytically by successive approximations.

BIBLIOGRAPHY

1952 SIESS, C. P., VIEST, I.M., and NEWMARK, N.M., "Studies of Slab and Beam Highway Bridges - Part III: Small - Scale Tests of Shear Connectors and Composite T - Beams", University of Illinois Engineering Experiment Station, Bulletin Series No. 396, Urbana, February, 1952.

VIEST, I.M., SIESS, C.P., APPLETON, J.H., and NEWMARK, N.M., "Studies of Slab and Beam Highway Bridges, Part IV: Full - Scale Tests of Channel Shear Connectors and Compsoite T - Beams," University of Illinois Engineering Experiment Station, Bulletin Series No. 405, Urbana, December 1952.

1955 VIEST, I.M., "Shear Connector Engineering Test Data - Test of Stud Shear Connectors Part III", Nelson Stud Welding, Lorain, Ohio, May 1955.

1956 VIEST, I.M., "Investigation of Stud Shear Connectors for Composite Concrete and Steel T - Beams, "Journal of the American Concrete Institute, Vol. 27, No. 8, April 1956.

1963 DAI, P. K. H., and SIESS, C. P. "Analytical Study of Composite Beams with Inelastic Shear Connection," University of Illinois, Civil Engineering Studies, Structural Research Series, No. 267, Urbana, June 1963.

ROBINSON, H., "Preliminary Investigation of a Composite Beam with Ribbed Slab Formed by Cellular Steel Decking", McMaster University, Hamilton.